NASA Tech Briefs

Transferring Technology to
American Industry and Government

September 1988
Volume 12 Number 8

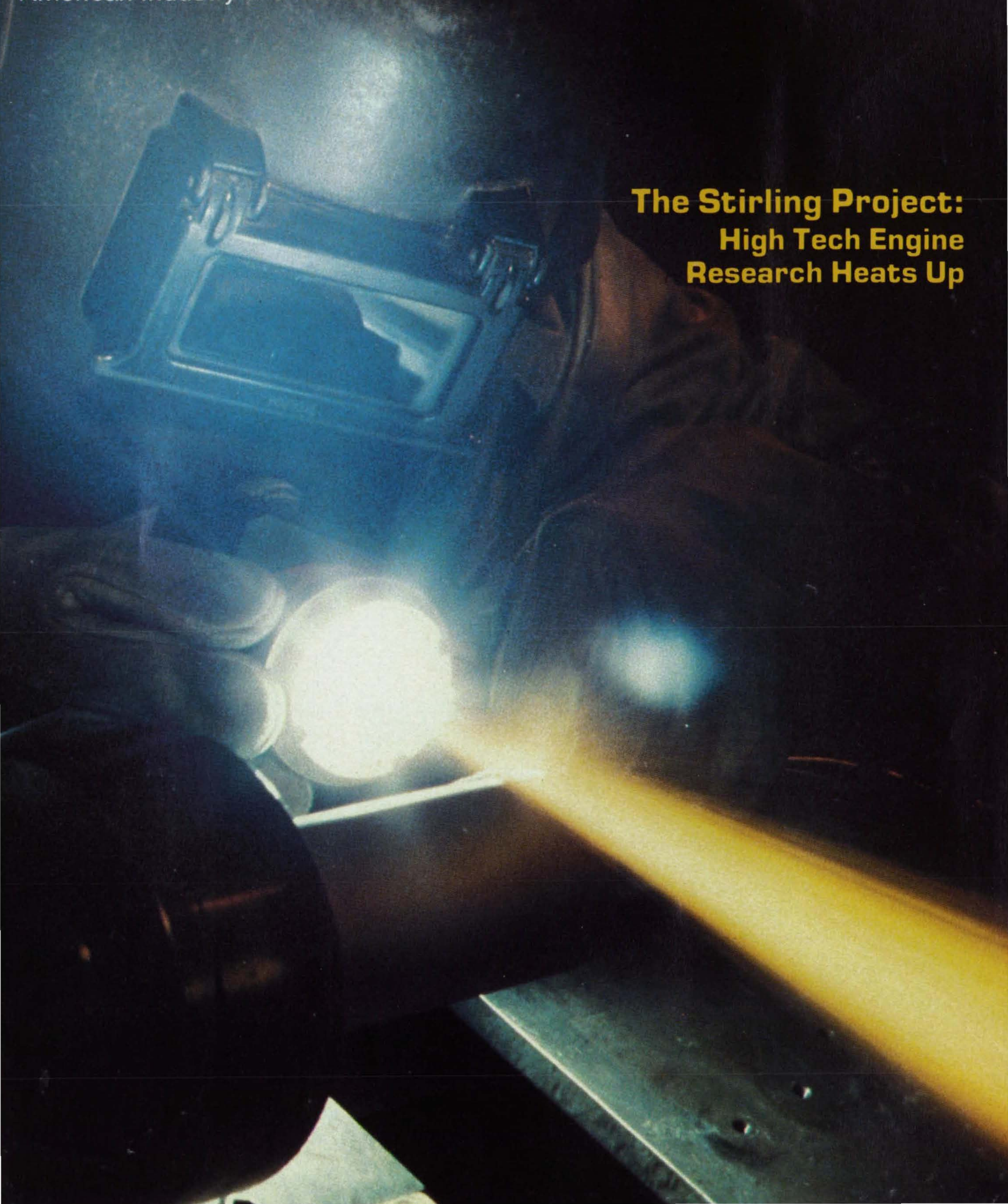

**The Stirling Project:
High Tech Engine
Research Heats Up**

Artisan Integrated Board The New

Why are so many test engineers in production and R&D welcoming the new Artisan A7000 full range tester?

Simply put, it's the most versatile tester you can use and, when you factor in its amazing simplicity, probably the least expensive.

Artisan's A7000 offers easy configurability for prototype test, the speed and ease of use required in full scale

Defines Functional Test. A7000.

production and straightforward fault reporting necessary for field service debug. Different problems, different environments, different skill levels—the same tester.

The A7000 speaks in a language you'll understand. Menus and function keys handle all test preparation, execution, and evaluation operations. The system guides you through every step of testing.

The evaluation of test results, fault reporting, and documentation are taken care of automatically.

The price? A very affordable $45,000. Low enough to pay for itself in a matter of months.

Training? One on one, at your site, and on your board.

Service? If you have a problem with our product, it's our problem. We'll make sure that you're up and running within 24 hours.

Artisan's A7000 Integrated Test System. The first tester built to be your *only* tester.

Call for more information or a personal demonstration: (203) 871-7322.

artisan

Artisan Development Corporation

Circle Reader Action No. 636

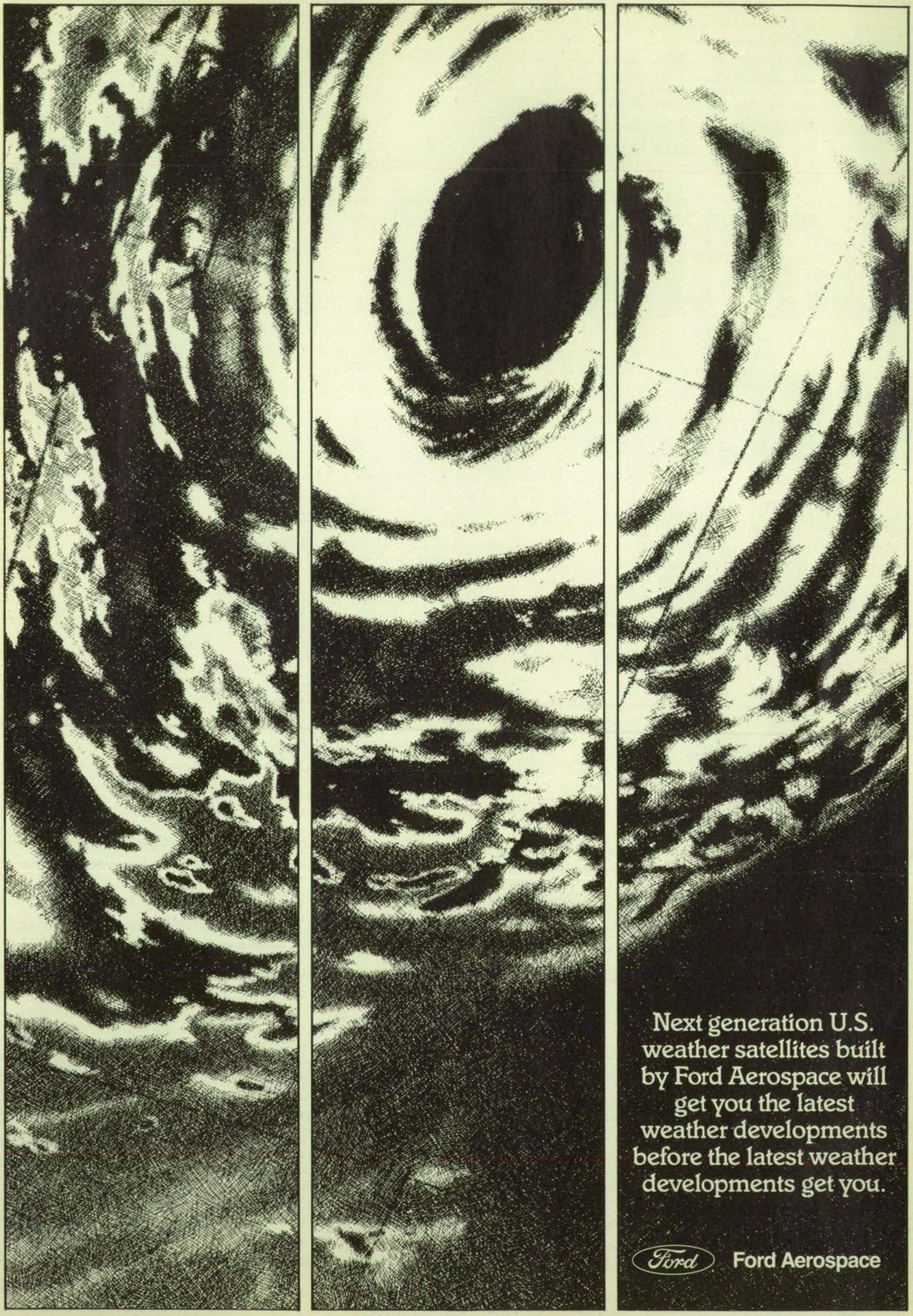
Next generation U.S. weather satellites built by Ford Aerospace will get you the latest weather developments before the latest weather developments get you.
Ford
Ford Aerospace


Generation to Generation.
Recyclable engineering materials today promise an even greater legacy than immediate reductions of costs and waste.
Generation and regeneration: from packaging to automotive to construction. The energy isn't lost. Our promise for the future. Advanced technology plastics offering long-term productivity and potential.
Recyclable. Reusable. Responsible.
For an informative outlook on recycling engineering plastics, request our free Recyclability Brochure today:
(800) 845-0600.
Recyclable
Reusable
Responsible
GE Plastics
GE Plastics
Circle Reader Action No. 615

NASA Tech Briefs

National Aeronautics and
Space Administration

SEPTEMBER 1988
Volume 12 Number 8

A computational fluid dynamics simulation of the airflow surrounding a high-speed airfoil. Designed by McDonnell Douglas Corp. for NASA, the airfoil features small wedges at its lower-surface trailing edges which increase effective camber and reduce drag. See page 66.
(Photo courtesy Douglas Aircraft Co., Long Beach, CA)

SPECIAL FEATURES

TECHNICAL SECTION

DEPARTMENTS

On The Cover: A technician at NASA's Lewis Research Center flame-sprays a high-temperature lubricant coating onto the cylinders of a Stirling engine. The chromium carbide-based coating will help increase the Stirling's power and efficiency, and may be applied to diesel engines as well. See page 14.
(Photo courtesy NASA)

This month's Mission Accomplished describes the Stirling engine, an alternative automotive power plant featuring a unique external combustion system. The Stirling employs an external heater head (shown at left), where continuous combustion takes place. For more information turn to page 14, and the related technical brief on page 61. *(Photo courtesy NASA)*

NASA Tech Briefs, ISSN 0145-319X, USPS 750-070, copyright © 1988 in U.S., is published monthly except July/August and November/December (10x per year) by Associated Business Publications Co., Ltd. 41 E. 42nd St., New York, NY 10017-5391. The copyrighted information does not include the individual Tech Briefs which are supplied by NASA. Editorial, sales, production and circulation offices at 41 E. 42nd Street, New York, NY 10017-5391. Subscriptions for non-qualified subscribers in the U.S., Panama Canal Zone, and Puerto Rico, $75.00 for 1 year; $125.00 for 2 years; $200 for 3 years. Single copies $15.00. Remit by check, draft, postal or express orders. Other remittances at sender's risk. Address all communications for subscriptions or circulation to NASA Tech Briefs, 41 E. 42nd Street, New York, NY 10017-5391. Second-class postage paid at New York, NY and additional mailing offices.

POSTMASTER: please send address changes to NASA Tech Briefs, 41 E. 42nd Street, Suite 921, New York, NY 10017-5391.

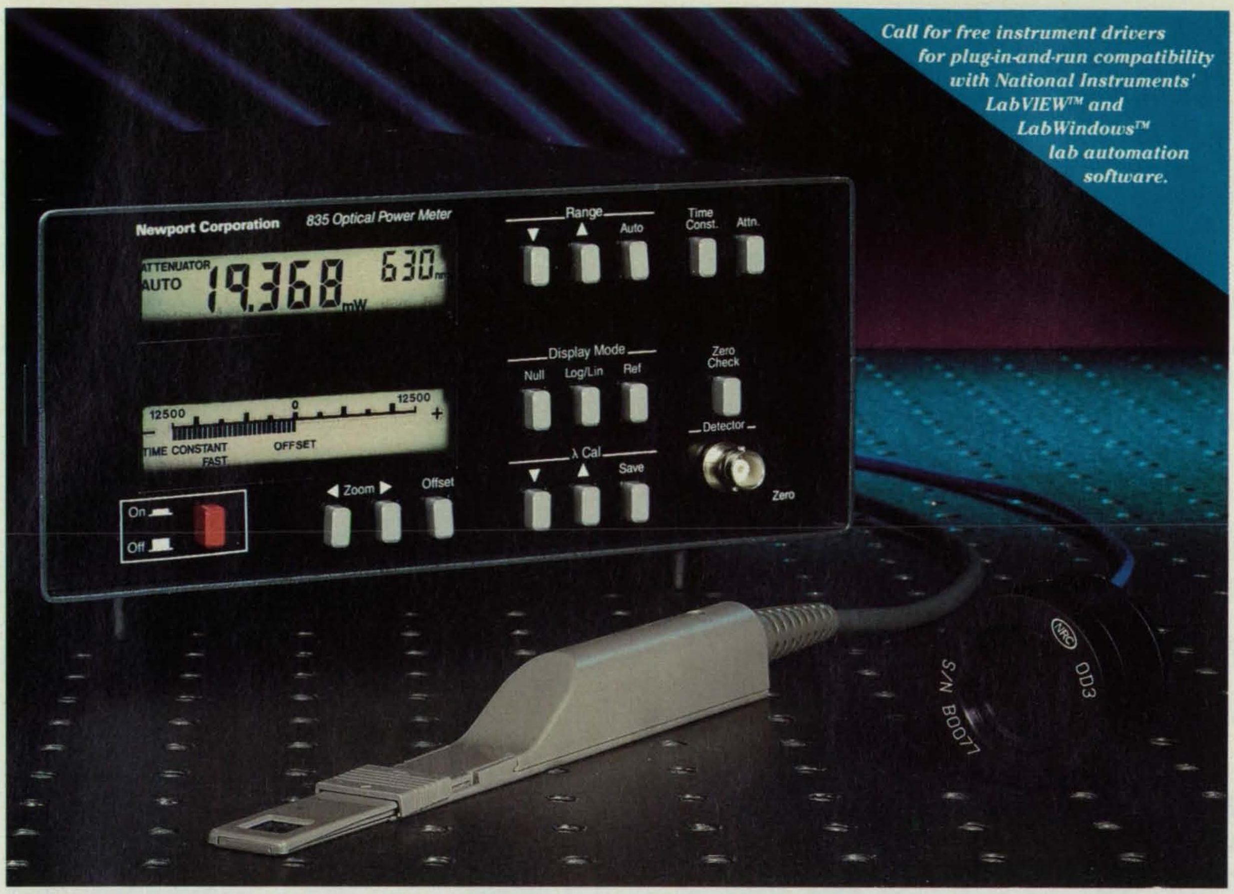

A full-featured Optical Power Meter for half the price!*

Consider these features:

- 0.1 picowatt/-100 dBm sensitivity with 0.1 dB resolution
- Built-in wavelength compensation at 10 nm intervals over the entire spectrum with high accuracy, NBS-traceable calibration
- Choice of standard or *new* UV-enhanced silicon detectors or IR germanium detector
- Auxiliary bar-graph analog backlit display and linear, log (dBm, dB) and ratio readout modes with background nulling function
- External 0-2 volt analog output

Options include rechargeable battery operation, fiberoptic adaptors, and IEEE-488 interface.

*Until now, these features were only available in meters that cost over twice as much as our popular Model 835 Digital Pico-Watt Power Meter.

For detailed information about this new product and other power meters, including measurement capabilities of up to 1 kilowatt, call or send for your free copy of the Newport Catalog.

714/965-5406

Newport Corporation
18235 Mt. Baldy Circle
Fountain Valley, CA 92708
Europe: Newport GmbH, Ph. 06151-26116
U.K.: Newport Ltd., Ph. 05827-69995

Newport

Circle Reader Action No. 540

NASA Tech Briefs

National Aeronautics and Space Administration

ABP BPA

NASA Tech Briefs:

Published by .... **Associated Business Publications**
Editor-in-Chief/Publisher .... **Bill Schnirring**
Associate Publisher .... **Frank Nothaft**
Associate Publisher .... **Robin J. DuCharme**
Managing Editor .... **R. J. Laer**
Associate Editor .... **Joseph T. Pramberger**
Technical Advisor .... **Dr. Robert E. Waterman**
Production Manager .... **Rita Nothaft**
Traffic Manager .... **James E. Cobb**
Circulation Director .... **Anita Weissman**
Marketing Research Manager .... **Leo D. Kluger**
Advertising Coordination Manager .... **Erving Dockery, Jr.**
Telecommunications Specialist .... **Evelyn Mars**
Reader Service Manager .... **Arlene Berrios**

Technical Staff:
Briefs prepared for National Aeronautics and Space Administration by **Logical Technical Services Corp.**, NY, NY
Technical/Managing Editor .... **Ted Selinsky**
Art Director .... **Ernest Gillespie**
Administrator .... **Elizabeth Texeira**
Chief Copy Editor .... **Lorne Bullen**
Staff Editors .... **Dr. James Boyd, Dr. Larry Grunberger, Jordan Randjelovich, George Watson, Oden Browne, Joseph Renzler, Dr. Theron Cole, Jr.**
Technical Advisers .... **Dr. Arthur Gilman, Dr. Jay Kirschenbaum**
Graphics .... **Luis Martinez, Vernald Gillman, Charles Sammartano**
Editorial & Production .... **Bill Little, Frank Ponce, Ivonne Valdes, Paul Marcus**

NASA:
NASA Tech Briefs are provided by the National Aeronautics and Space Administration, Technology Utilization Division, Washington, DC:
Administrator .... **Dr. James C. Fletcher**
Assistant Administrator for Commercial Programs .... **James T. Rose**
Deputy Assistant Administrator (Programs) .... **Henry J. Clarks**
Deputy Director TU Division (Publications Manager) .. **Leonard A. Ault**
Manager, Technology Utilization Office, NASA Scientific and Technology Information Facility .... **Walter M. Heiland**

Associated Business Publications
41 East 42nd Street, Suite 921, New York, NY 10017-5391
(212) 490-3999
President .... **Bill Schnirring**
Executive Vice President .... **Frank Nothaft**
Vice President .... **Domenic A. Mucchetti**
Vice President Marketing .... **Mark J. Seitman**
Controller .... **Felecia D'Amato**

Advertising:
New York Office: (212) 490-3999 FAX (212) 986-7864
Sales Manager .... **Robin DuCharme**
Regional Sales Manager (Mid-Atlantic) .... **Michelle Larsen**
Account Executive .... **Debby Crane** at (201) 967-9838
Account Executives (Midwest) ...... **Jack Cartwright** or **Paul Lesher** at (312) 501-4140
Account Executives (Eastern MA, NH, ME, RI) **Lee Arpin** or **Brian Clerkin** at (617) 899-5613; **Bill Doucette** at (617) 278-7792
Account Executive (Western MA, CT, VT) **George Watts** or **David Haggett** at (413) 253-9881
Account Executive (No. Calif., UT) .... for Area Codes 415/408 —**Janice Richey King** at (415) 656-3613
Account Executives (So. Calif., AZ, NV, NM) .... for Area Codes 818/213/805—**Thomas Stillman** or **Dana Gindoff** and for Area Codes 619/714—**Leslie Alley** or **Melanie Binkley** at (213) 372-2744

NTBM-Research Center
Account Supervisor .... **Lourdes Del Valle**

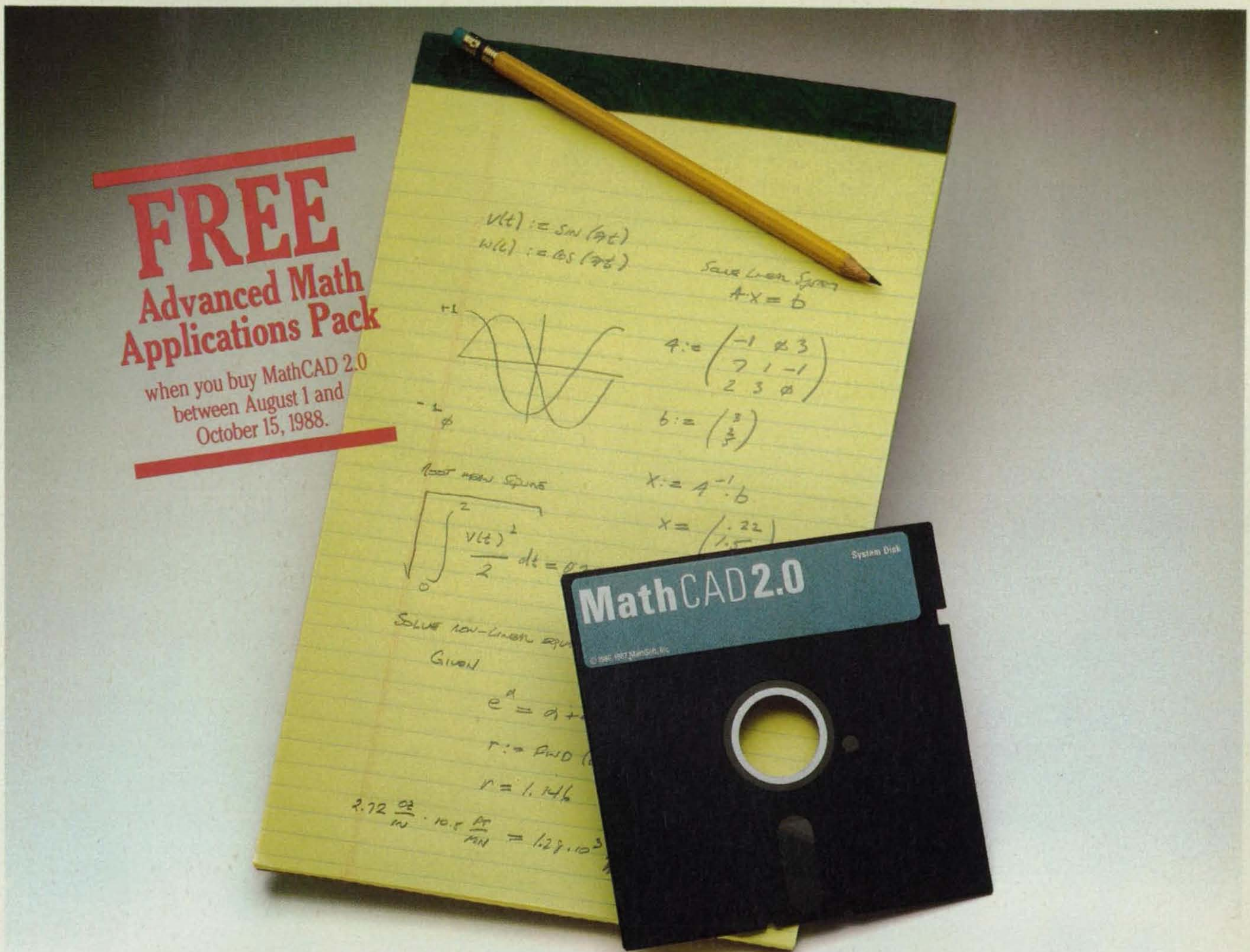

Your pad or ours?

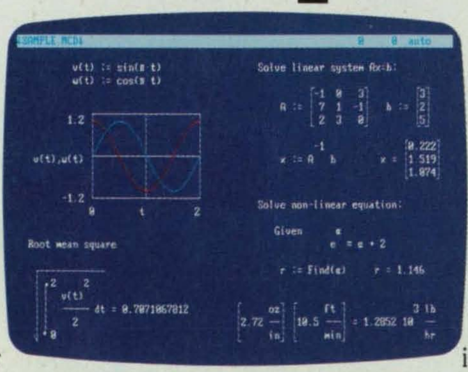

If you perform calculations, the answer is obvious.

MathCAD 2.0.

It's everything you appreciate about working on a scratch-pad – simple, free-form math – and more. More speed. More accuracy. More flexibility.

Just define your variables and enter your formulas anywhere on the screen. MathCAD formats your equations as they're typed. Instantly calculates the results. And displays them exactly as you're used to seeing them – in real math notation, as numbers, tables or graphs.

MathCAD is more than an equation solver. Like a scratchpad, it allows you to add text anywhere to support your work, and see and record every step. You can try an unlimited number of what-ifs. And print your entire calculation as an integrated document that anyone can understand.

Plus, MathCAD is loaded with powerful built-in features. In addition to the usual trigonometric and exponential functions, it includes built-in statistical functions, cubic splines, Fourier transforms, and more. It also handles complex numbers and unit conversions in a completely transparent way.

Yet, MathCAD is so easy to learn, you'll be using its full power an hour after you begin.

Requires IBM PC® or compatible, 512KB RAM, graphics card.
IBM PC® International Business Machines Corporation.
MathCAD® MathSoft, Inc.

What more could you ask for? How about the new **Advanced Math Applications Pack**? A $55 value, it's yours *free* when you purchase MathCAD between August 1 and October 15, 1988. The Advanced Math Pack includes a custom binder, software and documentation for 16 advanced applications such as:

- Runge-Kutta Solution of First Order Differential Equation
- Solution of Second-Order Differential Equation
- Eigenvalues and Eigenvectors of a Symmetric Matrix
- Convolution and Correlation of Sequences
- Convolutions using FFT's
- And many more!

If you're tired of doing calculations by hand or writing and debugging programs, come on over to MathCAD.

For more information contact your local dealer or call **1-800-MATHCAD, ext. 2775** (In MA: 617-577-1017, ext. 2775).

MathCAD®

MathSoft, Inc., One Kendall Sq., Cambridge, MA 02139

Circle Reader Action No. 628

New Product Ideas

New Product Ideas are just a few of the many innovations described in this issue of *NASA Tech Briefs* and having promising commercial applications. Each is discussed further on the referenced page in the appropriate section in this issue. If you are interested in developing a product from these or other NASA innovations, you can receive further technical information by requesting the TSP referenced at the end of the full-length article or by writing the Technology Utilization Office of the sponsoring NASA center (see page 18). NASA's patent-licensing program to encourage commercial development is described on page 18.

Contactless Coupling for Power and Data

An experimental flat-plate coupling transmits digital data signals and electrical power across a small gap between two modules. Unlike multiple-pin electrical connectors, the two halves of the coupling do not have to be aligned precisely for mating and can be assembled by robots, remote manipulators, or people working in protective clothing. (See page 22).

Solid-State Single-Photon Counter

A commercial avalanche photodiode can be used to detect single photons if it is cooled to an optimum temperature and overbiased beyond its breakdown voltage. Avalanche photodiodes used in this mode offer two to three times the sensitivity of the photomultiplier tubes commonly used for photon detection. (See page 27).

Yaw Control at High Angles of Attack

In a conventional airplane, the rudder becomes ineffective when the craft is operating at a very high angle of attack. The problem is solved by the use of articulated, conformal forebody strakes. Wind-tunnel tests have confirmed the effectiveness of this arrangement at angles of attack between 10° and 70° and sideslip angles of 20°. (See page 76).

Shaping Plastic Covers Quickly and Cheaply

An inexpensive, compact fixture enables the thermal forming of custom-contoured plastic covers in only half an hour. Previously, two workers needed 12 hours to form such a cover by hand. The fixture includes an aluminum baseplate and an aluminum forming plate with an opening cut out to match the cover outline. (See page 90).

This symbol appears next to technical briefs which describe inventions having potential commercial applications as new products. The process for developing a product from a NASA invention is described at the top of this page.

OPA111/883B

RAD-HARD & READY TO SERVE

The World's Best Op Amp Just Earned Its Stripes!

OPA111/883B combines unmatched performance and radiation hardness. Our customers tell us it could be the best military op amp available. It's based on our industry-leading monolithic ***Difet***® design, and we make it fully compliant to MIL-STD-883C, Class B, on our DESC-certified lines. We hope you'll consider it for your precision military instrumentation, data acquisition, optoelectronics, and test equipment applications.

Key OPA111/883B Features

- Fully compliant MIL-STD-883C processing
- Dielectrically isolated FET design provides superior radiation hardness
- Low noise: 100% tested, 8nV/$\sqrt{\text{Hz}}$ max (10kHz)
- Low bias current: 2pA max
- Low offset: 500μV max
- Low drift: 10μV/°C max
- High open-loop gain: 114dB min
- Hermetic metal TO-99 package, full −55/+125°C MIL temp range

Contact your Burr-Brown technical rep for full details and evaluation samples, or call Applications Engineering, (602) 746-1111. Burr-Brown, P.O. Box 11400, Tucson, AZ 85734.

BURR-BROWN®

Difet® Burr-Brown Corp.

Circle Reader Action No. 435

Mission Accomplished

The Stirling Engine

NASA's High Tech Power Plant

A joint research effort between NASA and the Department of Energy has resulted in a new breed of automotive engine that delivers high miles per gallon on anything from the cheapest gasoline to kerosene or home heating oil. This revolutionary power plant, the Stirling heat engine, can be applied to cars, buses, trucks—even spacecraft.

Like standard auto engines, the Stirling burns a mixture of air and fuel to drive pistons and thereby transmit power to the wheels. The Stirling differs from conventional internal combustion engines in that it employs an external heater head, where continuous combustion of a working gas takes place, located outside the cylinders.

"The Stirling's external combustion system allows virtually any liquid or gaseous fuel to be burned without degrading performance," said Dr. William Ernst, Manager of Kinematic Programs for Mechanical Technology Inc. (MTI), NASA's prime contractor for the Stirling development project. "This is advantageous to both the engine manufacturer who could use the same design and hardware for any fuel and for the consumer who could shop for the cheapest fuel and be immune to shortages of any one type of fuel."

The Stirling design also offers environmental benefits, including reduced exhaust emissions and lower noise levels than internal combustion engines. As part of an industry-government test program, General Motors Research Laboratories conducted emission evaluations on a first-generation, or Mod I, Stirling which was installed in an AMC Spirit and driven for over 1,000 miles. General Motors reported that the Mod I met federal emission standards with a "comfortable margin," despite the fact that the engine was operated without a catalytic converter.

Separate tests performed by MTI confirmed that a 20 decibel noise reduction can be obtained from a Stirling engine over a comparable diesel engine. "By employing a continuous combustion process, the Stirling eliminates pressure pulsations from the engine exhaust and is therefore relatively quiet," explained Dr. Ernst.

Low maintenance costs and long service life are further advantages the Stirling holds over conventional engines. The Stirling has no carburetor, spark plugs, muffler, or catalytic converter, requires minimal lubrication, and never needs an oil change. In addition, the Stirling's kinematic components are free of the contaminants found in internal combustion systems.

Though the concept for the Stirling engine dates back to the early 19th century, substantial research on this engine cycle has occurred only in the last few decades. "For years the engineering community considered the Stirling to be a laboratory curiosity, nothing more," said Ernst. The first Stirling-based engines, produced in the Netherlands during World War II and later improved in Sweden, were slow-running machines that could not compete with the more versatile spark-ignition systems.

United States interest in the Stirling began during the oil crisis of the early 1970's, when the Environmental Protection Agency was searching for an alternative automobile engine that would conserve energy and reduce reliance on fossil fuels. In 1978, the Department of Energy initiated a program to transfer Stirling technology to the United States and assigned NASA's Lewis Research Center the task of developing the high-temperature materials and sealing techniques required to transform the external combustion concept into a practical power plant.

Lewis and its contractors developed substitute metal alloys that reduced the engine's fabrication costs by eliminating cobalt and other strategic materials. Lewis engineers also invented a high-temperature lubricant coating for the Stirling that could provide a ten percent increase in engine power. When applied to the cylinder walls, the coating allows the piston rings to be moved from a cold area at the piston's lower end to a 700°C zone on top of the piston. "A considerable

Above: A wood-sculpted model of the Mod II Stirling engine built for checking precise dimensions prior to machine tooling of parts. (Photo courtesy Mechanical Technology Inc., Latham, NY)

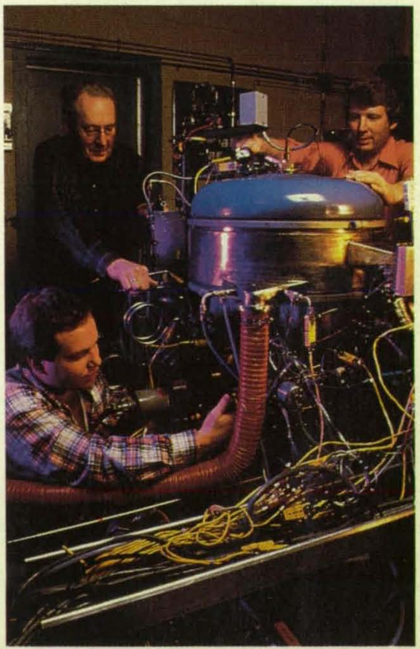

Engineers hook up a Stirling engine to a dynamometer prior to a test cell run at various speeds and loads.

amount of power is lost in the gap between the top and bottom of the piston," explained Michael Tomazic, Stirling Project Manager for Lewis. "By installing a ring near the top of each piston dome we can seal the gap and thereby boost engine power."

A Testing Ground

Before the Stirling can be mass-produced for automobiles, it must first prove its mettle in smaller starter markets. "We're looking for markets with low production rates," said Tomazic. "That way we can gain the necessary commercial experience with less financial risk."

Potential starter market applications include engine generators, heat pumps, irrigation pumps, and solar electric units. Initial applications are likely to come in the specialty vehicle market, which is the current focus of Stirling testing. Mod I engines installed in Air Force pickup trucks and vans have logged over 18,000 urban and highway miles while operating on a variety of fuels—including unleaded gasoline, jet fuel, kerosene, and diesel fuel. Throughout these evaluations, Air Force drivers reported no differences in acceleration or response due to fuel changes.

This month NASA will begin field testing of a Mod II engine in a U.S. postal van. The Mod II, which has fewer parts and weighs less than its predecessors, should improve the van's fuel efficiency by about 28 percent—from 23.1 to 29.6 miles per gallon.

With the kinematic engine technology as a base, NASA has expanded its research into free-piston Stirling engines, which could be used to generate electricity aboard NASA's planned Space Station. The free-piston Stirling has no contacting parts and is therefore less susceptible to wear than conventional engines.

While the free-piston Stirling will require years of research before it is commercially viable, the kinematic version is "ready right now for preproduction engineering by a manufacturer," according to Ernst. "We've taken the kinematic Stirling out of the laboratory and turned it into a practical engine with realistic applications," he said. "Today there are non-technical personnel driving Stirling-powered vehicles around the country as if they were out for a ride in the family car." □

The four-cylinder Mod II Stirling features three basic engine systems: First, the external heat system converts energy in the fuel to heat flux. Next, the hot engine system contains the working gas in a closed volume to transform this heat flux into a pressure wave that acts on the pistons. Finally, the cold engine/-drive system transfers piston motion to connecting rods and the reciprocating rod motion is converted to rotary motion by a crankshaft.

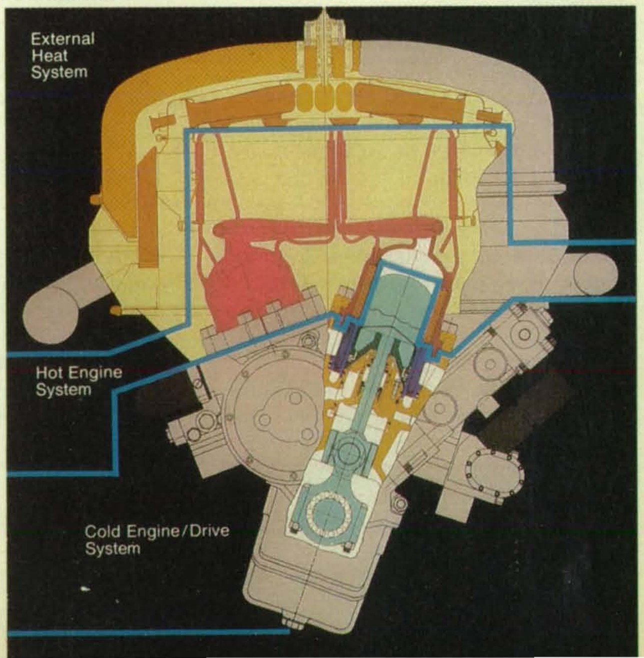

HOW YOU CAN BENEFIT FROM NASA's TECHNOLOGY UTILIZATION SERVICES

If you're a regular reader of TECH BRIEFS, then you're already making use of one of the low- and no-cost services provided by NASA's Technology Utilization (TU) Network. But a TECH BRIEFS subscription represents only a fraction of the technical information and applications/engineering services offered by the TU Network as a whole. In fact, when all of the components of NASA's Technology Utilization Network are considered, TECH BRIEFS represents the proverbial tip of the iceberg.

We've outlined below NASA's TU Network—named the participants, described their services, and listed the individuals you can contact for more information relating to your specific needs. We encourage you to make use of the information, access, and applications services offered by NASA's Technology Utilization Network.

How You Can Utilize **NASA's Industrial Applications Centers**—A nationwide network offering a broad range of technical services, including computerized access to over 100 million documents worldwide.

You can contact NASA's network of Industrial Applications Centers (IACs) for assistance in solving a specific technical problem or meeting your information needs. The "user friendly" IACs are staffed by technology transfer experts who provide computerized information retrieval from one of the world's largest banks of technical data. Nearly 500 computerized data bases, ranging from NASA's own data base to Chemical Abstracts and INSPEC, are accessible through the nine IACs located throughout the nation. The IACs also offer technical consultation services and/or linkage with other experts in the field. You can obtain more information about these services by calling or writing the nearest IAC. User fees are charged for IAC information services.

Aerospace Research Applications Center (ARAC)
Indianapolis Center for Advanced Research
611 N. Capitol Avenue
Indianapolis, IN 46204
Dr. F. Timothy Janis, Director
(317) 262-5036

Central Industrial Applications Center/NASA (CIAC)
Southeastern Oklahoma State U.
Station A, Box 2584
Durant, OK 74701
Dr. Dickie Deel, Director
(405) 924-6822

North Carolina Science and Technology Research Center (NC/STRC)
Post Office Box 12235
Research Triangle Park, NC 27709
H. Glenn Reese, Director
(919) 549-0671

NASA Industrial Applications Ctr. 823 William Pitt Union
University of Pittsburgh
Pittsburgh, PA 15260
Dr. Paul A. McWilliams, Exec. Director
(412) 648-7000

NASA/Southern Technology Applications Center
P. O. Box 24
Progress Ctr., One Progress Blvd.
Alachua, FL 32615
J. Ronald Thornton, Director
(904) 462-3913
(800) 354-4832 (FL only)
(800) 225-0308 (toll-free US)

NASA/UK Technology Applications Program
University of Kentucky
109 Kinkead Hall
Lexington, KY 40506-0057
William R. Strong, Director
(606) 257-6322

NERAC, Inc.
One Technology Drive
Tolland, CT 06084
Dr. Daniel U. Wilde, President
(203) 872-7000

Technology Application Center (TAC)
University of New Mexico
Albuquerque, NM 87131
Dr. Stanley A. Morain, Director
(505) 277-3622

NASA Industrial Applications Center (WESRAC)
University of Southern California Research Annex
3716 South Hope Street, Room 200
Los Angeles, CA 90007
Radford G. King, Exec. Director
(213) 743-8988
(800) 642-2872 (CA only)
(800) 872-7477 (toll-free US)

NASA/SU Industrial Applications Center
Southern University Department of Computer Science
Baton Rouge, LA 70813-9737
Dr. John Hubbell, Director
(504) 771-6272

If you represent a public sector organization with a particular need, you can contact NASA's Application Team for technology matching and problem solving assistance. Staffed by professional engineers from a variety of disciplines, the Application Team works with public sector organizations to identify and solve critical problems with existing NASA technology. **Technology Application Team, Research Triangle Institute, P.O. Box 12194, Research Triangle Park, NC 27709. *Doris Rouse, Director,* (919) 541-6980**

How You Can Access Technology Transfer Services At NASA Field Centers: **Technology Utilization Officers & Patent Counsels**—Each NASA Field Center has a Technology Utilization Officer (TUO) and a Patent Counsel to facilitate technology transfer between NASA and the private sector.

If you need further information about new technologies presented in *NASA Tech Briefs,* request the Technical Support Package (TSP). If a TSP is not available, you can contact the Technology Utilization Officer at the NASA Field Center that sponsored the research. He can arrange for assistance in applying the technology by putting you in touch with the people who developed it. If you want information about the patent status of a technology or are interested in licensing a NASA invention, contact the Patent Counsel at the NASA Field Center that sponsored the research. Refer to the NASA reference number at the end of the Tech Brief.

Ames Research Ctr.
Technology Utilization Officer: Laurance Milov
Mail Code 223-3
Moffett Field, CA 94035
(415) 694-4044
Patent Counsel: Darrell G. Brekke
Mail Code 200-11
Moffett Field, CA 94035
(415) 694-5104

Lewis Research Center
Technology Utilization Officer: Daniel G. Soltis
Mail Stop 7-3
21000 Brookpark Road
Cleveland, OH 44135
(216) 433-5567
Patent Counsel: Gene E. Shook
Mail Code 301-6
21000 Brookpark Road
Cleveland, OH 44135
(216) 433-5753

John C. Stennis Space Center
Technology Utilization Officer: Robert M. Barlow
Code GA-00
Stennis Space Center, MS 39529
(601) 688-1929

John F. Kennedy Space Center
Technology Utilization Officer: Thomas M. Hammond
Mail Stop PT-TPO-A
Kennedy Space Center, FL 32899
(407) 867-3017
Patent Counsel: James O. Harrell
Mail Code PT-PAT
Kennedy Space Center, FL 32899
(407) 867-2544

Langley Research Ctr.
Technology Utilization Officer: John Samos
Mail Stop 139A
Hampton, VA 23665
(804) 865-3281
Patent Counsel: George F. Helfrich
Mail Code 279
Hampton, VA 23665
(804) 865-3725

Goddard Space Flight Center
Technology Utilization Officer: Donald S. Friedman
Mail Code 702
Greenbelt, MD 20771
(301) 286-6242
Patent Counsel: R. Dennis Marchant
Mail Code 204
Greenbelt, MD 20771
(301) 286-7351

Jet Propulsion Lab.
NASA Resident Office
Technology Utilization Officer: Gordon S. Chapman
Mail Stop 180-801
4800 Oak Grove Drive
Pasadena, CA 91109
(818) 354-4849
Patent Counsel: Paul F. McCaul
Mail Code 180-801
4800 Oak Grove Drive
Pasadena, CA 91109
(818) 354-2734
Technology Utilization Mgr. for JPL: Norman L. Chalfin
Mail Stop 156-211
4800 Oak Grove Drive
Pasadena, CA 91109
(818) 354-2240

George C. Marshall Space Flight Center
Technology Utilization Officer: Ismail Akbay
Code AT01
Marshall Space Flight Center, AL 35812
(205) 544-2223
Patent Counsel: Leon D. Wofford, Jr.
Mail Code CC01
Marshall Space Flight Center, AL 35812
(205) 544-0024

Lyndon B. Johnson Space Center
Technology Utilization Officer: Dean C. Glenn
Mail Code IC-4
Houston, TX 77058
(713) 483-3809
Patent Counsel: Edward K. Fein
Mail Code AL3
Houston, TX 77058
(713) 483-4871

NASA Headquarters
Technology Utilization Officer: Leonard A. Ault
Code CU
Washington, DC 20546
(202) 453-2119
Assistant General Counsel for Patent Matters: Robert F. Kempf, Code GP
Washington, DC 20546
(202) 453-2424

A Shortcut To Software: **COSMIC®**—For software developed with NASA funding, contact COSMIC, NASA's Computer Software Management and Information Center. New and updated programs are announced in the Computer Programs section. COSMIC publishes an annual software catalog. For more information call or write: **COSMIC®** 382 East Broad Street, Athens, GA 30602 *John A. Gibson, Dir.,* (404) 542-3265

If You Have a Question . . . **NASA Scientific & Technical Information Facility** can answer questions about NASA's Technology Utilization Network and its services and documents. The STI staff supplies documents and provides referrals. Call, write or use the feedback card in this issue to contact: **NASA Scientific and Technical Information Facility,** Technology Utilization Office, P.O. Box 8757, Baltimore, MD 21240-0757. *Walter M. Heiland, Manager,* (301) 859-5300, Ext. 242, 243

THE CHALLENGE: "MACHINE HIGHLY COMPLEX AEROSPACE COMPONENTS WITH PRECISE REPEATABILITY. AND REDUCE COSTS SIGNIFICANTLY."

We were able to meet this challenge because at Howmet we work closely with our customer-partners. Our engineer-to-engineer approach allows us to take charge from concept through prototype to finished product and provide our customers with capabilities our competitors can't match.

ECM equipment is integrated with customer CAD/CAM data.

GREATER DESIGN FREEDOM AND COST EFFECTIVENESS. At our New England Aircraft Products Division, in Farmington, CT, we produce airfoils up to 14" in length by electrochemical machining (ECM). As a "stress-free" process, ECM permits thinner, more complex shapes which are otherwise extremely costly or impossible to manufacture. And our CAD/CAM technology permits your design to be duplicated precisely. With no final polishing required and a low scrap rate, manufacturing costs are reduced as much as 10%.

Howmet's Winsted Machining Center, in Winsted, CT, specializes in small to medium airfoils. Our state-of-the-art encapsulation system and CNC continuous dress creep feed grinders triple the removal rates while improving accuracy and throughput.

At Whitehall, MI, our Whitehall Machining Division specializes in medium to large airfoils and integral nozzles and rotors. We also run small lots and prototype work, offering fast turn time and low cost for special needs. Our creep feed grinders reduce machining time while increasing precision and flexibility.

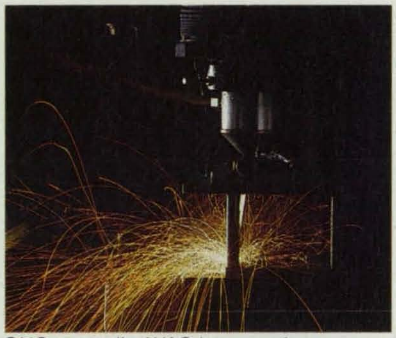

CNC-controlled YAG laser performs cutting, welding and drilling.

IMPOSSIBLE? CHALLENGE US. At Howmet, we employ the most advanced technologies to meet the strict requirements of our customer-partners. We will work closely with you, engineer to engineer, to

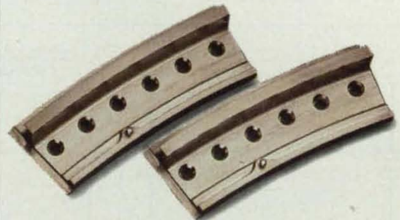

These retainer plates are typical of our precision-machined hardware.

bring your product cost-effectively from prototype work into production. For more information on our machining capabilities, write our Sales Department, Howmet Corporation, 475 Steamboat Road, Greenwich, CT 06836-1960. Or phone the Sales Manager at New England Aircraft Products Division, (203) 677-1376, Whitehall Machining Division, (616) 894-5686, or Winsted Machining Center, (203) 379-3314.

HOWMET CORPORATION

Partners. Challenge by Challenge.

New England Aircraft Products Division, Farmington, CT
Whitehall Machining Division, Whitehall, MI
Winsted Machining Center, Winsted, CT

ECM'd fan and compressor blades for P&W jet engines.

Circle Reader Action No. 335

Switching Voltage Regulator

Both pulsed and continuous outputs are available.

NASA's Jet Propulsion Laboratory, Pasadena, California

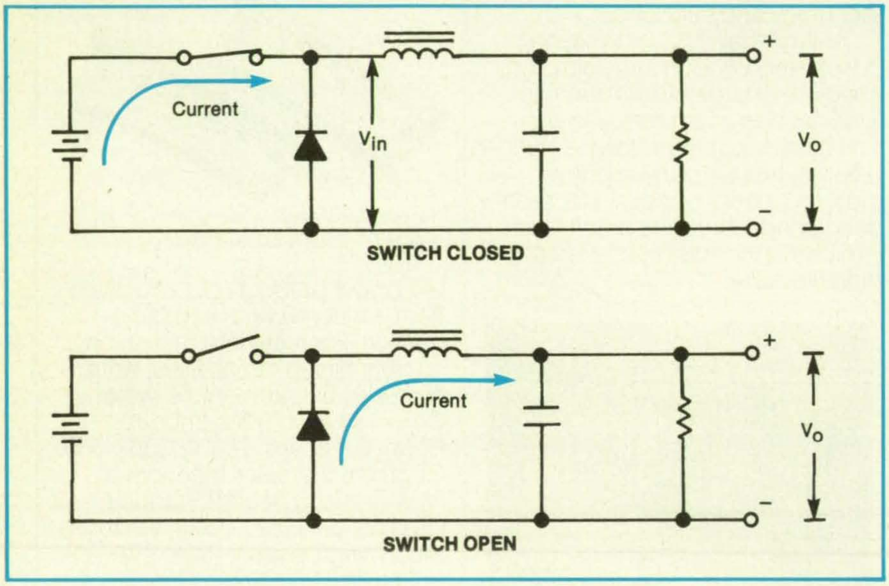

A switching power-supply circuit converts the input power from two 9-V batteries in series to an output of 5 Vdc regulated within 1.5 percent, either at a continuous current of 5 mA or at a current of 500 mA in 0.5-s pulses at 1-min intervals. The power supply operates for at least 100 h on a pair of batteries. It is at least 50 percent efficient at a 5-mA load and 76 percent efficient at a 500-mA load.

Figure 1. This **Simplified Schematic Diagram** illustrates the principle of operation—inductive and capacitive filtering of controlled pulses of battery voltage.

Figure 2. This **Power Supply** converts unregulated 12- to 18-Vdc input to regulated 5-Vdc output.

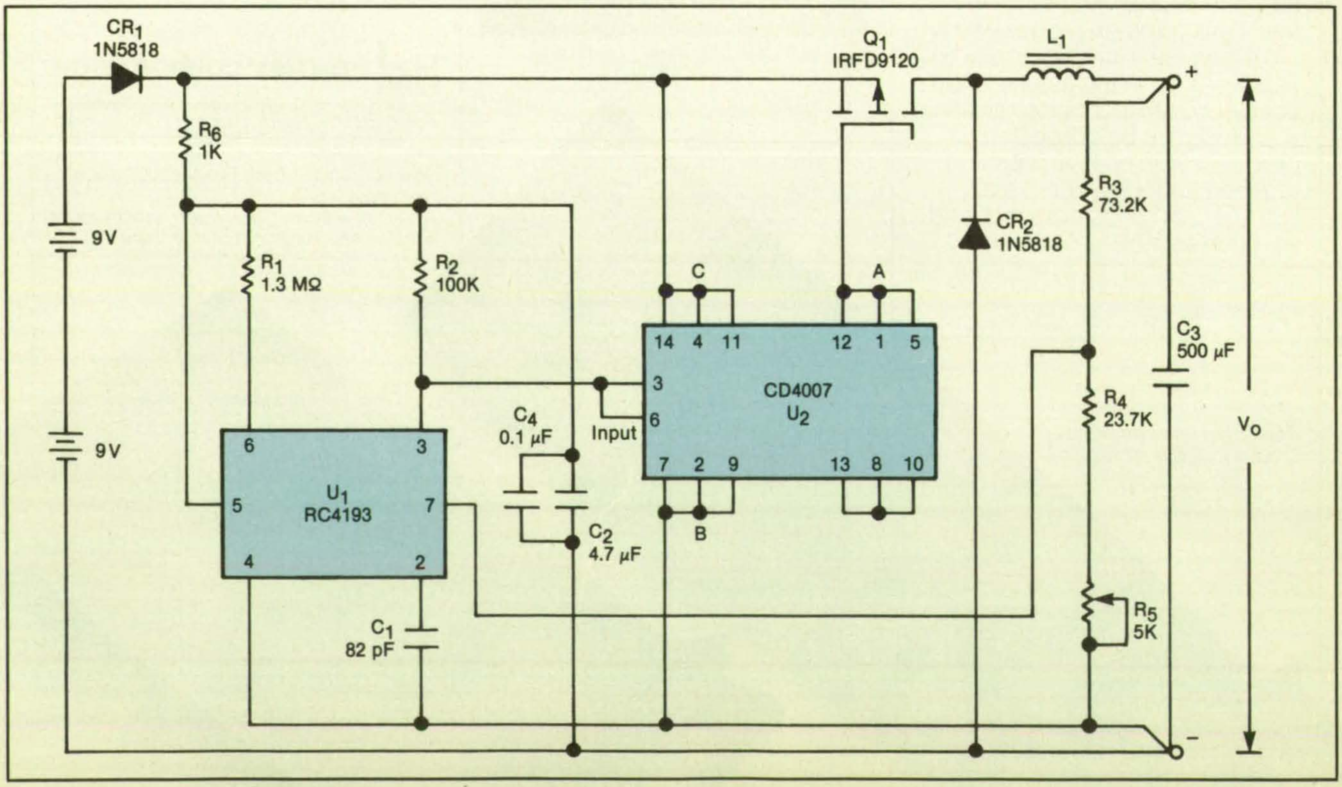

The power supply is essentially a buck converter (see Figure 1). An electronic switch alternately connects the battery to and disconnects it from the input end of an inductor-and-capacitor filter. The inductor suppresses the input current transients, and the capacitor suppresses the output voltage transients. Provided that the switching frequency is much greater than the resonant frequency of the inductor-and-capacitor combination, the average dc output voltage V_o in the steady state is given approximately by

$$V_o = DV_{in}$$

where D = the duty cycle (the fraction of the switching cycle during which the switch is closed), and V_{in} = the input voltage (the battery voltage minus any voltage drop in the switching circuit).

The power supply (see Figure 2) maintains V_o nearly constant even though V_{in} decreases as the batteries are used up; it does this by sensing V_o and adjusting D accordingly. A voltage proportional to V_o is coupled to micropower switching-regulator integrated circuit U_1 via sensing resistors R_3, R_4, and R_5. Voltage V_o is set by choosing the ratio $R_3/(R_4 + R_5)$, and R_5 is adjusted to compensate for the tolerance in an internal Zener-diode voltage reference and associated components in U_1.

Circuit U_1 contains an oscillator, the frequency of which (of the order of 30 kHz) is determined in part by C_1. The sensed voltage on terminal 7 is compared with the internal reference voltage; the difference between them controls the duty cycle of a pulsed version of the oscillator signal at output terminal 3.

Transistor Q_1 is the power switch at the input end of inductor L_1. Integrated circuit U_2 serves as an analog multiplexer that alternately connects the gate of Q_1 to the negative side of the battery or to the source of Q_1, under the control of the output of U_1. Thus, pulses of battery voltage are applied to L_1 at the oscillator frequency and at a duty cycle controlled by V_o.

Inductor L_1 and capacitor C_3 must be chosen carefully to cope with transient loads and to remain within specified limits on size and weight. In this case, L_1 was chosen to be a swinging choke (a nonlinear inductor); as the current increases from light to heavy loads (from 5 to 500 mA), the core of L_1 saturates, causing the inductance to decrease from about 400 mH to 100 mH. Although a linear version of L_1 could be used, tests show that the nonlinear version responds better to transient loads.

This work was done by Colonel W. T. McLyman of Caltech for **NASA's Jet Propulsion Laboratory**. *For further information, Circle 42 on the TSP Request Card. NPO-16889*

Contactless Coupling for Power and Data

The alignment of this flat-plate interface is not critical.

Goddard Space Flight Center, Greenbelt, Maryland

An experimental flat-plate coupling transmits digital data signals and electrical power across a small gap between two modules. Unlike multiple-pin electrical connectors, the two halves of the coupling do not have to be aligned precisely for mating; thus, the coupling concept may be a useful substitute for electrical connectors in equipment that has to be assembled by robots, remote manipulators, or humans working in protective clothing or otherwise restricted in dexterity.

The coupling includes a power transformer operating at a frequency of 20 kHz. Each of the mating modules contains half of the pot-shaped core of the transformer and a spiral winding (see figure). Two versions have been built: one to transfer

When the call to TDRSS doesn't go through...

there's no getting your dime back.

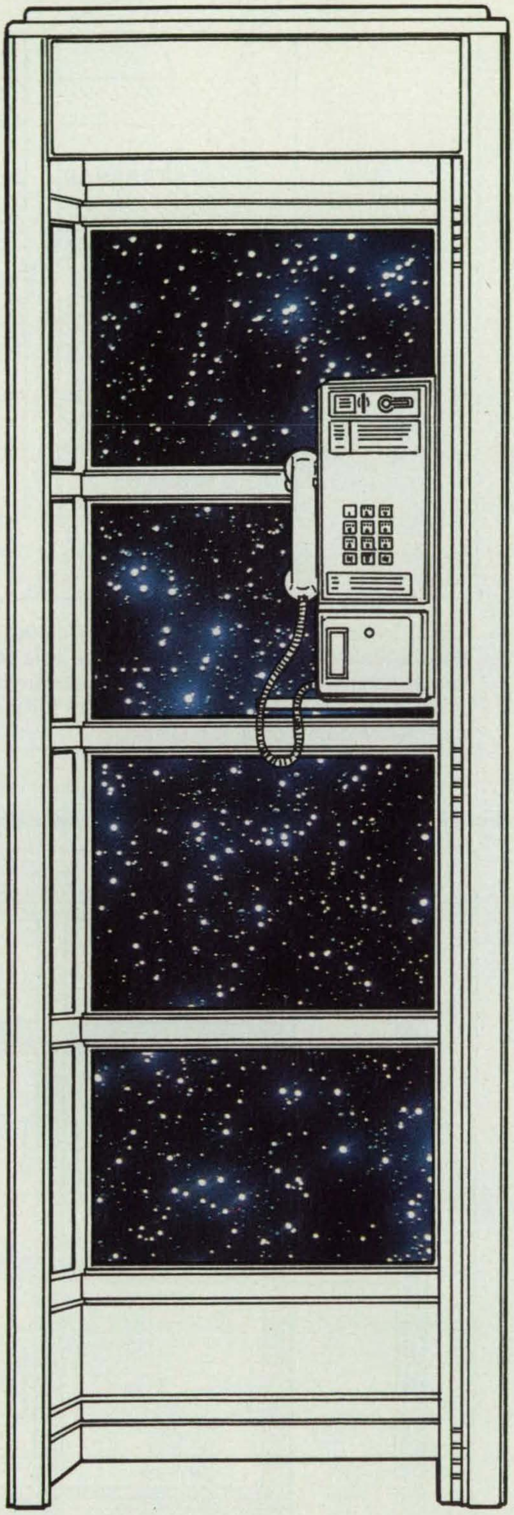

System availability and reliability are the big issues for NASA as it acquires its Second TDRSS Ground Terminal (STGT). Delivery of data to users depends on it.

The Nation's commitment is too great to demand anything less than the objective NASA has established: 0.9999 availability. That's why GE is competing to build STGT; we can respond to the challenge. That's why GE is proposing an all-new distributed data system architecture for reliable operations.

We've designed for low life cycle cost too, by significant reductions in equipment and personnel—to be achieved in hardware, automated operations and proven command and control concepts from current successful programs.

And we've made the human, financial and technical commitment to deliver to NASA on time and within cost.

As the first user of TDRSS, we know how vital STGT is. So, while offering the technical solution that NASA asked for, we're more than just a supplier. We've been there.

STGT will play a key role in Earth/Space communications for years to come...and GE is committed to making 0.9999 availability a reality.

GE Aerospace

Ground Systems Department
Valley Forge, Pennsylvania

Circle Reader Action No. 556

STGT-1

100 W of power, the other to transfer 1,000 W.

The transformer is designed to operate at maximum efficiency with a gap of 10 to 20 mils (0.25 to 0.5 mm) between the halves of the core. This eliminates the need to force the halves into contact and thereby also minimizes wear of the mating surfaces. The 100-W version of the transformer has been tested for its performance with various gaps, lateral displacements, and angular misalignments. Within the tolerance range, the transformer exhibits an efficiency as high as 97 percent.

The data-transmission system includes light-emitting diode (LED) transmitters, positive/intrinsic/negative (PIN) diode receivers, and Motorola (or equivalent) emitter-coupled-logic supporting electronic circuitry. The transmitting and receiving diodes are equipped with lenses that give some divergence to the transmitted light beam and field of view, respectively. Consequently, the digital-signal coupling also has some tolerance to separations and misalignments. The data-transmission system has been tested with a 50-MHz signal representative of a 100-Mb/s nonreturn-to-zero pulse code.

This work was done by John C. Moody and Joseph W. Foley of OAO Corp. for **Goddard Space Flight Center**. *No further documentation is available. GSC-13059*

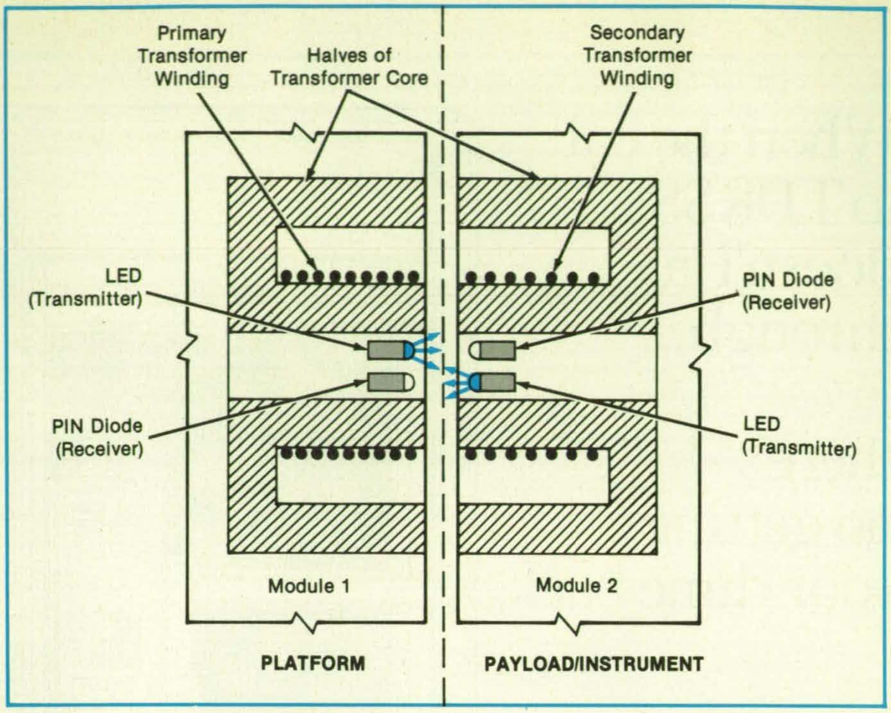

A **Split Transformer and Optoelectronic Components** transmit electrical power and digital signals, respectively, across a small gap. This coupling would be useful in robotically assembled equipment because it tolerates some misalignment. The coupling offers also higher reliability due to one overall alignment mechanism as opposed to multiple pin/socket alignment requirements.

Multiple-Coil, Pulse-Induction Metal Detector

A large area is scanned rapidly.

John F. Kennedy Space Center, Florida

A multiple-head, pulse-induction metal detector scans an area of 72 ft^2 (6.7 m^2) with a combination of eight detector heads, each 3 ft (0.9 m) square. The new detector, designed for the recovery of Space Shuttle debris, replaces an earlier version that had only one 3-ft-square head and that was based on the tuned-coil principle.

In the tuned-coil principle, the resonant frequency of the coil in the detector head is changed by the detected metal. This principle is not suitable for a multiple-head detector because each head would have to be tuned to a different frequency, and this would entail an impractically large bandwidth. However, the pulse-induction method used in the new detector is suitable for multiplexed operation and does not impose a severe bandwidth requirement.

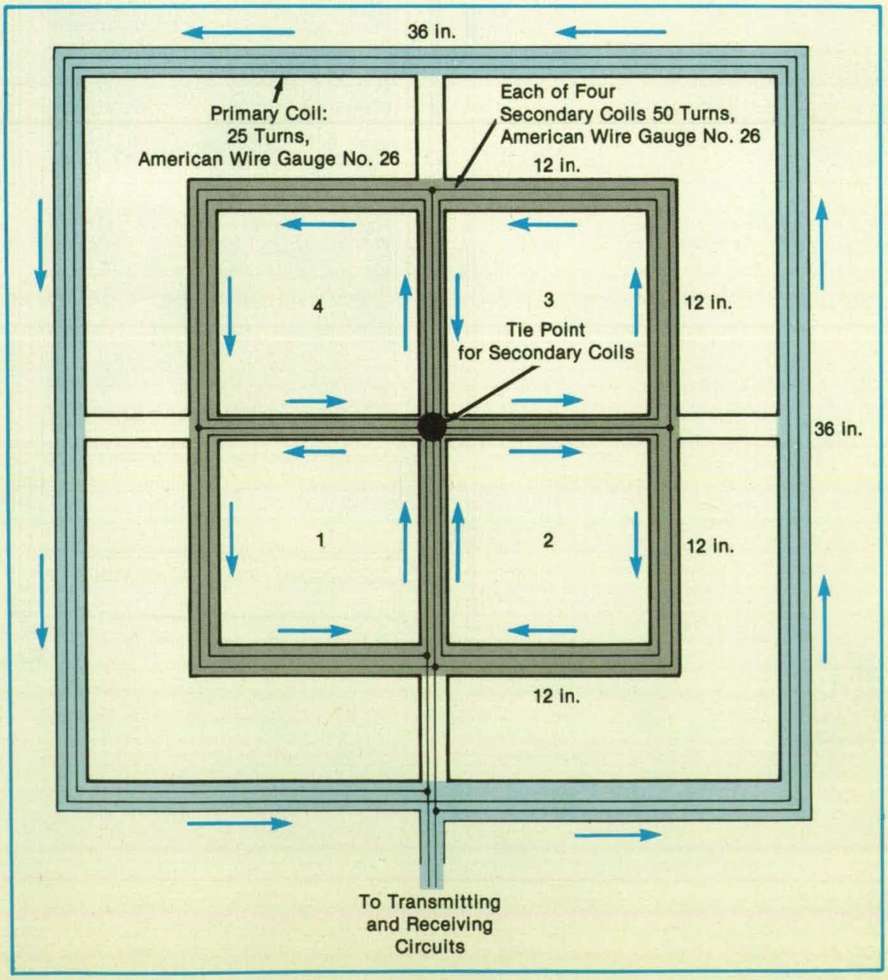

Figure 1. A **Detector Head** includes a large primary coil that induces current in the smaller secondary coils. An array of eight such heads enables a searcher to cover a large area relatively quickly.

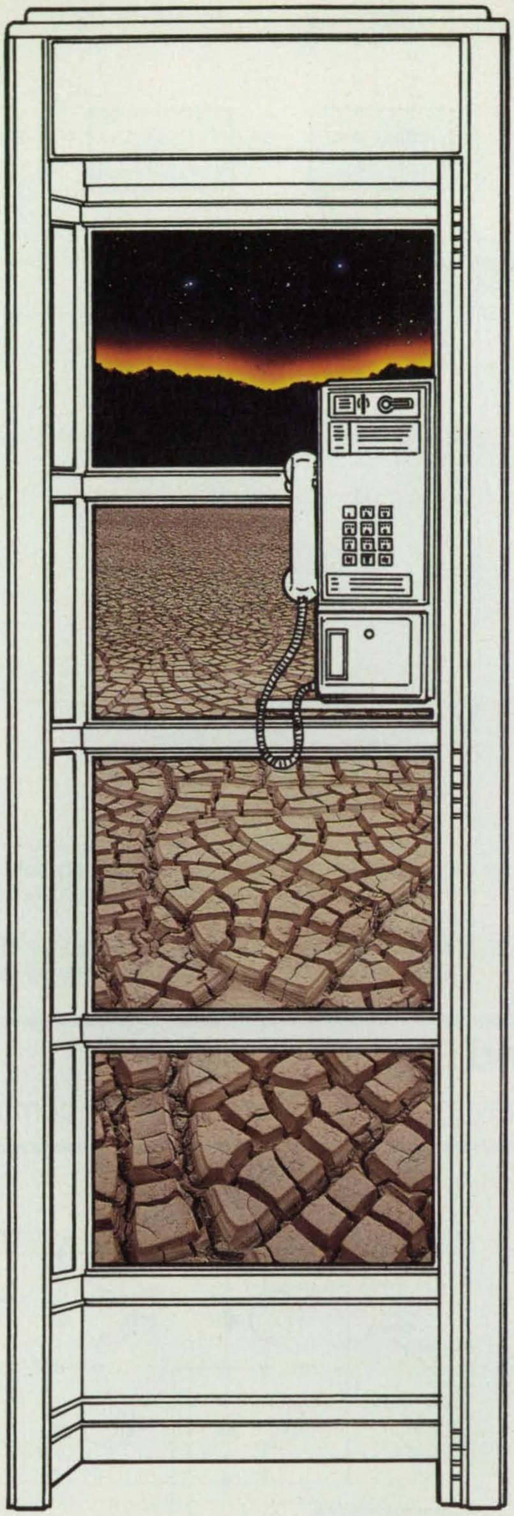

Each detector head (see Figure 1) includes a large, square primary (transmitting) coil, within which are located four smaller secondary (receiving or sensing) coils. The four sensing coils are connected in parallel in such a way that three of them aid the primary-coil induction and one of them opposes it.

An oscillator having a frequency of 250 Hz switches a solid-state relay (see Figure 2) with a voltage of about 8 V. The relay generates a positive voltage pulse for the primary coils every 2 ms. For multiple-head operation, a sequential counter sends the pulses to each detector head in turn. The pulsed current in each primary coil induces a voltage in its secondary coils. This voltage is amplified, rectified, and compared with a reference dc voltage that corresponds to no metal in the detector field.

When metal is present in the detector field, the secondary-coil voltage deviates from the reference level. A departure of ±5 mV from the reference level causes the comparator to saturate at about 13 V output. The comparator output causes a driver to apply power to an indicator. In tests, the detector indicated a 3- by 3-in. (7.6- by 7.6-cm) box 17 in. (43 cm) from the detector head and a 7- by 12-in. (18- by 30-cm) box up to 24 in. (61 cm) from the detector head.

This work was done by Edward S. Lesky, Alan M. Reid, Wilton E. Bushong, and Duane P. Dickey of **Kennedy Space Center**. *No further documentation is available.*

Inquiries concerning rights for the commercial use of this invention should be addressed to the Patent Counsel, Kennedy Space Center [see page 18]. Refer to KSC-11386.

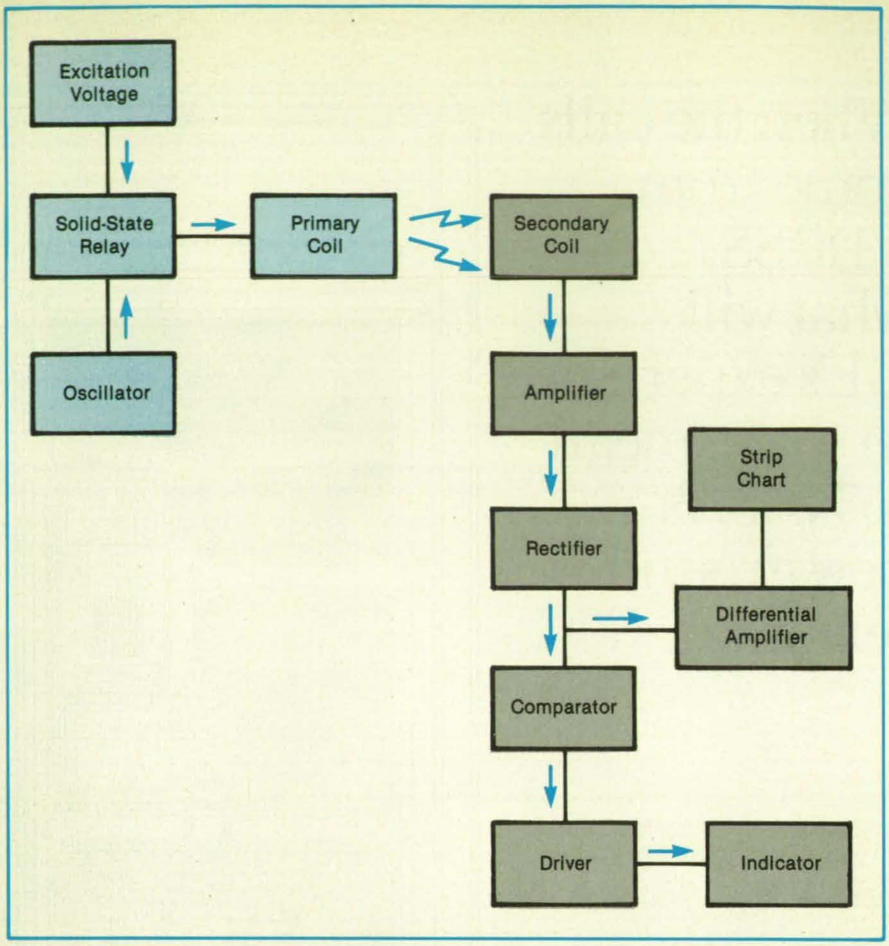

Figure 2. **Pulses Are Applied** to the primary coil, and the pulses induced in the secondary coils are measured to determine whether metal is present within the range of the detector head.

Integrated Inverter and Battery Charger

A dual-function circuit would obviate duplication of electrical components and structural parts.

NASA's Jet Propulsion Laboratory, Pasadena, California

A proposed circuit would combine the functions of dc-to-ac inversion (for driving an ac motor in a battery-powered vehicle) and ac-to-dc conversion (for charging the battery from an ac line when the vehicle is not in use). The circuit would automatically adapt to either mode; there is no need to set switches and relays or disconnect cables.

The design of the integrated inverter/charger would eliminate the need for duplicate components, save space, and reduce the weight and cost of the vehicle. It would offer similar advantages in such other applications as load-leveling systems, standby ac power systems, and uninterruptible power supplies.

The circuit would include a three-phase bridge inverter employing pulse-width modulation, an input capacitor, a line filter, a line rectifier, and control circuitry (see figure). For inverter operation, the controller would switch transistors Q_1 through

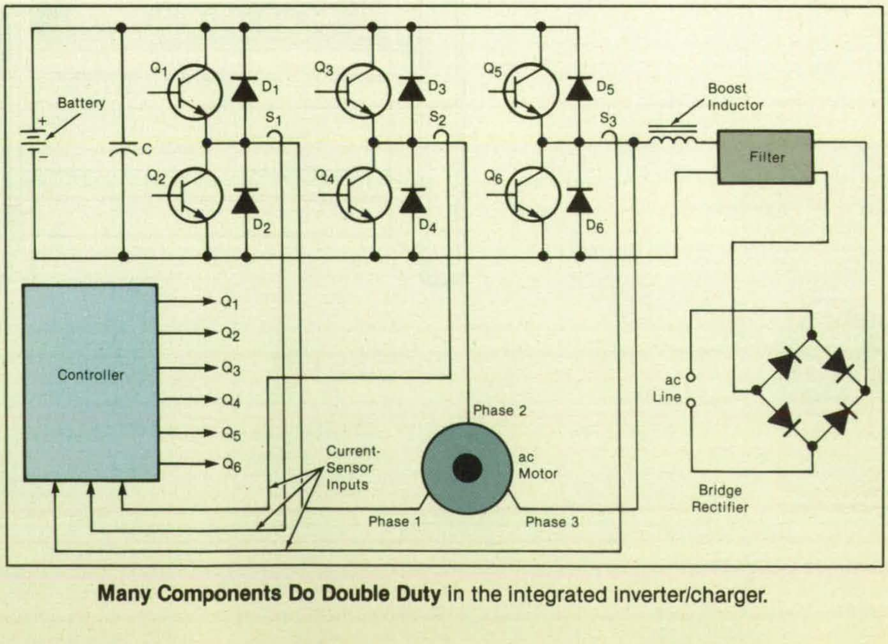

Many Components Do Double Duty in the integrated inverter/charger.

Q_6 so that voltages and currents of the appropriate magnitude, frequency, and phase would be applied to the motor. Regenerative and reactive currents would be returned to the input capacitor C and the battery by the six antiparallel diodes D_1 through D_6.

The input capacitor would isolate ac components from the battery, acting as a filter that has an impedance to transients lower than that of the battery. The input capacitor would also supply the inverter current pulses to drive the motor, drawing power from the battery on a steady, averaged basis rather than in pulses. Sensors S_1, S_2, and S_3 would measure the currents of the three phases for the controller.

For operation in the charging mode, the controller would modulate the duty cycle of transistors Q_6 to transfer power from the ac line, through the rectifier bridge, the filter, the boost inductor, and diode D_5 to the battery. The controller would act so that the instantaneous line current would be proportional to the instantaneous line voltage; that is, the circuit would operate at a power factor of 1. As in inverter operation, the input capacitor would isolate the battery from transients. The filter would isolate the ac line from the high-frequency components of the modulation pulses. Sensor S_3 would provide a charging-current signal to the controller.

While the battery is being recharged, the controller would keep the other transistors in the off state. Therefore no currents would enter the motor even though a voltage is present at the junction of D_5 and Q_6, because there would be no return paths. The motor would not have to be disconnected during recharging.

The leakage inductance of the motor could be used in place of the boost inductor. The low value of this inductance allows some ripple in the charging current, but the ripple would not be objectionable at the high charging rates that are likely to be used to recharge vehicles quickly. If the ripple were too high for the application, the discrete boost inductor could be retained in the circuit.

Many electrical components could be shared by the inverter and charger portions of the integrated inverter/charger. Other parts that would not have to be duplicated include the battery-connector plug, bus connections, heat sinks, cooling fan, housing, and supporting structure.

This work was done by Wally E. Rippel of Caltech for **NASA's Jet Propulsion Laboratory**. *For further information, Circle 89 on the TSP Request Card.*

Inquiries concerning rights for the commercial use of this invention should be addressed to the Patent Counsel, NASA Resident Office-JPL [see page 18]. Refer to NPO-17133.

Solid-State Single-Photon Counter

Under the right conditions, an avalanche photodiode performs better than a photomultiplier tube.

NASA's Jet Propulsion Laboratory, Pasadena, California

A commercial avalanche photodiode can be used to detect single photons if it is cooled to an optimum temperature and overbiased beyond its breakdown voltage. Avalanche photodiodes used in this mode offer two to three times the sensitivity of the photomultiplier tubes commonly used for photon detection. Moreover, they are not subject to the disadvantages of photomultipliers: low quantum efficiency, fragile vacuum-tube packages, and anode potentials of about 1,600 V. Avalanche photodiodes thus bring the advantages of solid-state devices to a variety of applications requiring low-level light detection; for example, optical communication, astronomy, remote sensing, optical metrology, and optical signal processing.

When cooled to reduce the number of thermal carriers, an avalanche photodiode can be reverse-biased beyond its normal breakdown voltage to give it an extremely-high internal gain of 10^7 to 10^8. The performance characteristics of an avalanche photodiode as functions of temperature and voltage were studied in a set of experiments and compared with those of a photomultiplier tube.

An avalanche photodiode was mounted on a cold stage in a small evacuated refrigerator and connected to an external quenching circuit (see figure). The photomultiplier tube, which had a gallium arsenide photocathode sensitive to infrared, was cooled to −30 °C in a separate thermoelectric refrigerator. The light from a laser diode at a wavelength of 822 nm was directed at both detectors.

A calibrated beam splitter directed a known fraction of the laser light to an optical-power meter to enable the determination of the level of light incident on the detectors. Calibrated neutral-density filters attenuated the laser light to a few photons per pulse. A second beam splitter divided the beam between the avalanche photodiode and the photomultiplier tube.

The light source produced 50-ns pulses at a rate of 15 kHz. Corresponding voltage pulses from the light source gated a logic circuit so that it transmitted the avalanche-photodiode counts during a laser pulse ("true" counts) or those during the dark period between pulses ("false" counts), or all counts.

The photomultiplier tube measured the beam intensity after attenuation. From this measurement, the quantum efficiency of the photomultiplier, and the efficiencies of the optical components, the intensity of the light incident on the avalanche photodiode was calculated. Detection probabilities were calculated from this intensity and from the measured number of events detected by the avalanche photodiode.

The optimum temperature for the avalanche photodiode was found to be 200 K. At this temperature and an overbias of 1.5 V (Breakdown voltage was about 175 V.), the single-photon detection probability was 27 percent, compared with 12

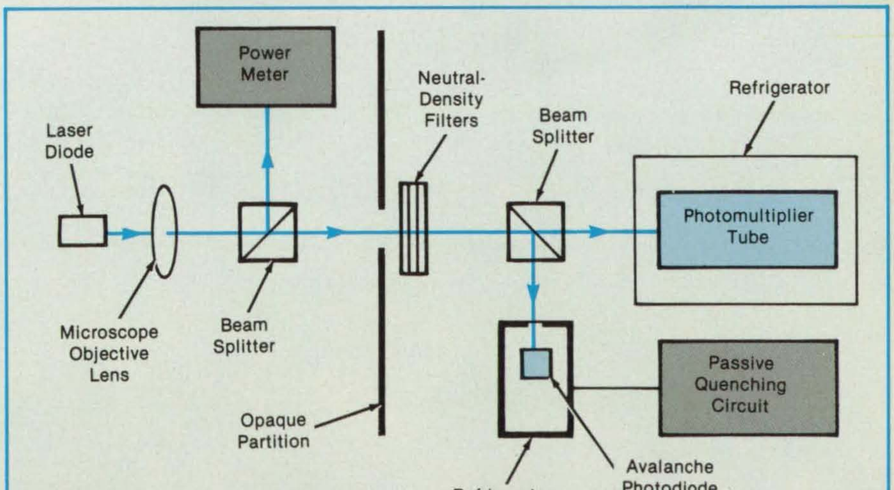

The sensitivity of the **Avalanche Photodiode** was measured by comparing with the known sensitivity of a photomultiplier tube. The data were collected and reduced by a pair of time-interval counters, a storage oscilloscope, and a microcomputer.

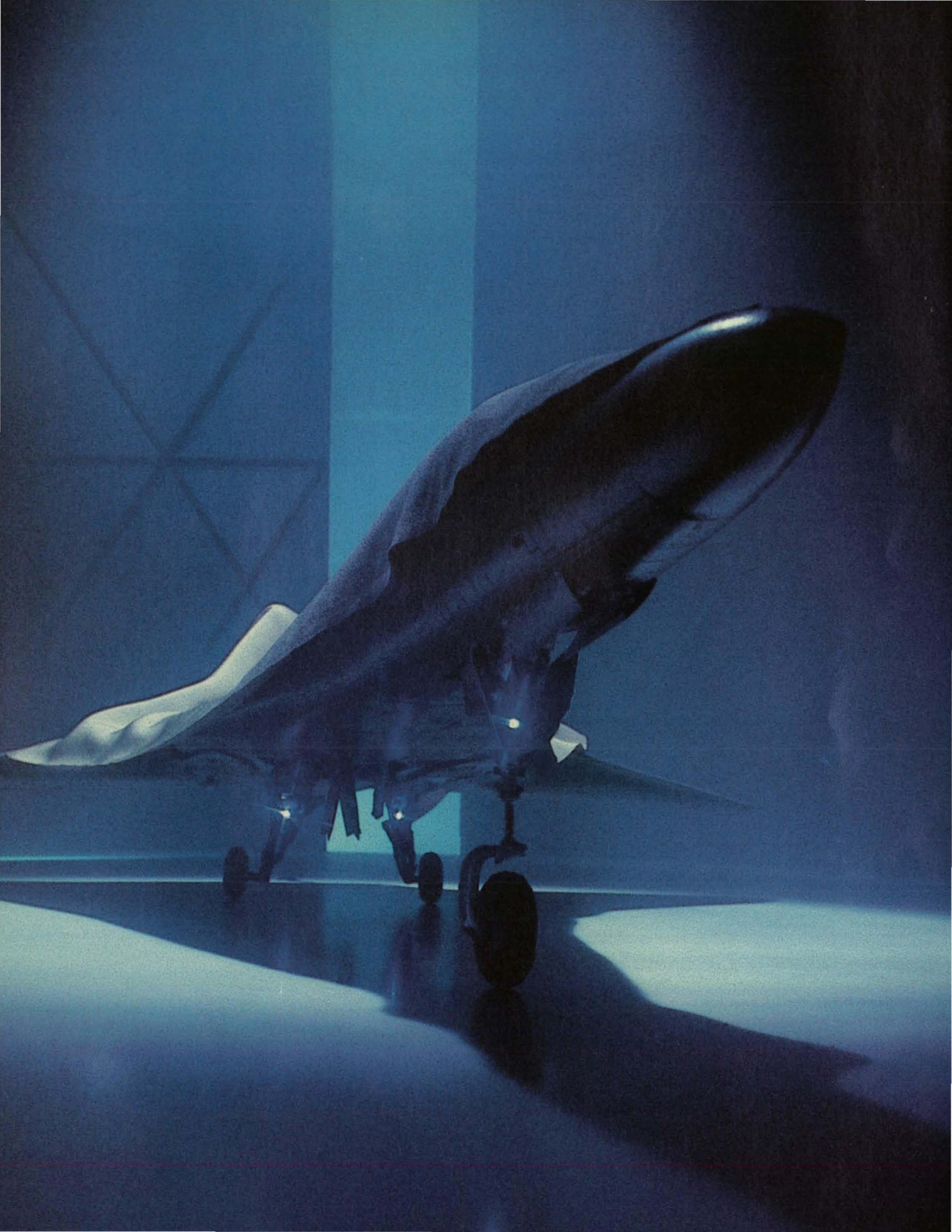

percent for the photomultiplier operating at −30 °C and an anode potential of 1,600 V. The probability increased to 50 percent when the overbias was raised to 10 V, but the dark count also increased, nearly equaling the true count.

This work was done by D. L. Robinson and B. D. Metscher of Caltech for **NASA's Jet Propulsion Laboratory**. *For further information, Circle 45 on the TSP Request Card.*
NPO-17103

Books and Reports

These reports, studies, handbooks are available from NASA as Technical Support Packages (TSP's) when a Request Card number is cited; otherwise they are available from the National Technical Information Service.

Bipolar-Battery Construction

The components are configured so that the processing steps can be automated.

Bipolar batteries can be fabricated in a continuous quasi-automated process. The components of the battery are configured so that the processing steps can be run sequentially. The key components of the battery, the bipolar plate and bipolar separator, are fabricated separately and are later joined together.

The sequential steps of the process are cutting, masking, etching, plating, folding, and sealing the bipolar plates; inserting bipolar separators; and then compressing, binding, and filling the combination with electrolyte. The assembly of successive battery plates can expand and contract to compensate for thermal and mechanical stresses and volume changes.

This work was done by Wally E. Rippel and Dean B. Edwards of Caltech for **NASA's Jet Propulsion Laboratory**. *For further information, Circle 81 on the TSP Request Card.*

Title to this invention has been waived under the provisions of the National Aeronautics and Space Act [42 U.S.C. 2457(f)], to the California Institute of Technology. Inquiries concerning licenses for its commercial development should be addressed to

Edward Ansell
Director of Patents and Licensing
Mail Stop 301-6
California Institute of Technology
1207 East California Boulevard
Pasadena, CA 91125

Refer to NPO-15315, volume and number of this NASA Tech Briefs issue, and the page number.

Electronic Systems

Asynchronous Communication Scheme for Hypercube Computer

Average delays are reduced.

NASA's Jet Propulsion Laboratory, Pasadena, California

A generalized scheme has been devised for an asynchronous-message communication system for the Mark III hypercube concurrent-processor network. The scheme is intended to support applications that require the passage of both polled or solicited and unsolicited messages.

The network may consist of up to 1,024 processing elements connected electrically as though they were at the corners of a 10-dimensional cube. Each node contains two Motorola 68020 processors along with the Motorola 68881 floating-point processor utilizing up to 4 megabytes of shared dynamic random-access memory.

The primary goal in designing the software for the communication system is to take advantage of the highly parallel architecture of each node, allowing the main processor to proceed with computations while the input or output is in progress. Secondary goals include offering both packet switching (for single-packet messages) and virtual-circuit switching (pipelining of paths for multipacket messages), along with the ability to expand and reconfigure to support various applications specified by the user.

The scheme includes a regular-message-transfer and a fast-message-transfer mode for communication between nodes. It also addresses such issues as control of the flow of messages, routing, buffering, detection and correction of collisions, and the control of congestion to prevent deadlock.

In the regular transfer mode (for single-packet messages), a single-packet message is transferred from the shared memory to the local transmitting buffer in the communication processor and is subsequently transmitted in the regular packet-switched mode to its eventual destination along one of the available paths. This path is determined by reference to the message-routing table to locate an available outbound channel.

Each intermediate node that receives the single-packet message either forwards the packet along the forward path if any one of the alternate channels is available or else returns (backtracks) the packet to the last forwarding node that sent this packet. The last forwarding node then reroutes the packet along a different path.

In the fast-message-transfer mode (to be used for multipacket messages), the communication processor starts the process of setting up a path (virtual circuit) to the destination node by using the message-routing table to determine the outbound channels. The technique of setting up a path prior to the transfer of data is called the prior-notification-of-intended-message-transfer/path-validation process and is particularly useful for long messages. Each of the successive intermediate nodes then establishes the path by pipelining the inbound channel-number specification to the outbound channel-number specification by use of a path-setup/reference table in the local memory of each node. At each node, a reverse path is also set up simultaneously for an end-to-end acknowledgment from the destination node.

The destination node attempts to allocate the requisite memory, then responds with an acknowledgment/error packet back to the source along the reverse path. Next, the forward path is confirmed at all intermediate nodes, and the source node is notified to transmit the multipacket message. Meanwhile, the reverse path is deallocated at all the intermediate nodes soon after the acknowledgment. All intermediate nodes en route to a given destination simply perform a direct-memory-access transfer of data, thus speeding up the data-transfer process by an order of magnitude. The pipelined path in each path-setup/reference table is destroyed when the requisite numbers of bytes have been transferred.

The effects of the communication on an 8-node and on a 16-node hypercube processor were examined in simulations performed on a VAX 11/780 computer. Among other things, the simulation showed that the average delay per packet is less for pipelined messages than it is for packet-switched messages (see figure). The optimal message size for which pipelining reduces the overhead below that of pure packet switching is in excess of 256 bytes.

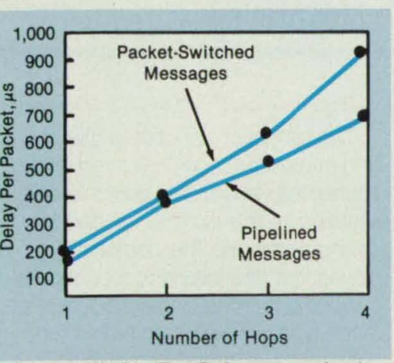

The Average End-to-End Delay per packet increases with the number of hops. This plot was obtained by simulations of the transmission of multipacket messages with an average size of 512 bytes.

This work was done by Herb S. Madan of Caltech for **NASA's Jet Propulsion Laboratory**. *For further information, Circle 53 on the TSP Request Card.*

This invention is owned by NASA, and a patent application has been filed. Inquiries concerning nonexclusive or exclusive license for its commercial development should be addressed to the Patent Counsel, NASA Resident Office-JPL [see page 18]. Refer to NPO-16860.

Force-Balance Dynamic Display

Six dynamic signals are simultaneously monitored on a single-trace oscilloscope.

Langley Research Center, Hampton, Virginia

A balance dynamic display unit (BDDU) is a compact system that conditions six dynamic analog signals so that they can be monitored simultaneously in real time on a single-trace oscilloscope. The instrument was originally designed to monitor the output of a strain-gauge force balance that measures the aerodynamic forces and moments generated about the three orthogonal axes of a model in a wind tunnel. The system features two display modes that are usable with a conventional, single-channel oscilloscope: a multiplexed six-channel "bar-graph" format and a single-channel display. A two-stage visual and audible limit alarm is provided for each channel.

The BDDU accurately monitors, multiplexes, and displays signals in the input range of ±100 mV to ±1 V at frequencies from 0 to 7,000 Hz. Sensitivity and zero-balance adjustments are provided for each channel. For full-scale input, the normalized output is 1 Vdc to both the oscilloscope and the individual buffered outputs. The six normalized buffered outputs provide access for additional recording or analyzing instrumentation.

In the scan mode (see figure), the six multiplexed signals appear as a single trace, on which each channel occupies one-sixth of the total trace width. This mode enables a quick visual overview of the total static and dynamic loads being applied in all axes. In the select mode, a single channel is displayed on the oscilloscope, and the average dc level is displayed on an integral digital panel meter. The BDDU has a thumbwheel switch that enables the selection of any channel for display on the oscilloscope for detailed viewing of any aspect of the signal by use of the normal oscilloscope functions.

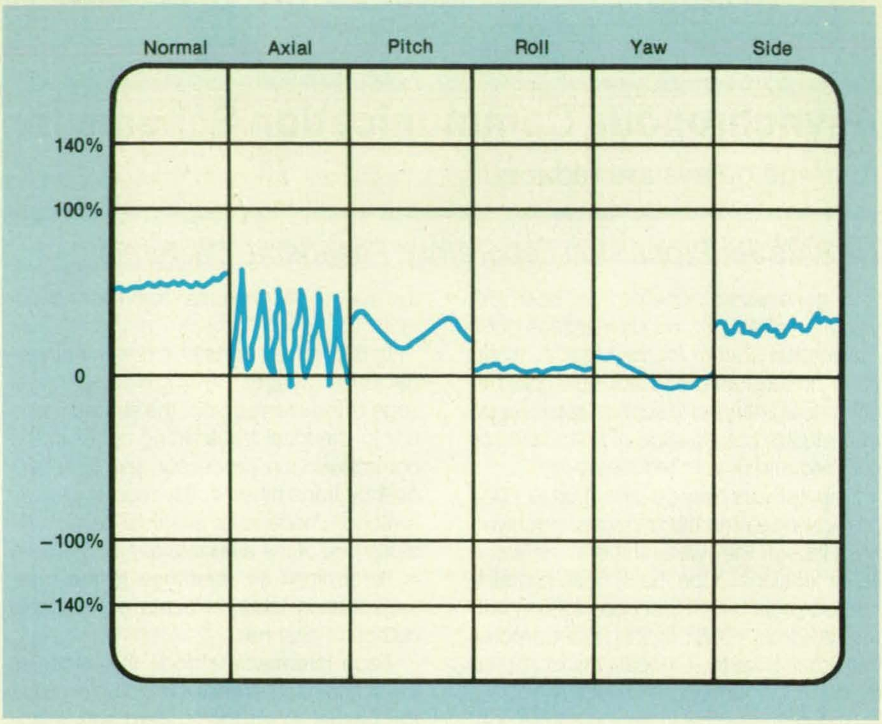

A Typical BDDU Oscilloscope Display in the scan mode shows each channel occupying one-sixth of the total trace.

Alarms are incorporated into each channel to provide an 8-s visual warning following any pulse of 20 μs or longer duration that exceeds ±100 percent of full scale, and a second visual and audible latching alarm is activated when the input signal of that channel exceeds ±140 percent of full scale for 700 μs or longer. An additional feature has been incorporated into the BDDU to enable the display of the sum and difference of the signals in channels 1 and 3 and of the signals in channels 5 and 6.

This work was done by Alice T. Ferris of **Langley Research Center** *and William C. White of Wyle Laboratories. For further information, Circle 63 on the TSP Request Card.*

Inquiries concerning rights for the commercial use of this invention should be addressed to the Patent Counsel, Langley Research Center [see page 18]. Refer to LAR-13658.

High-Speed Multiprocessing for Engine Simulation

Parallel microprocessors have the computational power and speed for realistic simulations.

Lewis Research Center, Cleveland, Ohio

A multiprocessor simulator uses parallel microprocessors to achieve the computing speeds needed for real-time engine simulation. The system has been used to simulate a small turboshaft engine to demonstrate the potential of multiprocessing in such applications.

Real-time simulation aids development of new digital engine controls because it enables the testing of hardware and software under realistic conditions. However, because of the massive amount of calculation required to model a complex engine, simulation in real time on a single processor demands a fast, dedicated mainframe computer. The new simulator has shown that multiprocessing is an effective alternative to mainframe computing.

In addition to the simulator hardware, a structured macroinstruction-based real-time multiprocessor language and an operating system were developed. The language enables engineers to develop simulation programs, and the operating system enables users to communicate interactively with the system.

The simulator concept is based on $2(n+1)$ processors and $2n$ shared memories connected via two data buses (see figure), where n is the number of parallel processing channels. The demonstration employed four channels and reduced the calculation time for a single processor of the same type by more than half. The processors selected for the demonstration were 16-bit chips; if more-advanced 32-bit chips had been used, even more time would have been saved.

Two processors are reserved for spe-

VXIbus from CDS

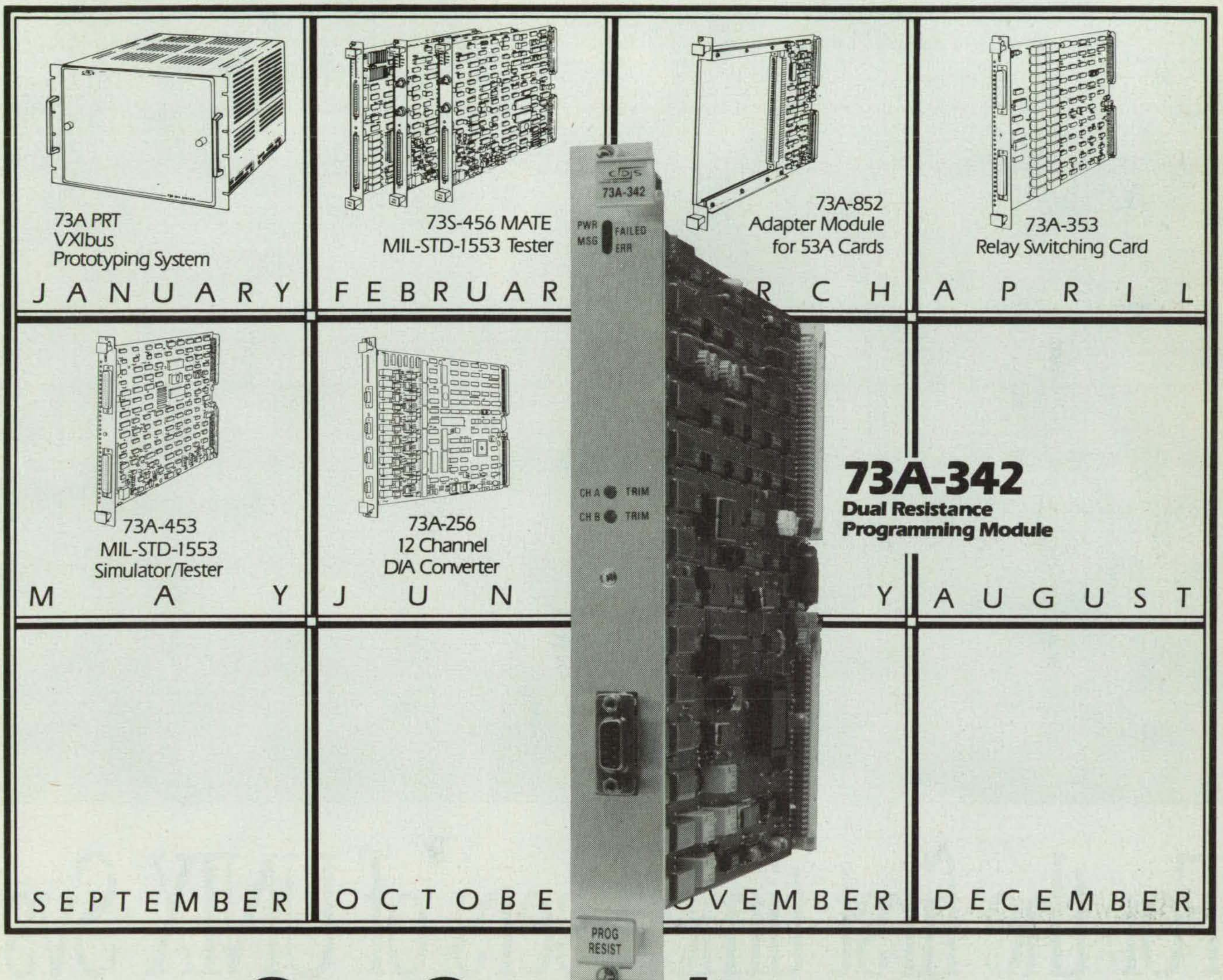

Our Commitment: A VXI Product Every Month

Innovation! Leadership! At CDS, these are not words, they are commitments. The VXIbus is just the latest example. While others are still trying to figure out what the VXIbus is, CDS has been building–and delivering–more than a product a month since January, with still more to come.

CDS
colorado data systems ®

Colorado Data Systems
3301 W. Hampden Ave., Unit C
Englewood, Colorado 80110
(303) 762-1640
TWX 910-933-0193
1-800-CDS-ATE1

Circle Reader Action No. 639

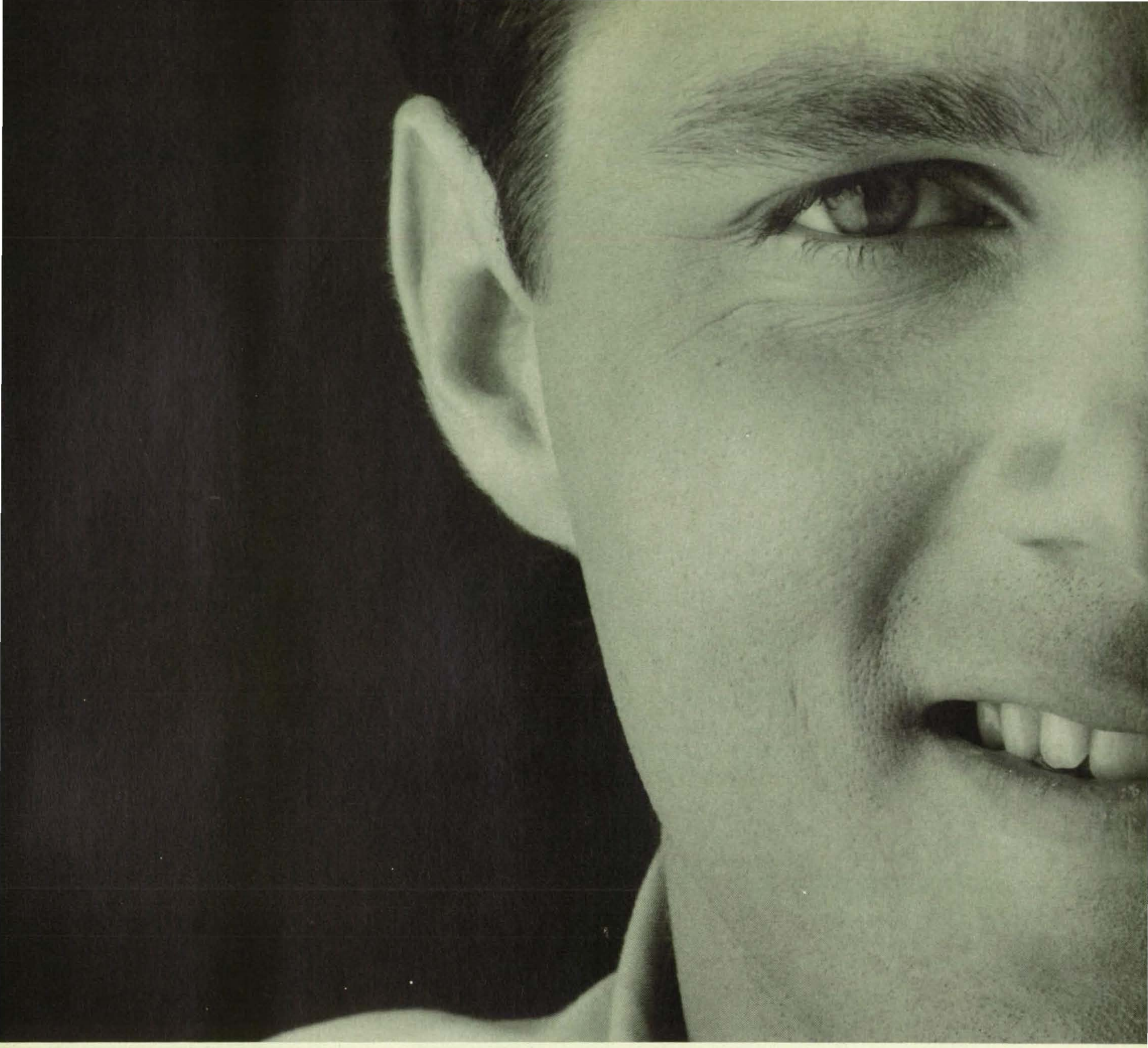

n V can talk to a true supercomputer.

JNIX System V and then compile and run them on any ETA10 Supercomputer—from the affordable ETA10-P, the ETA10-Q and ETA10-E to the world's most powerful supercomputer, the ETA10-G.

Now, all your present applications based on AT&T's JNIX System V can be ported easily to ETA10 Supercomputers. Programs that once took months to port now take hours. Because programs based on AT&T's UNIX System V don't have to be rewritten.

ETA is also developing a library of applications specifically for AT&T's UNIX System V users in higher education environments. These applications include SPSS, IMSL and DI3000.

If you know AT&T's UNIX System V, you now have a voice in supercomputing. Beginning today.

Talk to your Control Data representative, or: ETA Systems, Inc., 1450 Energy Park Drive, St. Paul, MN 55108. Phone: (612) 642-3460.

ETA10 SUPERCOMPUTERS.

CONTROL DATA

Circle Reader Action No. 626

cial input and output functions, and the remaining processors are available to operate on portions of the simulation. Each channel contains a preprocessor, a memory, and a computational processor. One of the reserved processors, the front-end processor, is the communication link between the user and the simulation. It enables the simulation to run interactively. The user can monitor the results and can make changes in key simulation parameters during a run. The other reserved processor, the real-time extension, is the communication link between the simulator and such external engine devices as actuators and controllers.

The model of the engine — a small unit with 20,000 lb (89 kN) thrust — includes mathematical representations of the following:

- A single-centrifugal-stage, five-axial-stage compressor with variable inlet guide vanes and variable stator vanes for the first two stages;
- A two-stage, axial, air-cooled gas generator turbine that drives the compressor rotor;
- Compressor-exit bleed air that cools the turbine; and
- A second two-stage turbine that is uncooled and has a coaxial drive shaft extending forward through the gas generator turbine to the engine output shaft.

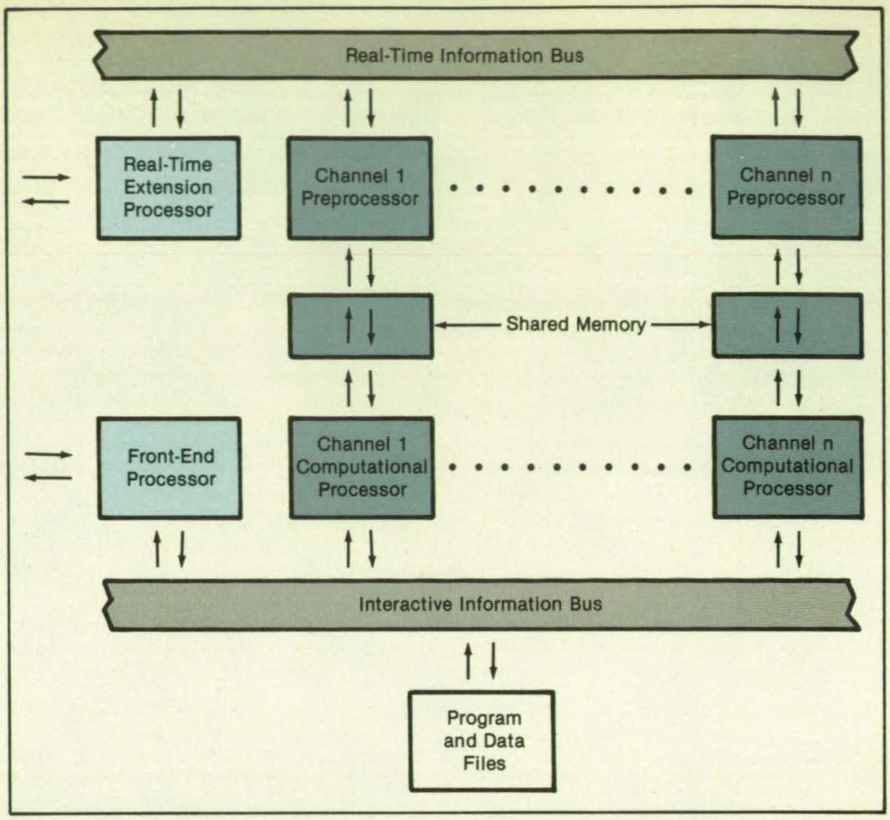

The **Interactive Information Bus** links the front-end processor and the computational processors. The real-time information bus links the real-time extension processor and the preprocessors. A computational processor and a preprocessor communicate through their shared memory.

The small-engine model proved to be ideal for demonstrating the system. It was complex enough to offer a challenging problem of partitioning the computations among processors. In determining what equations should go on the various processors, the model developers gained insight and produced generic partitioning algorithms. At the same time, the engine model had only six dynamic state variables and so did not require excessive execution time that would delay the development of the system.

This work was done by Edward J. Milner and Dale J. Arpasi of **Lewis Research Center**. *Further information may be found in NASA TM-87216 [N86-16221/NSP], "Simulating a Small Turboshaft Engine in a Real-Time Multiprocessor Simulator (RTMPS) Environment."*

Copies may be purchased [prepayment required] from the National Technical Information Service, Springfield, Virginia 22161, Telephone No. (703) 487-4650. Rush orders may be placed for an extra fee by calling (800) 336-4700.
LEW-14593

Simulating Line-of-Sight Radar Returns

Invisible terrain features are removed from further consideration.

Ames Research Center, Moffett Field, California

A computational method has been developed to model the return signals of a ground-mapping radar system for use in simulations where the terrain is in a polygonal form commonly used with computer-generated imagery (CGI). The approach involves the fast rejection of polygons not visible to the radar, to speed the simulation of the radar return. The computational technique can be used to determine which objects in a scene are visible from a specified vantage point and might also be used to determine movements of robot arms that avoid obstacles.

A real-time mathematical model of a forward-looking, ground-mapping radar must produce a range-versus-altitude profile of the CGI terrain along the present flightpath vector (FPV) of the aircraft. The profile is that determined by the intersection of the vertical plane containing the propagated FPV with the surface of the CGI terrain, given the simulated position of the aircraft and the coordinates of the vertexes of the CGI polygons. In this case, the radar model is for terrain following only. The guidance computations use the information from only one profile per computation cycle rather than from several profiles per computation cycle, as might be required in terrain avoidance.

The procedure begins with the precomputation of nonvarying parameters (prefight calculations) that are stored prior to the real-time computations. First, all of the labeled vertexes of the CGI system are stored. Next, the beginning and end points of the line segments are defined for the CGI data base. Also required are the angular bearings of all line segments (projection in the x-y plane), as referred to the beginning and end points of the lines.

Major circles (each enclosing three or more mountains) are used for quick elimination of as many CGI mountains as possible from the search. Each major circle is defined by the coordinates of the center, the radius, and the table of the mountains included within it. The selection of how many mountains and which ones to contain in a given major circle is arbitrary and is done by trial and error. A choice of three or four should be sufficient. Major circles should not intersect.

A minor circle encloses one mountain with a circle of minimum area. These minimum area circles are found by gradually

shrinking and adjusting an enclosing circle until two vertexes touching the circle define a diameter or three vertexes touching the circle form a triangle whose angles are all nonoblique. Under either of these conditions, the circle cannot be shrunk further and still enclose all the vertexes.

Major and minor circles allow the radar line-of-sight intersections with the data base to be determined rapidly by rejecting large portions of the data base with a simple test. If the distance from the line of sight to a major or minor circle is greater than the radius of the circle, then the line of sight cannot intersect anything enclosed in the circle (see figure).

The computational procedure was applied to the simulation of a terrain-following helicopter and required 17 ms to execute on a SIGMA 8 computer. In contrast, a previous method required about 120 ms. It should be possible to decrease the execution time significantly in future simulations.

This work was done by F. J. Moran and J. D. Phillips of **Ames Research Center**. *Further information may be found in NASA TM-88324 [N87-12967/NSP], "A Computational Method To Model Radar Return Range in a Polygonally Based, Computer-Generated-Imagery Simulation."*

Copies may be purchased [prepayment required] from the National Technical Information Service, Springfield, Virginia 22161, Telephone No. (703) 487-4650. Rush orders may be placed for an extra fee by calling (800) 336-4700.

Inquiries concerning rights for the commercial use of this invention should be addressed to the Patent Counsel, Ames Research Center [see page 18]. Refer to ARC-11783.

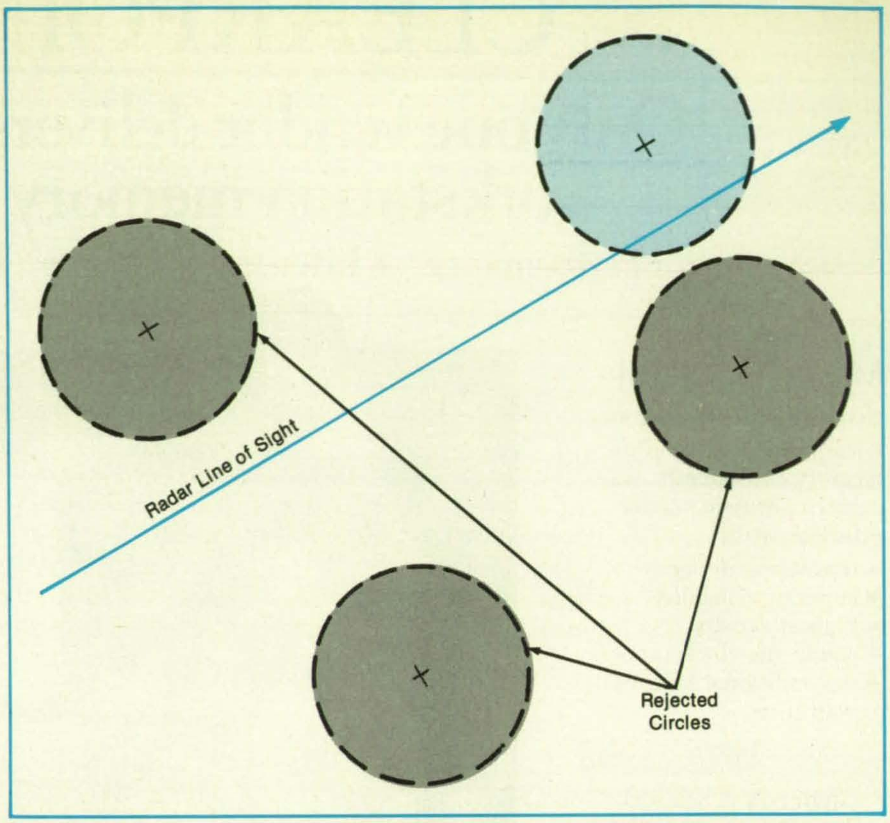

Test Circles are used in an algorithm that quickly rejects terrain features not traversed by the radar line of sight. If a circle does not cross the line of sight, then all the mountains in it are rejected.

Phase-Length Optical Phase-Locked-Loop Sensor (PLOPS)

This system provides high resolution without loss of dynamic range.

Langley Research Center, Hampton, Virginia

The PLOPS system is designed to provide a high-resolution measurement of the change in optical length from the optical-system source to any optical reflector, including a diffuse reflector. The system has the flexibility to operate from microdimensional to macrodimensional changes. Its use is broad and includes most measurement situations requiring information on length, vibration, and their derivatives. Thus, it can determine distances, structural modal displacements, and vibration frequencies from zero to the high-kilohertz range. Potential applications include building dynamics, remote sensing of vibrations in such systems as turbine-based machinery, monitoring of structural dynamics, noncontacting sensing of surface contours, measurement of large strains as in earthquake monitoring, measurement of atmospheric dynamics and turbulence, high-resolution sensing of humidity, detection of surface acoustic waves by optical microscopy, and related areas.

One version of the optical phase-locked loop (see figure) includes a laser beam as a carrier of an intensity-modulated energy source. The laser beam passes through a modulator to a transmitting mirror. The modulator varies the intensity of the laser beam at a frequency controlled by the modulation oscillator.

The optical beam is directed by the transmitting mirror to a target. Light reflected from the target is focused by a lens, then deflected by a receiving mirror onto an optical detector that converts the intensity signal into an electrical signal. The signal is amplified and enters a mixer, where the sum frequency is removed by a filter, and the difference frequency is used as a measure of the phase of the modulated signal with respect to that of the modulation oscillator.

The resulting signal is at zero frequency (or dc) and is either a positive voltage or negative voltage, depending on the phase difference between the modulation oscillator and the detected optical signal. At one quadrature point, the voltage will be zero, and the signal integrator will provide a stable operation point for the system by

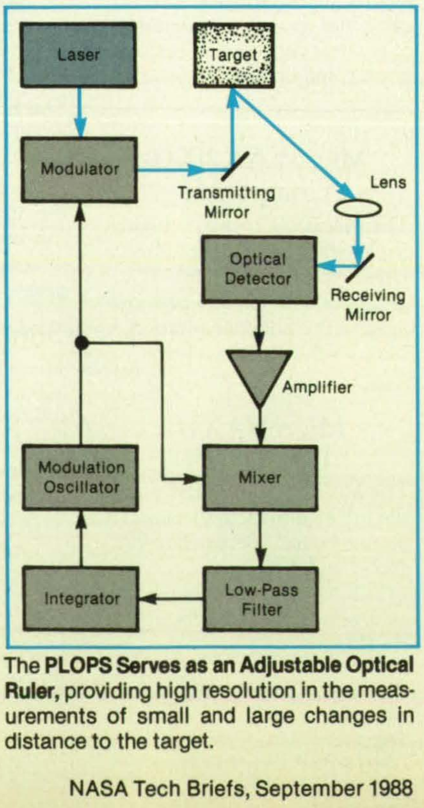

The **PLOPS Serves as an Adjustable Optical Ruler,** providing high resolution in the measurements of small and large changes in distance to the target.

feedback control to the frequency of the modulated oscillator. At that point, the frequency of the modulator sets up an exact number of wavelengths in the optical path.

When the phase-locked loop is locked, the condition of quadrature is maintained so that the phase of the system does not change. Any change in the optical-path length, therefore, changes the modulation frequency. As the target moves, the lock frequency will remain at quadrature, and the change in distance to the target can be monitored from the change in modulation frequency. In addition, the device can be aimed to specific targets, spatially locking onto them with an x,y beam wiggler that operates in a bandwidth different from that of the modulator. Thus the PLOPS can stay locked onto a moving target both spatially and dimensionally.

The PLOPS system has the advantage of high resolution without loss of wide dynamic range. In effect, the choice of the modulation frequency determines the degree of sensitivity of the system. The PLOPS does not depend on coherent reflection from the target and can measure targets that do not have special preparation or corner reflectors. The use of carrier modulation achieves high resolution without the problems of high-speed, short-pulse-duration systems. Thus the PLOPS has the advantage of simplicity, low cost, and small size without sacrificing resolution.

This work was done by Joseph S. Heyman and Robert S. Rogawski of **Langley Research Center**. *For further information, Circle 23 on the TSP Request Card.*

This invention is owned by NASA, and a patent application has been filed. Inquiries concerning nonexclusive or exclusive license for its commercial development should be addressed to the Patent Counsel, Langley Research Center [see page 18]. Refer to LAR-13387.

Books and Reports

These reports, studies, handbooks are available from NASA as Technical Support Packages (TSP's) when a Request Card number is cited; otherwise they are available from the National Technical Information Service.

Microcomputer Board for Space Shuttle Payloads

A general-purpose unit can be configured to control experiments during flight.

A brief report describes the Space Flight 80C86 microcomputer board, which is a configurable general-purpose microcomputer board designed specifically for near-Earth space-flight applications. The architecture of the microcomputer board supports a dual-bus structure.

A local bus provides the essential elements for stand-alone computer operations, and the system bus provides for communication with the subsystems unique to a specific application. The microcomputer board provides for 64 Kilobytes of static random access memory or programmable read only memory, six counters, eight interrupts, and a serial interface. The majority complementary metal-oxide/semiconductor (CMOS) integrated circuits allow for low power and high immunity to noise. The integrated circuits are all screened to Military Specification 883B, which is sufficient for most attached Space Shuttle payload projects.

This work was done by Mitchell L. Davis of **Goddard Space Flight Center**. *To obtain a copy of the report, "Main Control Processor User's Guide," Circle 108 on the TSP Request Card.*
GSC-13143

Photometer Tracks the Sun

An instrument is designed for use aboard an aircraft.

Ames Research Center, Moffett Field, California

An airborne Sun-tracking photometer enables observations of the Sun to be made during a much greater portion of flights than was previously possible, without special maneuvers of the airplane. Instead of being mounted in an airplane and viewing through a cabin window like previous photometers, the new instrument occupies a dome atop the airplane (see figure). Rotatable over wide azimuth and elevation ranges, the new instrument commands a far larger range of views than was possible through a cabin window. Moreover, the new instrument can be calibrated without removing it from the airplane. The previous instrument and its window had to be removed for calibration after every flight.

The photometer assembly is mounted in a cylinder in the dome. The elevation drive motor, acting through a belt-and-gear connection, rotates the cylinder in a meridional slot to the desired elevation. In a similar manner, the entire dome is rotated to the desired azimuth angle by the azimuth drive motor through a belt-and-gear linkage.

The photometer housing contains six round ports for its six measuring photodetector channels and a square port for four Sun-tracking photoresistors near its exterior end. A transparent optical flat isolates the atmosphere inside the photometer housing. The Sun-tracking photoresistors are parts of a feedback loop that controls the elevation and azimuth of the photometer so that the photometer housing points toward the Sun. The electronics for the control system are located in the dome. The data from the six photodetector channels are sent to the computer located inside the aircraft passenger area.

A resistance heater in the photometer housing maintains a nearly constant temperature for the photodetectors. The optical flat is exposed to outside air at temperatures as low as −60 °C. To prevent the flat from fogging because of internal moisture, dry nitrogen is circulated inside the photometer housing.

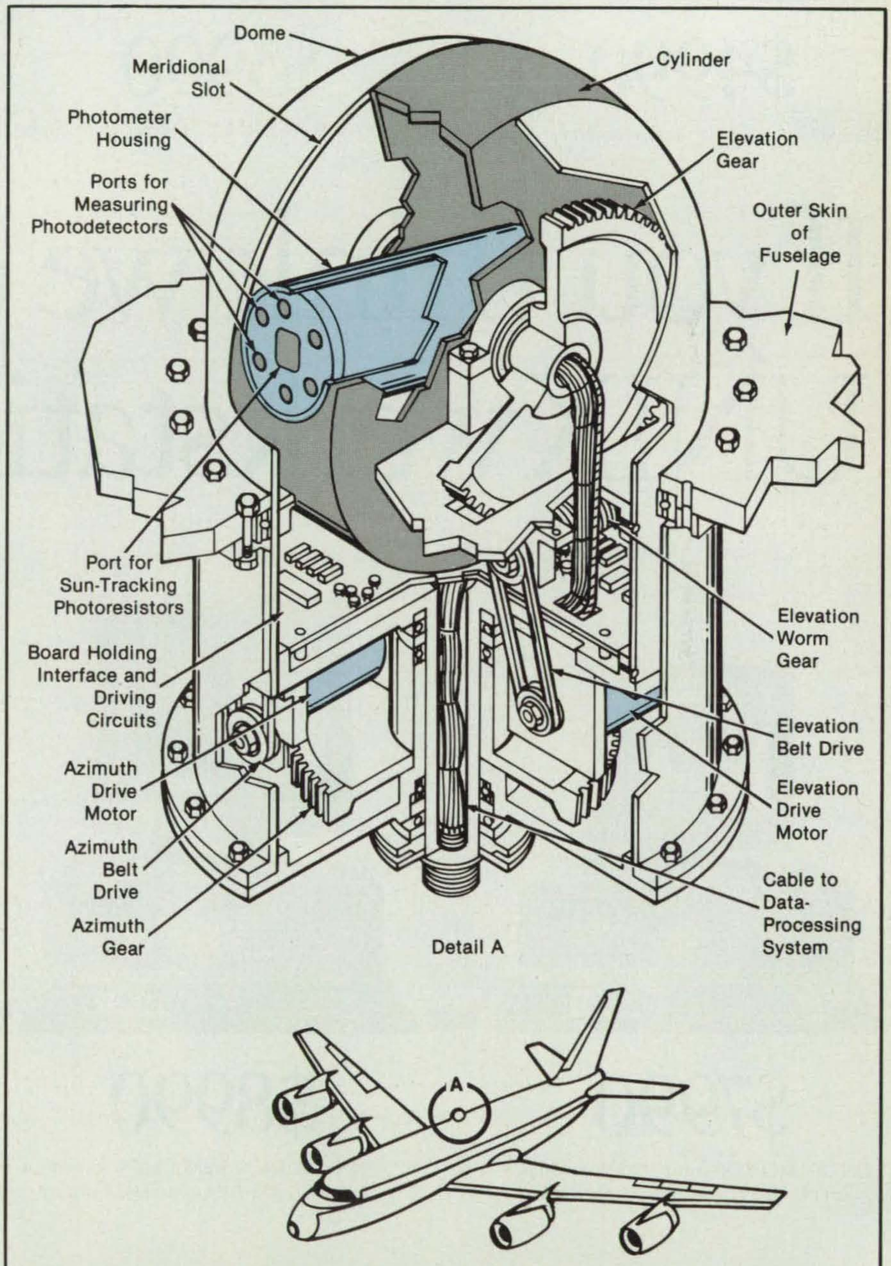

A Fiberglass Dome Protects a Photometer and rotates to aim the photometer in azimuth and elevation to track the Sun. The dome provides a controlled environment for the instrument, including its mechanical and electronic parts.

This work was done by Tak Matsumoto, Cesar Mina, Philip Russell, and William Van Ark of **Ames Research Center**. *For further information, Circle 105 on the TSP Request Card.*

This invention is owned by NASA, and a patent application has been filed. Inquiries concerning nonexclusive or exclusive license for its commercial development should be addressed to the Patent Counsel, Ames Research Center [see page 18]. Refer to ARC-11622.

$4990

DN3000 with 15" 1024 x 800 monochrome display

$5990

DN3000 with 19" 1280 x 1024 monochrome display

$8900

DN3000 with 15" 1024 x 800 color display

If you think we don't have UNIX workstation for unc

$7990

DN3500 MC68030-based 4-MIPS workstation with 15" 1024 x 800 monochrome display

$8990

DN3500 MC68030-based 4-MIPS workstation with 19" 1280 x 1024 monochrome display

$9990

DN3500 MC68030-based 4-MIPS workstation with 15" 1024 x 800 color display

Open Software
FOUNDATION Apollo is proud to be a founding sponsor of the Open Software Foundation.

At Apollo, we believe that the real test of a computer company is not only how often it introduces new technology, but also how quickly it makes that technology available at a truly affordable price.

As testimony to this, we offer not simply one workstation under $10,000, but two entire families of workstations, one of which starts at under $5,000.

Consider the Series 3000™. A Personal Workstation™ powered like a Porsche® but priced like a PC. $4,990, to be exact. And the new Series 3500™. An MC68030 machine that brings high performance to a new low. Making it possible for the first time to obtain a

a single high-performance
r $10,000, you're right.

4-MIPS monochrome system for less than $8,000, and a 4-MIPS color system for less than $10,000.

Prices that even include 4MB of memory, a floating-point coprocessor, an IBM PC AT®-compatible bus, and a choice of Ethernet® or Apollo Token Ring networks.

In addition, like all Apollo workstations, these provide support for industry standards such as UNIX® (System V.3 and Berkeley 4.3), PHIGS, X Window System™ and a host of others, as well as network computing and PC compatibility.

The Apollo Series 3000 and Series 3500. Technology as high as the price is low.

apollo

For more information, call 1-800-323-1846, and in Massachusetts (1-800-847-1011) or write Apollo, 330 Billerica Road, Chelmsford, MA 01824.

Circle Reader Action No. 635

Stand for Infrared Multiple-Internal-Reflection Mount

Infrared MIR spectra are more reproducible, and MIR crystal suffers less damage.

Langley Research Center, Hampton, Virginia

A new technique prevents lateral movement between the elements in a multiple-internal-reflection (MIR) cell during its assembly. The cell is used in infrared spectroscopy. The reproducibility of infrared MIR spectra relies on the ability to maintain the condition of the crystal, which is the MIR element, and to control the contact between the crystal and the sample. A newly developed yet simple stand does both by eliminating the movement of the mount pieces as pressure is applied and by providing a more consistent way of handling the specimen.

The stand aligns a three-piece mount (see figure), which holds a crystal and a specimen for infrared MIR spectroscopy. The mount is stacked vertically beginning with a bottom piece, which can hold either a liquid or an additional solid sample. A middle piece, which contains the crystal with a solid sample behind, is placed over the bottom piece with the crystal facing down, matching a triangular arrangement of holes. A cover, which supplies the pressure, is oriented with its three holes in the same manner as that of the first two pieces.

Screws are placed into the three holes and tightened. This assembly stand prevents the movement of the pieces of the mount during the tightening process and thereby prevents the scratching of the crystal. (The scratching of the crystal would reduce the sharpness of the spectrum, resulting in a loss of information.)

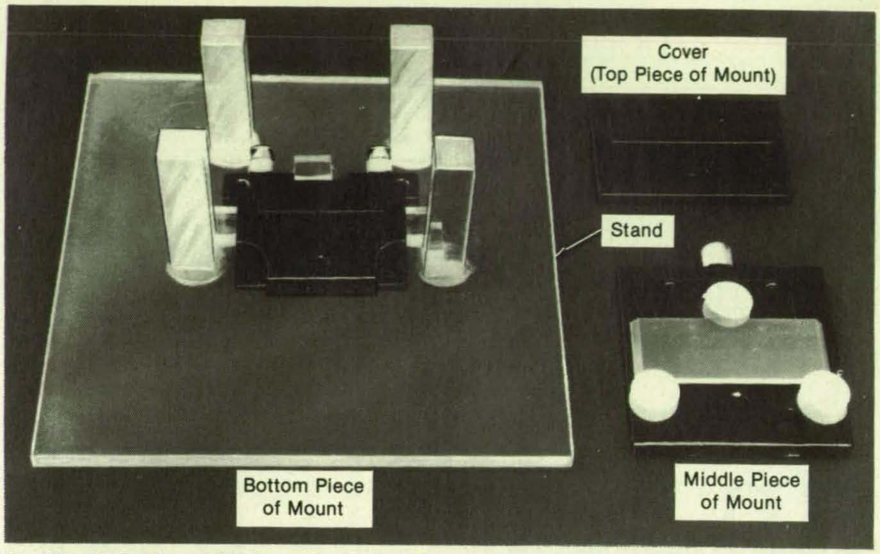

The **Simple Design of the Stand** facilitates the accommodation of any commercially-available mount system.

The stand is constructed of acrylic pieces bonded with epoxy adhesive. On the base are columns of two lengths. The three shorter columns match the thickness of the bottom piece of the mount and hold this piece in place. The four longer columns exceed the total thickness of the three pieces of the mount to accommodate any thickness of sample. These longer columns securely hold the center piece, which contains the crystal, and maintain the position of the top piece, which is as wide as the middle section.

The stand greatly reduces the marring of the crystal caused by the relative movement of the components of the mount/crystal/specimen stack during assembly. The lifetime of the crystal is increased by approximately an order of magnitude. In addition, the stand reduces the time spent mounting the specimen and increases the reproducibility of the infrared spectra.

This work was done by Edward R. Long, Jr., of **Langley Research Center** *and Cynthia A. Bradbury of Old Dominion University. No further documentation is available.*
LAR-13610

Furnace for Rapid Melting and Freezing

An experiment could be conducted in less than 1 minute.

Marshall Space Flight Center, Alabama

A proposed furnace would rapidly heat and cool specimens in material-processing experiments. The furnace would be particularly useful for experiments that require the artificial low gravitation produced by flying KC-135 airplanes in parabolic trajectories. To prevent gravitationally driven sedimentation and convection, the melting of a sample must be started after the airplane has entered the trajectory, and the sample must be completely frozen before the airplane reaches the end of the trajectory, which usually lasts no longer than 30 seconds.

Specimens would be assembled by placing the mixtures of materials to be melted in disk-shaped crucibles. A large disk area would be used to facilitate the transfer of heat to and from the specimens, and the disk would be thin to minimize the heating and cooling time. Before an experiment, a crucible would be fastened to the end of a specimen holder in the lower zone of the furnace, and the furnace would be preheated to a temperature somewhat below the melting temperature of the specimen (see figure).

In preparation for the experiment, a block of large thermal mass and high thermal conductivity (for example SiN or SiC) in the upper zone of the furnace would be preheated above the melting temperature. Immediately after the beginning of the brief experimental interval, the furnace would be moved downward to bring the specimen into contact with the preheated mass. A contact pad made of metallic mesh or other porous, flexible material filled with molten gallium or other liquid of low vapor pressure would speed the transfer of heat to the specimen. The specimen would be held in this position until it melted completely.

The furnace would then be retracted from around the specimen. To quench the specimen rapidly, a flow of cooling gas would be directed onto one face of the crucible through a distributor in the speci-

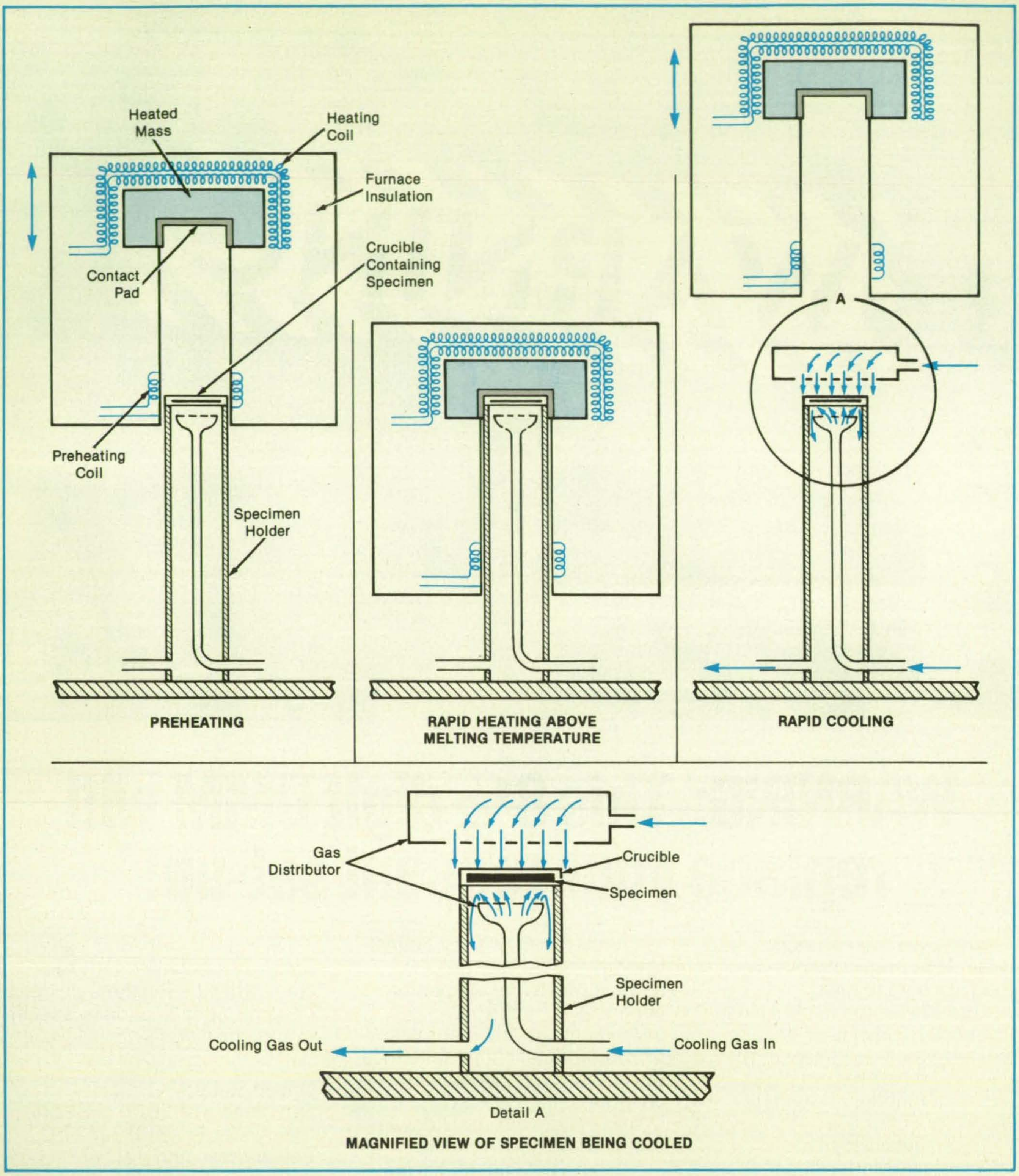

A **Preheated Specimen Would Be Heated Rapidly** above its melting temperature by contact with a hotter, more massive object. Once molten, it would be cooled rapidly with flowing gas.

men holder, while an external distributor would direct the cooling gas at the other face. The crucible would then be detached from the holder and replaced by the crucible for the next experiment.

The use of the furnace would be a relatively inexpensive alternative to longer low-gravity experiments in orbit or in parabolic rocket trajectories. Many experimental materials could be processed in the furnace, including oxidation-resistant superalloys with dispersions of refractory powders, fiber-reinforced glasses and ceramics, electrical contacts with refractory powders dispersed in lower-melting-temperature conductors, high-temperature superalloys reinforced by ceramic fibers, ceramic/metal dispersions, immiscible glasses, alloys of immiscible metals, and foamed ceramics and metals.

This work was done by Edwin C. Ethridge of **Marshall Space Flight Center**. *For further information, Circle 80 on the TSP Request Card.*

Inquiries concerning rights for the commercial use of this invention should be addressed to the Patent Counsel, Marshall Space Flight Center [see page 18]. Refer to MFS-28195.

Laser Pyrometer for Spot Temperature Measurements

The emissivity of the target is measured to assure accuracy.

NASA's Jet Propulsion Laboratory, Pasadena, California

A laser pyrometer makes a temperature map by scanning a measuring spot across a target. Unlike some other optical pyrometers, this one requires no a priori assumption about the local emissivity of the target at the measuring spot. The emissivity is measured as an integral part of the overall measuring process. The scanning laser pyrometer is particularly useful for the noncontact measurement of temperature distributions in the processing of materials; for example, at the liquid/solid interface in a semiconductor melt.

The system (see figure) includes a laser of wavelength λ and a photodetector that has a highly linear response and is equipped with a band-pass filter at wavelength λ. The laser and the photodetector are mounted with appropriate lenses and mirrors so that they both focus on the same small measuring spot.

From the Planck radiation law, the absolute temperature T of the measuring spot on the target is given by

$$T = [T_b^{-1} + (\lambda/C_2)\ell n(\varepsilon R_b/R_t)]^{-1}$$

where T_b is the temperature of a blackbody furnace used as a radiation standard, C_2 is a constant from the Planck radiation law, ε is the spectral emissivity of the target, R_b is the radiance of the blackbody at wavelength λ, and R_t is the radiance of the target at wavelength λ.

Because of the linear photodetector response, an absolute calibration of the photodetector is not required; it suffices to use

$$R_b/R_t = V_b/V_t$$

where V_b and V_t are the photodetector output voltage when observing the blackbody furnace and the target, respectively. The emissivity of the target is obtained from the response of the photodetector to the laser radiation reflected from the target ($V_{\ell t}$) and to the laser radiation reflected from a gold object ($V_{\ell g}$) that is shaped like the target and has a known reflectance r_g. Then the emissivity is given by

$$\varepsilon = 1 - r_g(V_{\ell t}/V_{\ell g})$$

A nonscanning prototype of the laser pyrometer has been tested with a laser at λ = 0.904 μm, stainless-steel and carbon spherical targets heated in a vacuum bell jar by radio-frequency induction, and a gold sphere of 0.99 reflectance. This system can attain a temperature resolution of about 5 °C at 1,300 °C. It is anticipated that with the use of a laser wavelength of 1.3 μm, a signal-to-noise ratio of 10, and a scanning rate of 10^5 picture elements per second, an imaging pyrometer will provide a temperature resolution of 1 °C at 1,300 °C and a spatial resolution of 10 μm.

This work was done by D. D. Elleman, J. L. Allen, and M. C. Lee of Caltech for **NASA's Jet Propulsion Laboratory**. *For further information, Circle 87 on the TSP Request Card.*

Inquiries concerning rights for the commercial use of this invention should be addressed to the Patent Counsel, NASA Resident Office-JPL [see page 18]. Refer to NPO-17024.

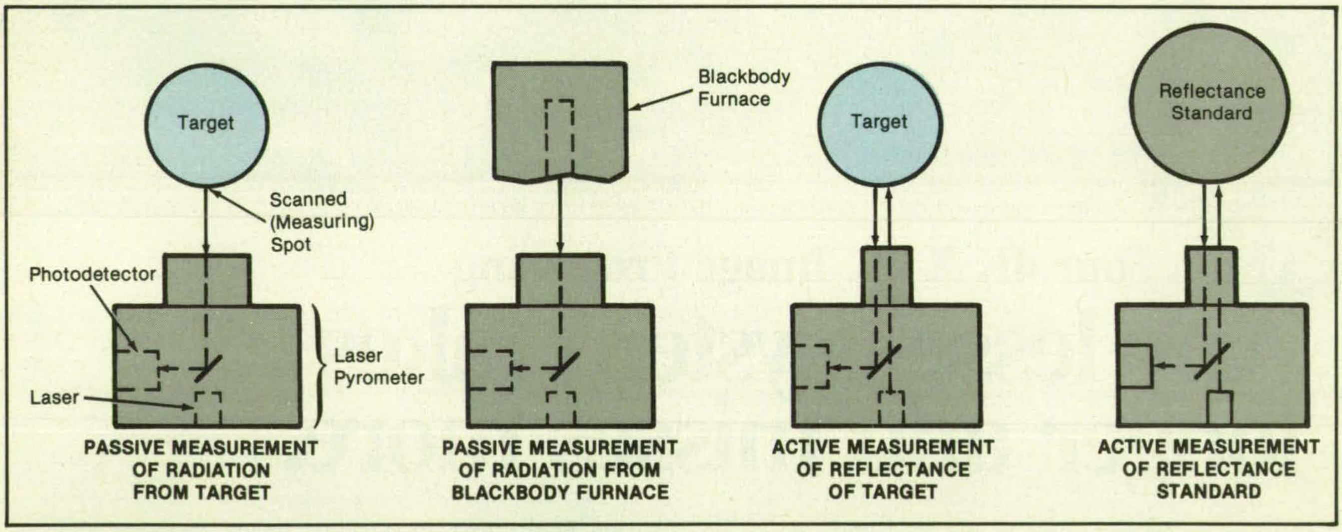

The **Scanning Laser Pyrometer** passively measures the radiation emitted by the scanned spot on the target and is calibrated by a similar passive measurement on a blackbody of known temperature. The laser beam is turned on for active measurements of the reflectances of the target spot and of a reflectance standard. From these measurements, the temperature of the target spot is inferred.

Temperature Fluctuations During Crystal Growth

Fluctuations of heat flow during Bridgman crystal growth are correlated with structural features.

Langley Research Center, Hampton, Virginia

A technique has been developed to deconvolve the period and relative amplitude of fluctuations of heat flow in Bridgman crystal growth. A temperature-measuring device with enough sensitivity and frequency response to make the desired measurements is inserted as close as possible to the substance that is to be monitored. The time-dependent temperature response is recorded, and then the time-domain response is converted to the frequency domain for further analysis. A fast Fourier transform (FFT) of the data on temperature oscillations shows particular behavior at some specific frequencies that corresponds with the striations, or defects, observed on the crystal.

In experiments, the temperature data were taken with a type K thermocouple. The thermocouple wires were 4 mils (0.1 millimeter) in diameter and provided high sensitivity for both temperature and frequency response. By the use of a computer-controlled waveform analyzer, the analog data were converted to digital data for temporary storage before conversion into FFT's. The original and transformed sets of data could then be stored on a computer disk for later use. A thermocouple meter

with analog output was used as the interface between the thermocouple and the waveform analyzer. The meter had a 3-Hz response, which was more than an order of magnitude faster than the highest frequency measured. The resulting FFT of typical data is shown in the figure.

The portion of the spectrum near zero frequency represents the steady decrease of temperature caused by the movement of the ampoule through the furnace. For this particular case, the interesting data are at 10 mHz, 25 mHz, and 47 mHz. Striations were found in the crystal at spatial intervals that correspond to the movement of the ampoule during intervals equal to the reciprocals of these frequencies.

This technique appears to be a useful procedure to help determine the sources of some growth-induced crystalline defects. The investigation of other processes that may be sensitive to small temperature fluctuations, such as diffusion, precipitation, and corrosion, may also benefit from this technique.

This work was done by Archibald L. Fripp, Jr., Ivan O. Clark, and William J. Debnam, Jr., of **Langley Research Center**; *Patrick G. Barber of Longwood College; Roger K. Crouch of NASA Headquarters; and Richard T. Simchick of PRC Kentron, Inc. No further documentation is available.*

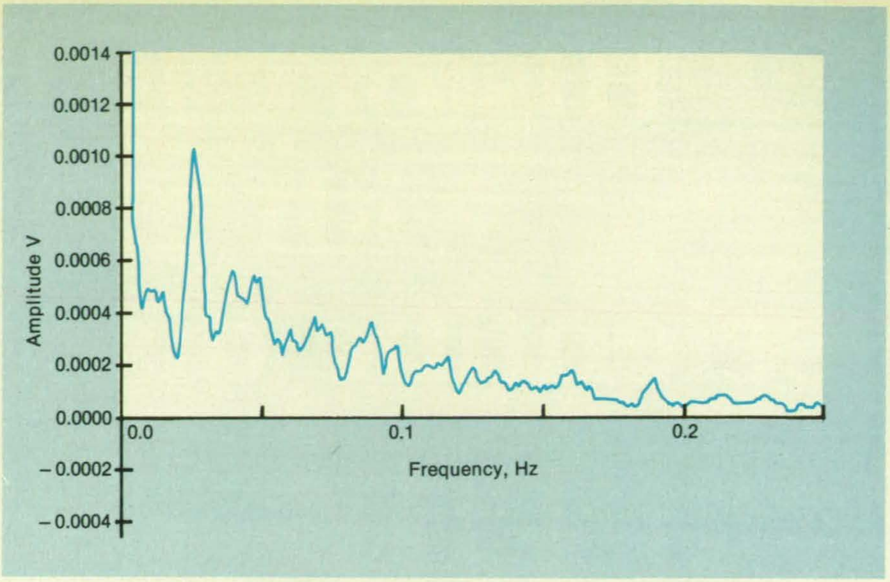

Fast Fourier Transforms of Temperature Signals indicate the spatial frequencies of striations that have been found in grown crystals.

Inquiries concerning rights for the commercial use of this invention should be addressed to the Patent Counsel, Langley Research Center [see page 18]. Refer to LAR-13670.

Detecting Space Dust Particles

The precise times of specific impacts are measured.

Langley Research Center, Hampton, Virginia

A new technique records the times the specific craters are formed in targets exposed in space and permits the determination of the direction in which the impacting particles were traveling at the times of the impacts. After recovery of the targets from space, the compositions of the impacting particles can be established through postflight laboratory analyses of the residual materials in the craters. On Earth, the technique may have industrial and military uses in the detection of fragments driven by explosions.

The principal parts of the device developed for this purpose (see figure) include a metal-oxide/silicon (MOS) capacitor; an electrical circuit, including a fuse, connected to the metal front plate of the MOS capacitor and the silicon-wafer substrate that forms the other plate of the capacitor; and an attached electronic system capable of maintaining a charge on the capacitor and capable of recording the precise time of discharge. The silicon dioxide layer grown on one surface of the silicon wafer is the dielectric of the capacitor.

A hypervelocity particle striking the electrically charged MOS capacitor produces a temporary conducting path between the metal front plate and the silicon substrate, initiating the discharge of the capacitor. With the proper relationship set between the energy stored in the capacitor and the thickness of the metal plate, the current density in the conducting path is sufficient to burn away the metal plate from a substantial region surrounding the impact crater. The removal of the metal around the conducting region terminates the discharge process.

When the attached electronic system attempts to recharge the capacitor, the recharge current blows the fuse, preventing recharge. (A built-in current-limiting device ensures initial charging of the capacitor.) Any particle impacts that occur when the capacitor is uncharged do not cause the removal of metal from the crater region: thus, the recorded impact time can be related to a single, specific, readily identifiable crater. The direction of the particle at time of impact is established by the known orientation of the MOS capacitor wafer on the spacecraft at the recorded impact time.

In addition to the study of space dust, studies of the orbital dynamics of particles produced by solid-propellant rocket-motor firings in space can be made using this technique. Because only one impact time can be recorded per capacitor, the total number of impact times recorded is a function of the number of individual capacitors flown. Large detection areas can be obtained by using multiple MOS capacitor wafers or by masking the front metal plates on a single MOS wafer to form multiple capacitors.

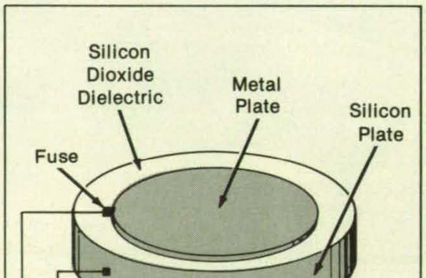

The **MOS Capacitor** is short-circuited by the impact of a particle striking it at high speed.

This work was done by William H. Kinard, Donald H. Humes and Philip C. Kassel, Jr., of **Langley Research Center**, *Jim Wortman of North Carolina State University, and S. Fred Singer and John Stanley of the University of Virginia. No further documentation is available.*

This invention is owned by NASA, and a patent application has been filed. Inquiries concerning nonexclusive or exclusive license for its commercial development should be addressed to the Patent Counsel, Langley Research Center [see page 18]. Refer to LAR-13392.

Books and Reports

These reports, studies, handbooks are available from NASA as Technical Support Packages (TSP's) when a Request Card number is cited; otherwise they are available from the National Technical Information Service.

Status of Sorption Cryogenic Refrigeration

Present equipment and anticipated development are described.

A report reviews the state of the art in sorption refrigeration. Developed in recent years for cooling infrared detectors, for cryogenic research, and for other advanced applications, sorption refrigerators have few moving parts, little vibration, and lifetimes of 10 years or more. The report describes the types of sorption stages, multistage and hybrid refrigeration systems, power requirements, cooling capacities, and the advantages and disadvantages of the various stages and systems.

In sorption refrigeration, low pressure gas is sorbed by physical adsorption (physisorption) on the surface of a material or by chemical absorption (chemisorption) within a solid material (the sorbent). The sorbent is then heated by 100 to 200 °C to desorb the gas at high pressure. The pressurized gas is passed through precooling stages, then expanded in a Joule-Thomson valve where it is partially liquefied and cooled to the final low temperature. The boiling of the liquid removes the heat from the equipment cooled by the low-temperature stage. The low pressure boiloff gas is then reabsorbed by the sorbents, thus completing the cycle.

Rules have been formulated to aid the selection and design of sorption stages to minimize the overall power consumptions and weights of refrigeration systems. The following Joule-Thomson stages and assemblies are recommended accordingly:

- Physisorption of methane on carbon to attain a temperature of 150 to 110 K;
- The preceding stage plus chemisorption of O_2 on $Pr_{1-n}Ce_nO_x$ to attain 90 to 55 K;
- The preceding stages plus chemisorption of H_2 on $LaNi_{4.5}Al_{0.5}$ to attain 30 to 14 K; and
- The immediately preceding system with the H_2 stage augmented by chemisorption of H_2 on slightly cooled palladium or similar material to lower the vapor pressure over the liquid hydrogen, causing it to solidify and sublime at 10 to 7 K.

Nonsorption stages can be combined with sorption stages to reach lower temperatures. A mechanical-compressor J-T helium system can be operated in conjunction with the 14-K hydrogen-chemisorption stage to reach 4 to 5 K. Such temperatures could also be reached by adiabatic demagnetization in series with a hydride stage or with helium physisorption, although this particular sorption stage is extremely inefficient. Future progress in 4 to 5 K long-life refrigerators will probably require the development of nonlubricated mechanical helium compressors or improved cryogenic regenerators for use in Gifford-McMahon or Sterling expansion schemes.

This work was done by Jack A. Jones of Caltech for **NASA's Jet Propulsion Laboratory**. *To obtain a copy of the report, "Sorption Cryogenic Refrigeration — Status and Future," Circle 116 on the TSP Request Card.*
NPO-17349

A FREE BROCHURE describes new books, posters, and videotapes available from NASA Tech Briefs. Circle Reader Action Number 700 for your free copy.

Materials

Improved "Green" Forming of Silicon Nitride

Advanced processing techniques reduce the incidence of critical flaws.

Lewis Research Center, Cleveland, Ohio

Silicon nitride (Si_3N_4) is being considered for many applications ranging from components of turbine engines to industrial heat exchangers. More widespread application has been hindered by the inability to make parts with reproducible properties. One reason for this is the uncontrolled introduction of fracture-initiating flaws during processing.

The critical flaws include pores caused by volatilization of organic contaminants, agglomerates that originate in the starting powders, and inclusions or metallic contamination introduced during various processing steps. The incidence of critical flaws induced by processing can be reduced by the processing of powders to avoid organic and metallic contamination and the combination of colloidal techniques with an innovative slurry-pressing technique that avoids agglomeration.

Advanced processing techniques like these were used with two different highly-pure Si_3N_4 powders. Both powders were combined with sintering additives to give a final composition of 87.8 weight percent of Si_3N_4, 6.4 weight percent of Y_2O_3, and 5.8 weight percent of SiO_2. The results with both powders indicate that slurry pressing of "green" (unheated) specimens improves the average flexural strength of the sintered Si_3N_4 by 10 to 15 percent when compared with a conventional dry-pressing procedure.

This improvement is attributed to the reduced sizes and volumes of pores and the elimination of metallic inclusions. The evaluation of the mixing containers indicated that reduced contact with plastic during processing resulted in a reduction in the number of critical flaws attributed to lenticular pores. Such flaws are thought to result from volatilization of plastic slivers during sintering.

It was shown that slurry pressing at a loading of 20 volume percent of solids is better than pressing at 30 volume percent of solids. The decreased sizes and volumes of pores in the material that contained 20 volume percent of solids may indicate that lower viscosity aids in the removal of voids during pressing. It was also found to be beneficial to mill the Y_2O_3 additive at least to the sizes of the particles of the starting Si_3N_4 powder before mixing the two powders together.

This work was done by Marc R. Freedman, William A. Sanders, and James D. Kiser of **Lewis Research Center**. *To obtain a copy of the reports, "Slurry Pressing of Silicon Nitride" and "The Effect of Powder Processing on the Properties of Slurry Pressed Sintered Silicon Nitride," Circle 83 on the TSP Request Card.*
LEW-14680

Annealing Reduces Free Volumes in Thermoplastics

Reductions reach asymptotic values after several annealing cycles.

Langley Research Center, Hampton, Virginia

High-temperature thermoplastics are excellent candidates for use in aerospace applications. Graphite-fiber composites that contain thermoplastic matrices could have wide applicability. However, previous work indicates that annealing would exert significant effects on the free volumes of thermoplastics. As a result, composites containing thermoplastics could suffer increasing internal stresses at the fiber/matrix interfaces as the free volumes in the matrices change due to variations of temperature during service. To assess the general suitability of thermoplastics for graphite/polymer composites, an investigation was conducted to determine the free volumes and the water-absorption characteristics of two types of thermoplastic polyimide as functions of their annealing histories.

The thermoplastic samples were weighed and immersed in distilled water at 90 °C. They were reweighed at 24-hour intervals and kept immersed until their weights stabilized. The samples were then transferred to a vacuum oven at 100 °C and weighed every 24 hours until they attained new steady weights. The difference between the two stabilized weights for a sample equals the saturation moisture content of the sample. For a noncrystalline sample, the saturation moisture content is directly proportional to its free volume.

Next, both types of samples were annealed for various multiples of 24 hours at a temperature of 200 °C, about 50 °C below their glass-transition temperatures. Both types of samples exhibited reductions in free volume following the annealing cycles. However, the free volumes reached asymptotic values after about four cycles. Finally, the samples were examined by x-ray diffraction to detect any changes that annealing may have produced in their levels of crystallinity. At a confidence level of 95 percent, no measurable changes in crystallinity were observed in any of the samples.

Because preanneal and postanneal x-ray-diffraction studies did not reveal any changes in the degree of crystallinity, it appears that any changes in the saturation-moisture weights are related to changes in the amorphous regions, where the primary absorption of water occurs. These regions, besides being generally disordered, also contain free volumes that may change as a result of annealing. The conclusion is that any changes in the saturation-moisture contents of the samples are directly proportional to changes in the free volumes in them. These results indicate that the annealing of thermoplastics reduces their free volumes but that the free volumes reach asymptotic levels beyond which no further reductions are observed.

This work was done by Jag J. Singh and Terry L. St. Clair of **Langley Research Center**. *No further documentation is available.* *LAR-13664*

Artificial Voids in Ceramic Materials

Small holes are made deliberately to help quantify techniques of nondestructive evaluation.

Lewis Research Center, Cleveland, Ohio

Silicon carbide and silicon nitride are high-temperature structural ceramic materials that are being considered for application in advanced gas-turbine engines. Pores, small cracks, inclusions, and variations in microstructure are strength-limiting defects commonly observed in these sintered silicon-base ceramics. The ability to detect and characterize voids (by sizes, shapes, and locations) in structural ceramics is vital for increasing the strengths and reliabilities of these materials. Ceramic samples containing seeded voids that have known dimensions and locations are essential for determining the quantitative capabilities of nondestructive evaluation techniques applied to structural ceramics.

A method for creating voids in ceramic specimens has been developed. In an example of the method, plastic microspheres of various sizes were pressed into the surfaces of silicon carbide and silicon nitride "green" bars placed in a die. Additional ceramic powder was added to cover the spheres, and the bars were compacted in such a way that the spheres were buried beneath the surfaces of the bars. The bars were heated to vaporize the spheres, thereby producing internal voids. The bars were then sintered to complete the processing cycle. Several hundred voids ranging in diameter from 25 to 500 μm were thus seeded in SiC and Si_3N_4 specimens.

These voids were fully characterized metallographically and the specimens examined by use of both conventional and projection x-radiography and scanning laser acoustic microscopy. Standard specimens produced and characterized in this way would be of interest to manufacturers of structural ceramic materials and to researchers and developers of nondestructive flaw detection equipment.

This work was done by Don J. Roth, Edward R. Generazio, and George Y. Baaklini of **Lewis Research Center**. *Further information may be found in NASA TM-88797 [N86-31913/NSP], "Quantitative Void Characterization in Structural Ceramics Using Scanning Laser Acoustic Microscopy."*

Copies may be purchased [prepayment required] from the National Technical Information Service, Springfield, Virginia 22161, Telephone No. (703) 487-4650. Rush orders may be placed for an extra fee by calling (800) 336-4700.
LEW-14586

Stabilizing PFAE Against Oxidation

Stabilized, noncorroding perfluoroalkylether can be used at 300 °C as a hydraulic fluid or lubricant.

Lewis Research Center, Cleveland, Ohio

A new process makes commercial perfluoroalkylether (PFAE) hydraulic fluid more stable in the presence of metals in hot oxidizing atmospheres. The viscosity and molecular weight of the treated fluid are almost identical with those of the untreated fluid.

The process consists of thermal oxidation in the presence of a catalyst (see figure) to remove weak links, followed by transformation of the newly-created functional groups into phospha-s-triazine linkages, which impart antioxidation and anticorrosion properties. A 66-percent yield of stable PFAE is obtained.

The thermal-oxidative stability of the treated fluid is better than that of the starting material by a factor of 2.6×10^3, on the basis of the amounts of volatile materials evolved during exposure for 8 hours to an oxidizing atmosphere in the presence of Ti(4Al, 4Mn) alloy. Furthermore, no corrosion occurred in the titanium alloy samples in these tests.

The fluid can be used as a lubricant, grease, or hydraulic fluid at temperatures from −55 to +300 °C in the presence of metals in an oxidizing atmosphere. No other lubricant now available offers this combination of properties.

This work was done by W. R. Jones, Jr., of **Lewis Research Center** *and K. Paciorek and R. Kratzer of Ultrasystems. Further information may be found in NASA TM-87276 [N86-25474/NSP], "Improved Perfluoroalkylether Fluid Development."*

Copies may be purchased [prepayment required] from the National Technical Information Service, Springfield, Virginia 22161, Telephone No. (703) 487-4650. Rush orders may be placed for an extra fee by calling (800) 336-4700.
LEW-14612

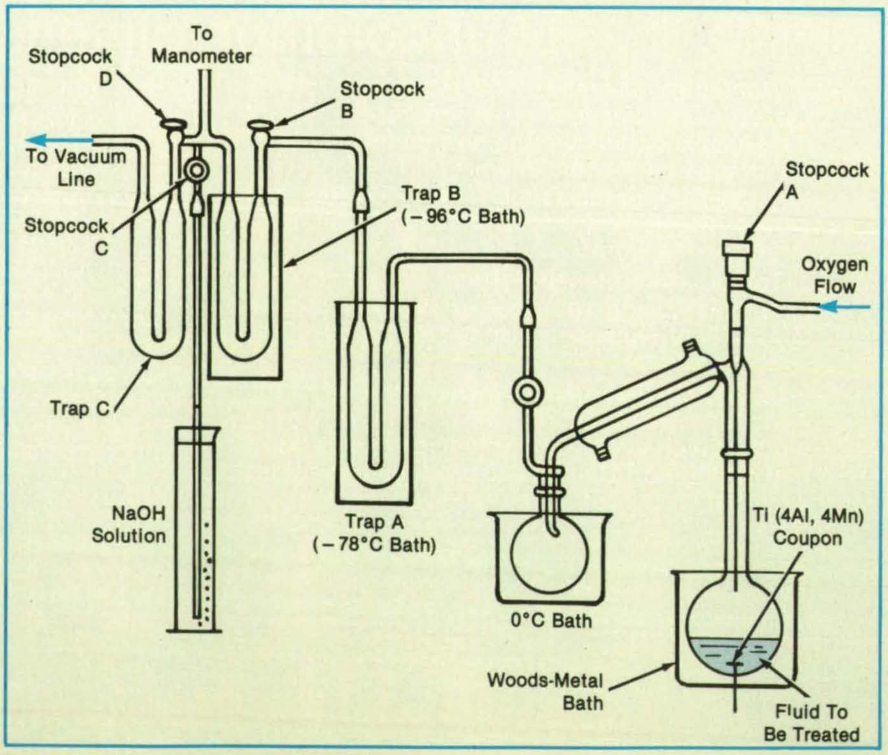

This **Laboratory Apparatus** is used in the first step of the production of stabilized PFAE. The traps are used to collect volatile fractions for analysis. The involatile residue is treated further to transform it into stabilized PFAE.

NON-DESTRUCTIVE TESTING: NOBODY ELSE OFFERS SO MANY WAYS TO LISTEN.

The extensive use of composite parts in the aerospace industry has created a need for fast, reliable, cost-efficient methods of testing.

As a major user of composites, McDonnell Douglas had reason to become a leader in ultrasonic testing.

We've developed four highly effective, state-of-the-art ultrasonic testing systems for our own needs. These systems are now available to you.

AUSS-IV, our fourth-generation Automated Ultrasonic Scanning System, is a computer-controlled machine and data handling system that automatically checks parts for anomalies.

AUSS-V, presently under development, will add totally new robotic, data imaging, and computer automation dimensions to ultrasonic testing.

ADIS, our Advanced Data Acquisition, Imaging, and Storage System, can update existing inspection units to provide state-of-the-art data acquisition, imaging, and plotting capabilities. Other features include depth measurements, cross sections, and histograms.

And MAUS, our Mobile Automated Ultrasonic Scanner, allows fast, in-place inspection of composite parts. It can scan the surface of compound curvatures without any special attachments.

To find out more about our systems, and how they can help you increase productivity while reducing costs, call or write:
McDonnell Aircraft Company,
Dept. 080, P.O. Box 516,
St. Louis, MO 63166
(314) 232-7454

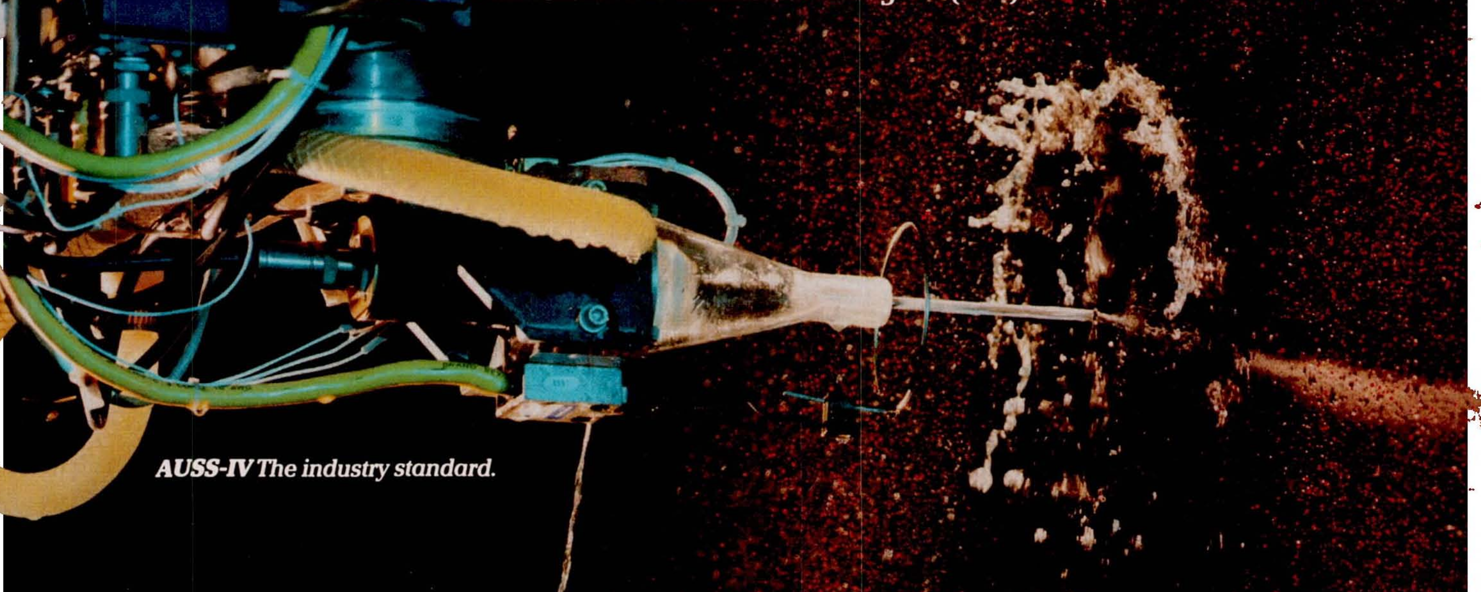

***AUSS-IV** The industry standard.*

***AUSS-V** Adds new dimensions to ultrasonic testing.*

***ADIS** Updates existing inspection units.*

***MAUS** Provides fast, in-place inspection of composite parts.*

MCDONNELL DOUGLAS

Circle Reader Action No. 372

Organoborosilane Polymers and Ceramic Products

Ceramics exhibit high thermo-oxidative stability.

Ames Research Center, Moffett Field, California

Processes have been developed to make polyorganoborosilane polymers. These polymers are useful principally as precursors to ceramics that withstand high temperatures. In a representative application, the polymer might be drawn into fibers, and then pyrolyzed to produce a ceramic cloth.

In the laboratory, polymers are prepared by coupling reactions of boron halides or organoboron halides with organic halosilanes in an aprotic solvent that has been dried and degassed to remove water and oxygen to the extent possible. In a typical reaction (see Figure 1), 4 to 6 equivalents of an alkali metal are freshly cut and added to the solvent at ambient temperature. The reactants are combined in equimolar amounts and slowly added dropwise to the solvent.

The reaction mixture of solvent plus reactants is refluxed at 120 to 160 °C for 16 to 24 hours. Then an alkyl iodide is added and the reflux continued for an additional time up to 4 hours to consume the excess alkali metal and thereby quench the reaction. The reaction products include the polymers and a precipitate consisting of the alkali halide.

After cooling, the reaction products minus the precipitate are filtered. The filtrate is washed with additional aprotic solvent, then dried in a partial vacuum to obtain the polymers, which usually have molecular weights of 800 to 1,300 daltons. The polymers are generally soluble in organic solvents and melt at temperatures below 150 °C.

To produce ceramic material, a polymer or mixture of polymers is pyrolized in nitrogen at temperatures from 600 to 1,100 °C. The resulting ceramic has high thermo-oxidative stability (see Figure 2): it resists both oxidation and weight loss when exposed in air to temperatures up to 1,100 °C.

This work was done by Salvatore R. Riccitiello of ***Ames Research Center*** *and Ming-ta Hsu and Timothy S. Chen of H. C. Chem Research and Service Corp. For further information, Circle 10 on the TSP Request Card.*

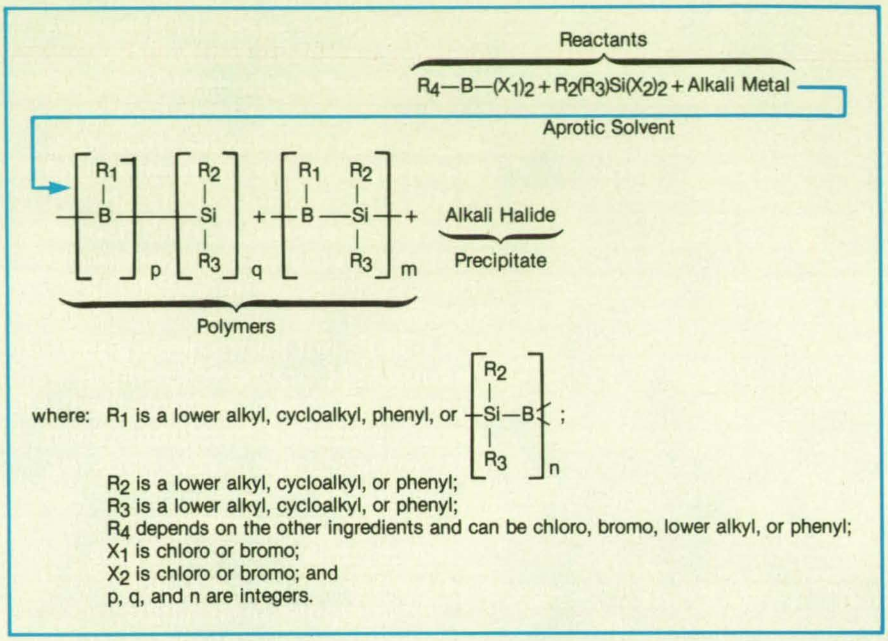

Figure 1. The **Precursor Polymers** are prepared by using an alkali metal to couple a boron halide with an organohalosilane.

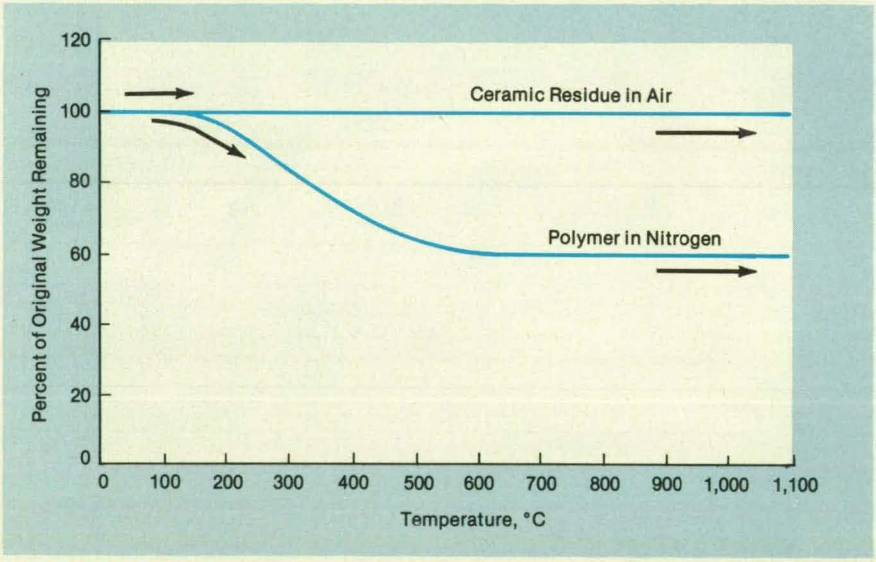

Figure 2. **Thermogravimetric Analysis** of a polymer prepared from dimethyldichlorosilane and methylboronidibromide shows the loss of weight as the polymer is heated in nitrogen. The resulting ceramic residue shows no weight loss or gain when subsequently heated in air.

Inquiries concerning rights for the commercial use of this invention should be addressed to the Patent Counsel, Ames Research Center [see page 18]. Refer to ARC-11649.

Dry PMR-15 Resin Powders

Shelf lives of PMR-15 polyimides are lengthened.

Lewis Research Center, Cleveland, Ohio

PMR-15 polyimides were developed at the NASA Lewis Research Center in response to the need for processable, high-temperature-resistant matrix resins for fiber-reinforced advanced composites. PMR-15 resins are commercially available from a number of suppliers and are currently being used in a variety of aerospace, aeronautical, and commercial applica-

tions.

During the manufacture of a PMR-15 resin, a resin solution is prepared by dissolving monomer reactant in an alcoholic solvent of low boiling temperature. The monomer solution is applied to a reinforcement and the bulk of the solvent removed to form prepreg material, which is then cured at high temperature and pressure to form a composite part.

Before curing, the composition of the resin is continually changing because of monomer reactions that occur during storage. The degree and type of these reactions depend on the storage conditions and the solvent content of the resin. Compositional changes in a resin include the formation of soluble higher esters, which severely affect the processability and properties of the composite, and insoluble imides, which precipitate from solution.

Prepreg materials containing low solvent levels (3 to 5 weight percent) can be stored at temperatures from 0 to 40 °F (−18 to +4 °C) for intervals of 6 months or longer before compositional changes in the resins markedly affect the processing and/or quality of the composites. The storage, before prepregging, of resin solutions that have solvent levels of 30 to 50 weight percent of solvent, is limited to a maximum time of 4 months at reduced temperatures before changes in the resins severely affect the processing and quality of composites. The shelf life of solutions stored at room temperature [75 °F (24 °C)] is limited to 20 days before the reacted materials precipitate.

In a recent study conducted at NASA Lewis Research Center, a simple procedure for significantly extending the room-temperature shelf life of PMR-15 polyimide resin material was developed. The procedure involves the quenching of monomer reactions by the vacuum drying of PMR-15 resin solutions at 70 to 90 °F (21 to 32 °C) immediately after preparation of the solutions. The absence of solvent eliminates the formation of higher esters and reduces the formation of imides to a negligible level. This procedure provides a fully-formulated dry PMR-15 resin powder that can be readily dissolved in the solvent at room temperature immediately before use. Graphite-reinforced composites prepared from dried resin reactant compositions that had been stored at room temperature for 4 months and 11 months provided PMR-15 composites with processing and mechanical properties identical to those of composites prepared from fresh PMR-15 solutions.

This work was done by Raymond D. Vannucci and Gary D. Roberts of **Lewis Research Center**. *No further documentation is available.*
LEW-14573

Powder-Metallurgy Process and Product

Rapid-solidification processing yields alloys with improved properties.

Langley Research Center, Hampton, Virginia

Ingot-metallurgy (I/M) 2XXX-series aluminum alloys based on Al/Cu and Al/Cu/Mg are widely used in aircraft structures where fatigue and fracture resistance and elevated-temperature strength are important design considerations. A systematic study was undertaken to extend the favorable property combinations of I/M 2XXX alloys through the recently developed technique of rapid-solidification processing using powder metallurgy (P/M). The benefits of rapid-solidification processing of P/M 2XXX aluminum alloy compositions over I/M processing were evaluated by comparison with an I/M control alloy.

Rapid-solidification processing, a technology that has greatly expanded the range of compositions and microstructures attainable in metallic materials, typically involves the impingement of a molten metal stream onto a rapidly-spinning chill block or through a gas medium using a gas atomization technique. The Al/Cu/Mg alloys used in this study, which contained various amounts of zirconium, were produced by air atomization of fine powders. The average powder size was maintained between 12 and 15 μm. After atomization, the powders were consolidated into billets and the billets extruded into bars. Standard metallographic procedures were used to examine the microstructures, and mechanical testing was performed with specimen configurations and procedures according to American Society for Testing and Materials standards. Standard tensile, Charpy V-notch, and fracture-toughness tests were performed on the extruded bar in naturally aged and artificially aged conditions.

By and large, the rapid-solidification-processed P/M alloys exhibited strength and toughness properties substantially improved over those of the I/M-produced alloys. Zirconium additions of as high as 0.6 weight percent were used successfully to enhance the alloy properties, while the practical limit of zirconium addition in I/M alloys is about 0.10 to 0.15 weight percent. One promising Al/Cu/Mg/Zr alloy composition was also evaluated in the product forms of plate and sheet. These product forms had a marked advantage in tensile properties and toughness due to the ability of the P/M microstructure to control better the recrystallization and the grain-growth processes. The results of this study indicate that rapid-solidification processing of P/M alloys has the potential of producing 2XXX-series aluminum alloys with strength and toughness properties superior to those of I/M-produced alloys.

This work was done by Henry G. Paris of Aluminum Co. of America for **Langley Research Center**. *Further information may be found in NASA CR-172521 [N87-20406/NSP], "Development of Powder Metallurgy 2XXX Series Al Alloy Plate and Sheet Materials for High Temperature Aircraft Structural Applications."*

Copies may be purchased [prepayment required] from the National Technical Information Service, Springfield, Virginia 22161, Telephone No. (703) 487-4650. Rush orders may be placed for an extra fee by calling (800) 336-4700.

Title to this invention has been waived under the provisions of the National Aeronautics and Space Act [42 U.S.C. 2457(f)], to the Aluminum Company of America. Inquiries concerning licenses for its commercial development should be addressed to

Manager, Technology Marketing Dept.
Aluminum Company of America
1501 Alcoa Building
Pittsburgh, PA 15219

Refer to LAR-13451, volume and number of this NASA Tech Briefs *issue, and the page number.*

Books and Reports

These reports, studies, handbooks are available from NASA as Technical Support Packages (TSP's) when a Request Card number is cited; otherwise they are available from the National Technical Information Service.

Effects of Radiation on Elastomers

Graphs and tables are presented for synthetic materials.

A report provides data on the effects of radiation on elastomers. It quantifies the effects by giving the minimum radiation levels to induce changes of 1 percent and 25 percent in given properties. Electrical, mechanical, and chemical properties are included in the data. The combined effects of heat and radiation are briefly considered. The data are summarized in a graphic form useful to designers.

Synthetic elastomers are especially prone to radiation damage but are essential for such parts as gaskets, seals, insulation, hoses, diaphragms, and o-rings. Radi-

ation tends to change an elastomer from a rubbery material to a brittle one that no longer fulfills its functions.

Graphs show the tensile-strength and elongation data for various materials, including fluorocarbons, silicones, and polybutadienes. Curves for the variation in electrical resistivities with radiation doses are also presented for selected elastomers.

Radiation-caused chemical changes are important because optical and thermal systems can become coated and because humans can be poisoned by gases given off by elastomers. The report tabulates outgassing by several elastomers and notes that polychloroprene and styrene/butadiene rubber evolve gases at particularly low rates.

The report calls for more work to define completely the responses of elastomers to nuclear radiation. The effects of radiation dose rates and the synergistic effects of temperature, radiation, and atmospheric constituents should be explored.

This work was done by Frank L. Bouquet of Caltech for **NASA's Jet Propulsion Laboratory**. *To obtain a copy of the report, "Radiation Data on Elastomers for Designers of Spacecraft and Nuclear Power Plants," Circle 120 on the TSP Request Card.*
NPO-16747

Choosing an Alloy for Automotive Stirling Engines

Twenty alloys are evaluated for resistance to corrosion, permeation by hydrogen, and high temperature.

A report describes a study of the chemical compositions and microstructures of alloys for automotive Stirling engines. Stirling engines offer the advantages of high efficiency, low pollution, low noise, and the ability to use a variety of fuels.

In an automotive Stirling engine, tubes containing hydrogen, the working fluid, are heated by flames from the burning fuel. For an adequate rate of transfer of heat to the hydrogen, the walls of the tubes must be no thicker than about 0.75 mm. The tube material must be strong enough to contain the hot, high-pressure hydrogen.

Automotive designs call for a peak hydrogen pressure of 21 MPa. The temperature on the flame side will be about 870 °C. Moreover, the tubes must last for at least 3,500 h under such conditions, corresponding to an engine driving life of 100,000 mi (160,000 km).

In the study, 20 alloys — 14 iron-based, 5 nickel-based, and 1 cobalt-based — were evaluated for resistance to oxidation and corrosion, permeability by hydrogen, and endurance. The iron-based alloys were considered the primary candidates because of their low cost. The nickel-based alloys were regarded as a second choice in case a suitable iron-based alloy could not be found. The cobalt-based alloy was included for comparison but was not a candidate, because cobalt is an expensive strategic material.

An iron-based alloy, CG-27, was selected as the material for Stirling-engine heater tubes. It was the only material that did not fail by creep rupture in engine tests. Moreover, it resisted oxidation and corrosion and formed thin, tenacious oxide layers on its surfaces that act as barriers to permeation by oxygen from outside and by hydrogen from inside the tube.

This work was done by Joseph R. Stephens of **Lewis Research Center**. *Further information may be found in NASA TM-87250 [N86-20541/NSP], "Alloy Chemistry and Microstructural Control to Meet the Demands of the Automotive Stirling Engine."*

Copies may be purchased [prepayment required] from the National Technical Information Service, Springfield, Virginia 22161, Telephone No. (703) 487-4650. Rush orders may be placed for an extra fee by calling (800) 336-4700.
LEW-14609

 Circle Reader Action No. 453

Computer Programs

COSMIC: Transferring NASA Software

COSMIC, NASA's Computer Software Management and Information Center, distributes software developed with NASA funding to industry, other government agencies and academia.

COSMIC's inventory is updated regularly; new programs are reported in *Tech Briefs*. For additional information on any of the programs described here, circle the appropriate TSP number.

If you don't find a program in this issue that meets your needs, call COSMIC directly for a free review of programs in your area of interest. You can also purchase the 1988 *COSMIC Software Catalog*, containing descriptions and ordering information for available software.

COSMIC is part of NASA's Technology Utilization Network.

COSMIC® — *John A. Gibson, Director,* (404) 542-3265
The University of Georgia, 382 East Broad Street, Athens, Georgia 30602

Computer Programs

These programs may be obtained at a very reasonable cost from COSMIC, a facility sponsored by NASA to make computer programs available to the public. For information on program price, size, and availability, circle the reference number on the TSP and COSMIC Request Card in this issue.

Physical Sciences

Four-Dimensional Global Reference-Atmosphere Model

Representative pressures, densities, temperatures, and winds are available for any location.

The Four-Dimensional Global Reference Atmosphere Model (GRAM) computer program was developed from an empirical atmospheric model that generates values for pressure, density, temperature, and winds, from the ground to orbital altitudes. This program can be used to generate values of the atmospheric parameters as functions of altitude along any simulated trajectory through the atmosphere.

The program was developed for design applications in the Space Shuttle program, such as the simulation of reentry trajectories of the external tanks. Other potential applications would be studies of global circulation and diffusion and the generation of plots or data for comparison with the results of such atmospheric-measurement techniques as temperature-vs.-altitude data obtained by satellites and infrasonic measurement of wind as a function of altitude.

The program is an amalgamation of two empirical atmospheric models for the low (25-km) and the high (90-km) atmosphere with a newly-developed latitude- and longitude-dependent model for the middle atmosphere. The high atmospheric region above 115 km is simulated entirely by the Jacchia (1970) model. The Jacchia sections of the program are in separate subroutines so that other thermospheric/exospheric models could easily be adapted if required for special applications.

The atmospheric region between 30 km and 90 km is simulated by a latitude- and longitude-dependent empirical model that is a modified version of the latitude-dependent empirical model of Groves (1971). Between 90 km and 115 km, a smooth transition between the modified Groves values and the Jacchia values is accomplished by a fairing technique. Below 25 km, the atmospheric parameters are computed by the four-dimensional worldwide atmospheric model of Spiegler and Fowler (1972). This set of data is not included. Between 25 km and 30 km, an interpolation is performed between the four-dimensional results and the modified Groves values.

The output parameters consist of components for latitude-, longitude-, and altitude-dependent monthly and annual means; quasi-biennial oscillations; and random perturbations to simulate partially the variability due to synoptic, diurnal, planetary-wave, and gravity-wave variations. Quasi-biennial and random-variation perturbations are computed from parameters determined by various empirical studies and are added to the monthly mean values.

The UNIVAC version of GRAM is written in UNIVAC FORTRAN and has been implemented on a UNIVAC 1110 under control of EXEC 8 with a central-memory requirement of approximately 30K of 36-bit words. The GRAM program was developed in 1976, and GRAM-86 was released in 1986. The monthly data files were last updated in 1986.

The DEC VAX version of GRAM is written in FORTRAN 77 and has been implemented on a DEC VAX 11/780 under control of VMS 4.X with a central-memory

requirement of approximately 100K of 8-bit bytes. The GRAM program was originally developed in 1976 and later converted to the VAX in 1986 (GRAM-86). The monthly data files were last updated in 1986.

This program was written by Dale Johnson of **Marshall Space Flight Center** *and Rhonda S. Blocker of Boeing Support Services. For further information, Circle 24 on the TSP Request Card.*
MFS-28293

Mathematics and Information Sciences

LONGLIB Graphics-Library Program

Curves, maps, histograms, and other graphical outputs can be generated.

The LONGLIB computer program is a set of subroutines designed for plotting vectors on cathode-ray tubes, plotting machines, and dot-matrix and laser printers. LONGLIB subroutines are invoked by program calls similar to standard CALCOMP routines. In addition to the basic plotting routines, LONGLIB contains an extensive set of routines to enable viewport clipping, extended character sets, graphic input, shading, polar plots, and three-dimensional plotting with or without the removal of hidden lines.

LONGLIB capabilities include surface plots, contours, histograms, logarithm axes, world maps, and seismic plots. LONGLIB includes 'master subroutines,' which are self-contained series of commonly-used individual subroutines. When invoked, the master routine initializes the plotting package and plots multiple curves, scatter plots, log plots, three-dimensional plots, and the like, and then closes the plot package, all with a single call.

Supported devices include VT100 terminals equipped with Selanar GR100 or GR100+ circuit boards; VT125's, VT240's, and VT220 terminals equipped with Selanar SG220, Tektronix 4010/4014, Tektronix 4107/4109, or other compatible boards; and Graphon GO-235 terminals. Dot-matrix printer output is available by using the raster-scan-conversion routines provided for DEC LA50 printers, Printronix printers, and high- or low-resolution Trilog printers. Other output devices include QMS laser printers, laser printers compatible with Postscript, and plotters compatible with HPGL. The LONGLIB package includes the graphics-library source code, an on-line help library, scan-converter and metafile conversion programs, and command files for installing, creating, and testing the library.

The latest version, 5.0, is significantly enhanced and has been made more portable. Also, the format of the metafile in the new version has been changed and is incompatible with that of previous versions. A conversion utility is included to port the old metafiles to the new format. Color-terminal plotting has been incorporated.

LONGLIB is written in FORTRAN 77 for batch or interactive execution and has been implemented on a DEC VAX-series computer operating under VMS. The program was developed in 1985 and last updated in 1988.

This program was written by David G. Long of Caltech for **NASA's Jet Propulsion Laboratory**. *For further information, Circle 159 on the TSP Request Card.*
NPO-17443

Divergent-Trailing-Edge Airfoil

A wedge concept is integrated into basic airfoil design.

Langley Research Center, Hampton, Virginia

In previous studies, tests of high-speed airfoils revealed the possibility of significant airfoil technology improvements through the application of trailing-edge design criteria different from those currently used. Small wedges were added to the airfoil lower-surface trailing edges, thereby producing significant increases in effective camber and an attendant compressibility-drag reduction. However, the wedge addition also introduced a base-drag penalty because of increased airfoil trailing-edge thickness. At the same time, design studies identified difficulties associated with flap structural-design constraints due to the supercritical airfoil thin aft end.

The current airfoil design, DLBA 238, was developed to produce an airfoil with superior geometric characteristics and equivalent cruise aerodynamic characteristics when compared to the baseline supercritical airfoil DLBA 032. The "trailing-edge wedge" concept, briefly investigated in previous studies, has been improved by integration into the basic airfoil design for the DLBA 238. In this design, the trailing-edge thickness and maximum thickness were constrained to be the same as those of the baseline DLBA 032. Hence, the base drag-penalty of a wedge is avoided. Additionally, the airfoil upper-surface geometry was held fixed.

The effective camber increase of the divergent trailing edge was offset by increasing the airfoil depth from approximately 50-to 95-percent chord along the lower surface. This increased depth is a significant structural benefit because this is the region of the wing that sets the flap and aileron structural depth. The figure shows geometric comparisons of the airfoil sections. The resulting divergent trailing edge is quite evident. In the flap spar region, the airfoil depth has been increased by 30 percent. Some depth is lost between 95-percent chord and the trailing edge. The resulting thickness is still considered quite reasonable.

Calculated upper-surface pressure distributions are nearly the same for both airfoils. The only notable exception is that the DLBA 238 recovers to a slightly lower pressure at the upper-surface trailing edge. However, a considerable difference is noted in the lower-surface pressure distributions. Increased velocities from approximately 56- to 94-percent chord relate roughly to the region of increased airfoil depth. The lower recompression gradient is nearly linear. Calculated drag-rise characteristics for the two airfoils are, by design, essentially the same, and calculated lift, drag, and pitching-moment characteristics of the two airfoils are quite similar at 0.74 mach. Experimental drag-rise characteristics show a slight drag benefit for DLBA238.

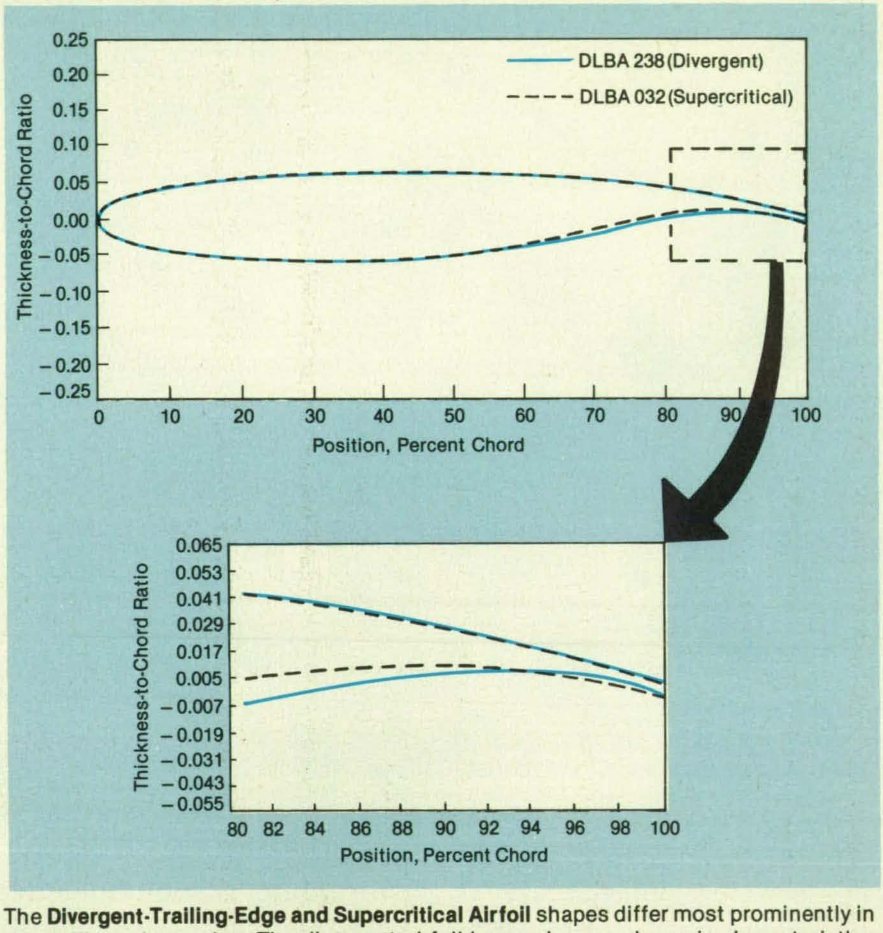

The **Divergent-Trailing-Edge and Supercritical Airfoil** shapes differ most prominently in the trailing-edge region. The divergent airfoil has cruise aerodynamic characteristics essentially equivalent to those of the supercritical airfoil.

This work was done by Preston A. Henne and Robert D. Gregg of McDonnell Douglas Corp. for **Langley Research Center**. *No further documentation is available.*

Title to this invention has been waived under the provisions of the National Aeronautics and Space Act [42 U.S.C 2457(f)], to the McDonnell Douglas Corp. Inquiries concerning licenses for its commercial development should be addressed to

Charles Hughes, H312, HQ-75-775
McDonnell Douglas Corp.
P.O. Box 516
St. Louis, MO 63166.

Refer to LAR-13374, volume and number of this NASA Tech Briefs *issue, and the page number.*

Relief Valve Opens and Closes Quickly

The valve reseats after a small pressure drop.

Lyndon B. Johnson Space Center, Houston, Texas

A relief valve opens quickly to relieve excess pressure and closes quickly when the pressure drops slightly below the relief pressure. Although the valve was designed for use aboard the Space Shuttle to vent pressurized hydrazine to vacuum, the valve concept may be useful in industrial applications where rapid opening, rapid closing, or low susceptibility to blockage by the vented fluid is required.

The valve is connected to the pressurized system through its externally threaded end, through which a channel leads to discharge ports (see figure). Normally, Belleville-spring washers push the relief-valve poppet forward until it bottoms on the sealing surface, compressing the O-ring so that it forms a seal at the sealing surface, the O-ring groove, and the discharge ports.

Under moderate pressure, the working fluid flows around the poppet stem, and the differential pressure forces the O-ring into the crack between the poppet and the sealing surface. In this condition, a tight seal is maintained. As pressure increases further, the poppet begins compressing the Belleville-spring washers, and the O-ring moves into the gap between the sealing surface and the poppet face, still maintaining a tight seal.

When the pressure rises to the preset relief pressure, the poppet compresses the washers more. As the O-ring is forced farther into the gap, it uncovers one of the discharge ports with a snap action, allowing the pressurized fluid to be expelled. Additional increases in pressure move the poppet farther and push the O-ring farther into the gap, uncovering additional discharge ports. At the highest pressure, the O-ring is forced completely out of its groove, uncovering all the discharge ports, but still maintaining a seal around the outside of the poppet.

As the pressure decreases, the combination of spring force on the poppet and O-ring elasticity drives the ring back into its groove, and thus the valve snaps closed. The valve reseats at only 5 to 10 lb/in.^{2} (35 to 69 kPa) below the relief pressure.

The reseating is fast because the primary movement is in the O-ring rather than the poppet. For example, as the pressure is raised from zero to a relief pressure of 1,000 lb/in.^{2} (6.89 MPa), the poppet moves a total of only 0.004 in. (0.1 mm). When the valve is reseated at 990 lb/in.^{2} (6.83 MPa), the poppet has retracted only 0.0005 in.

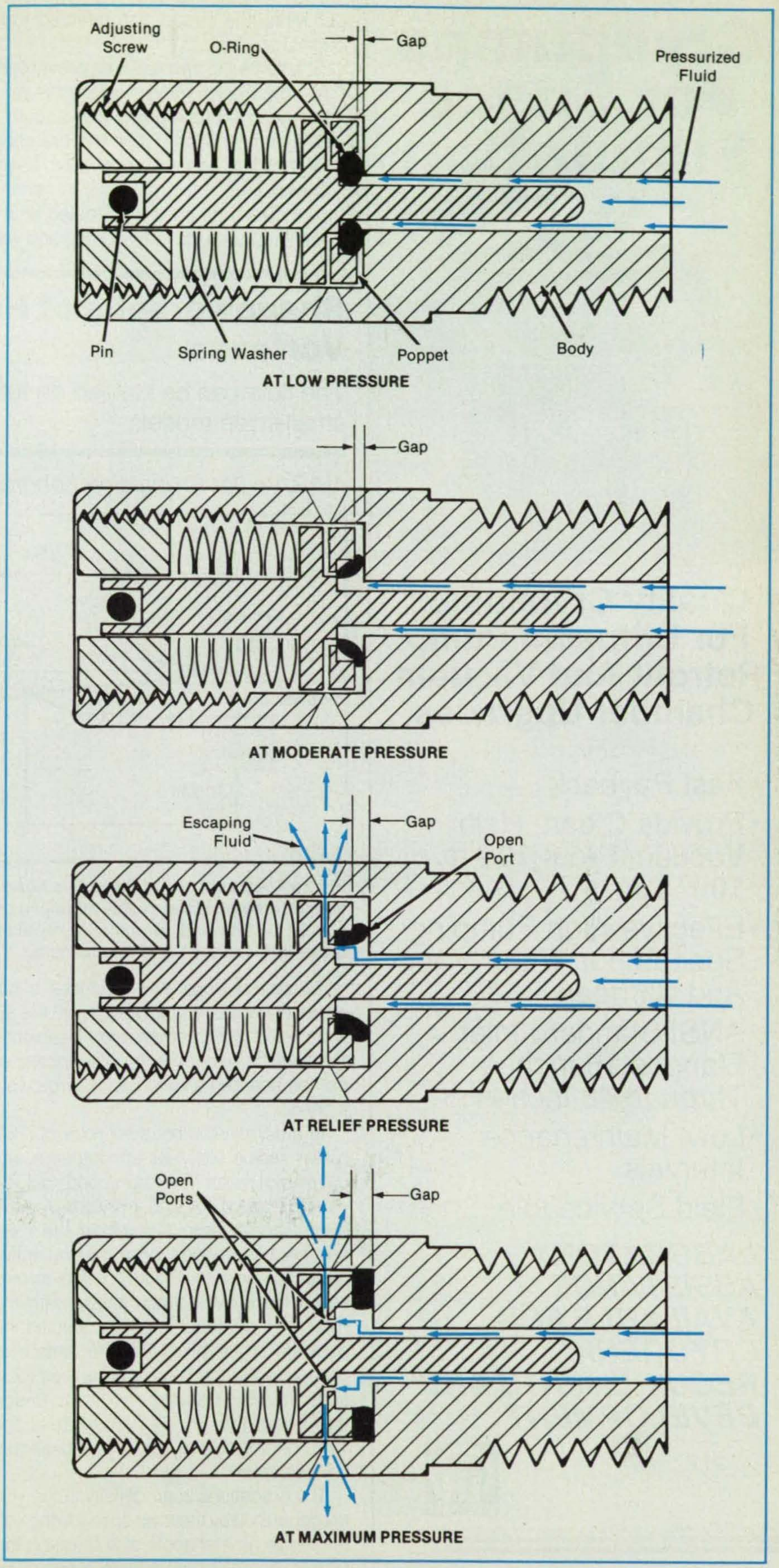

The **O-Ring Exposes One or More Ports** under high pressure, thus releasing excess pressurized fluid. The adjusting screw is used to change the compression on the Belleville-spring washers and thus to set the pressure at which the valve opens.

(0.013 mm). At a pressure of 500 lb/in.^{2} (3.5 MPa), the poppet has returned to its original position.

The following two features prevent the fluid from freezing and blocking the relief valve when it discharges into a vacuum:

1. The discharge-port channels are short, and the fluid passes through them at high speed.
2. The discharge ports are located on the low-pressure side of the O-ring and vent directly to the outside. As a consequence, the springs and the other parts that engage in relative motion are not wet by the fluid and are therefore unlikely to become stuck with frozen fluid.

This work was done by Paul A. Svejkovsky of Northrop Services, Inc., for **Johnson Space Center**. *For further information, Circle 114 on the TSP Request Card.*
MSC-21209

Shadowgraphs of Helicopter-Rotor-Tip Vortexes

The flow can be studied on full-size rotors instead of on small-scale models.

NASA's Jet Propulsion Laboratory, Pasadena, California

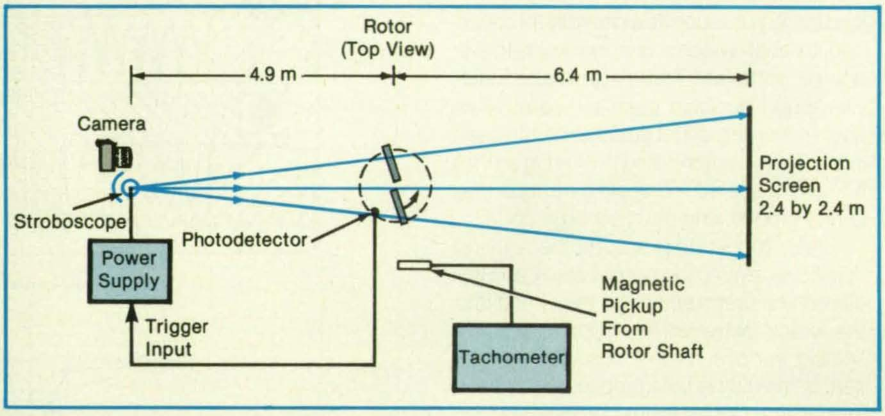

Figure 1. A **Stroboscope Projects a Shadow Image** of a helicopter rotor on a large, square screen. A commercial, highly reflecting projection screen is used; simply projecting the image on a white wall, for instance, would not yield enough light for photographing the vortexes with a standard 35-mm camera.

An optical apparatus produces a full-scale or larger shadowgraph of the tip vortexes of a helicopter rotor. Developed for outdoor experiments, the apparatus can be adapted also to use in large wind tunnels.

In a demonstration, a tail rotor of 0.65-meter radius was set up outdoors and driven by a motor. The rotor speed could be varied from 1,900 to 3,200 rpm. A point stroboscopic lamp illuminated the rotor and cast its shadow on a retroreflective projection screen (Figure 1). The stroboscopic lamp was synchronized with the rotor by a photodetector that sensed the passage of the blade tip. The lamp thus flashed when the tip passed a fixed location, thereby freezing the rotor image throughout the test. A camera near the lamp photographed the image projected on the screen.

The gradations in air density in the vortex generated by the rotor tip made the vortex visible as a shadow of a spiral on the screen. In the demonstration, a hair dryer was used to blow hot air to make the flow around vortex cores visible. The cores are visible (Figure 2) from natural density

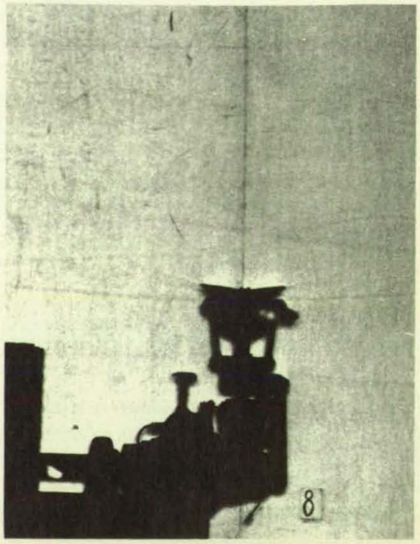

Figure 2. This **Shadowgraph** was taken with the apparatus of Figure 1. The flow around the vortex at the right was made visible by hot air from a hair dryer. The rotor tip in this shadowgraph faces the viewer. At the extreme right and left, the shadows appear darker because light rays pass tangentially through the vortexes. The mach number at the rotor tips is 0.64 and the angle of attack is 12°.

There's profit at the end of this tunnel. And it could be yours.

If your product, and profits, can be improved with wind tunnel testing, Boeing aerodynamic testing facilities are at your service through Boeing Technology Services. BTS specialists will work with you to understand your needs precisely, and then will help you tap into Boeing resources efficiently.

Boeing has subsonic, transonic, supersonic and hypersonic tunnels with on-line systems that deliver final plotted data within seconds. Our special services also include aeroacoustic testing, a captive trajectory system and a separate airflow calibration facility.

We can test your model. Or design and build one to your specifications. Or provide a complete package.

Boeing specialists also can help you develop a testing program to meet your technical requirements, timetable and budget. And we can handle projects that are classified or that require security for proprietary reasons.

For a full description of the Boeing aerodynamic testing facilities and services available to you, call Paula Royalty, Marketing Manager at (206) 277-4600. Or write to Boeing Technology Services, P.O. Box 3707, M/S 9R-28, Seattle, WA 98124-2207.

BOEING

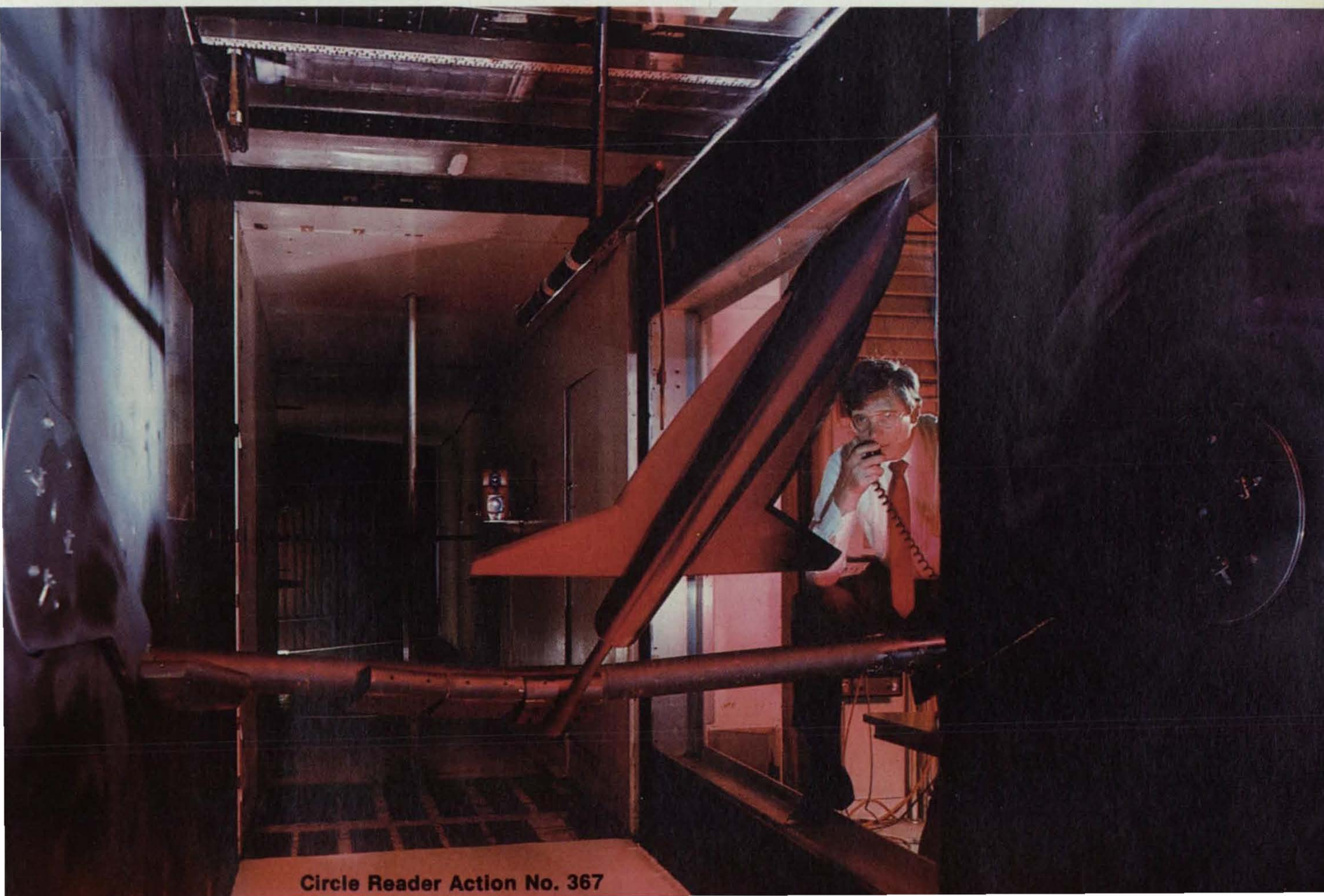

Circle Reader Action No. 367

changes, however.

In the demonstration, the vortexes were visible for a range of tip mach numbers from 0.38 to 0.64. The angles of attack ranged from 4° to 14°. Visibility improved with speed and angle of attack; at higher tip speeds, visibility would probably be even better. Variation of the distance between the rotor and screen was found to have little effect on the size and clarity of the image. Shadowgraphs at 4.4- and 6.4-meter separations looked similar. Even greater distances could be used with good results.

Two such optical systems could be set up with their axes oriented perpendicularly. It would then be possible to obtain information on tip vortexes in three dimensions.

This work was done by Shakkottai P. Parthasarathy, Young I. Cho, and Lloyd H. Back of Caltech for **NASA's Jet Propulsion Laboratory.** *For further information, Circle 135 on the TSP Request Card.* *NPO-16593*

Laminar-Separation Sensor

The sensor detects flow reversal in a boundary layer.

Langley Research Center, Hampton, Virginia

The accurate determination on laminar-flow surfaces of the location and cause of the boundary-layer transition from laminar to turbulent flow is important in basic research for the validation of theory and in developmental testing for the validation of design. Laminar boundary layers form in an accelerating flow with velocity components in the downstream direction. When the local flow decelerates, a laminar-separation bubble can form in the boundary layer. Within the bubble, at the surface, the flow direction is reversed so that the local flow is in the upstream direction. The resultant velocity profile is inflected. Transition to turbulence may occur along the free shear layer over the top of the bubble. The existence of laminar separation in the boundary layer may thus be detected using a method that senses the direction of local flow at the surface.

The laminar-separation sensor provides a means for detecting a laminar-separation bubble by the use of a very thin, surface-mounted sensor. The sensor consists of a flush array of three proximate thin films, as shown in the figure. The middle film is electronically heated by means of a constant-temperature anemometer (CTA). The outer films, one upstream and one downstream of the middle film, are incorporated into a bridge circuit to respond as resistance thermometers.

When the sensor is exposed to flow, the heat from the middle film is transferred to either the upstream or downstream resistance thermometer, depending on the direction of the flow. The differential heating of the resistance thermometers is measured by a differential amplifier, and the direction of flow becomes evident from the direction of the signal output. By the proper selection of the film spacing (h), the sensor signals can be made to respond to the smallest laminar-separation bubbles of practical interest. The approximate spacing between elements for typical high-speed subsonic applications is 0.0625 in. (1.59 mm) or less. The orientation of the long dimension of the sensing element in the spanwise direction provides for greater

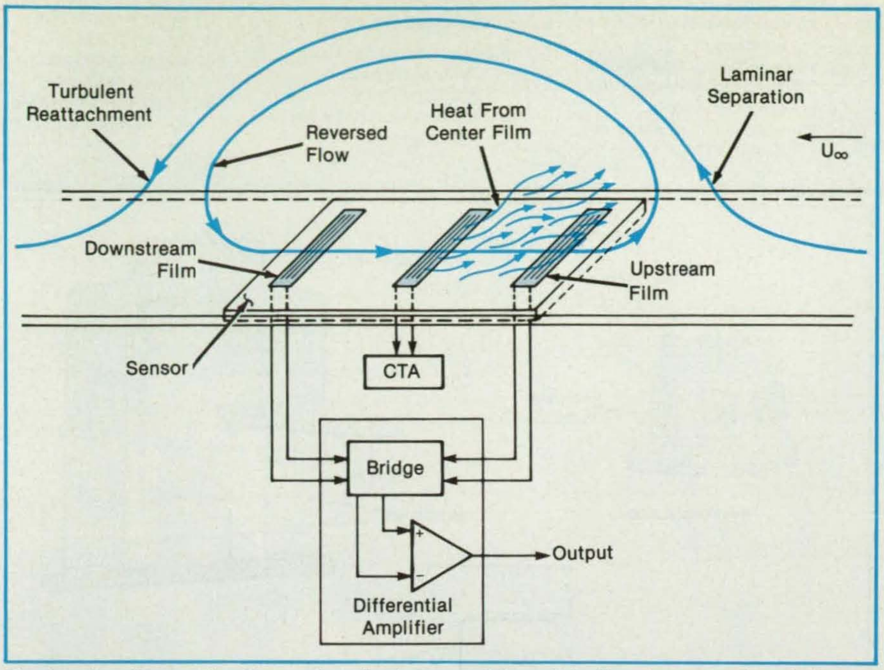

The **Laminar-Separation Sensor** is a flush array of three thin-film elements placed along a streamline.

sensitivity of the element to small laminar bubbles.

The three elements consist of a series of polymer-backed thin-film nickel sensors that are dissected to create a predetermined sensor configuration and electrical resistance. They are then placed in a matrix on a thin polymer sheet and bonded with a suitable adhesive. The resulting sensor thickness is small enough not to cause boundary-layer transition to turbulence in most applications of interest. The CTA's used to heat the middle films are commercially available units, and the film elements are designed to be compatible with these units.

The nominal resistance of a film is 6.5 ohms or greater to provide the necessary sensitivity. Since the sensors can be manufactured with very uniform resistances, several middle films can be multiplexed onto one anemometer with no adjustment to the system. The sensors can be installed in a staggered fashion or fabricated into one continuous multielement strip of sensors, providing for the measurement of the streamwise movement of laminar separation with changes in the angle of attack.

This sensor is easier to install and involves less circuitry than do systems involving three surface-buried hot wires. In flight at high Reynolds numbers, where the length of a laminar separation bubble may be quite small, this sensor provides the only known surface-mounted means for positively identifying the presence of laminar separation as a cause of boundary-layer transition.

This work was done by Bruce J. Holmes, Harlan K. Holmes, Thomas C. Moore, Gregory S. Manuel, and Cynthia C. Croom of **Langley Research Center** *and Debra L. Carraway of Old Dominion University. For further information, Circle 25 on the TSP Request Card.*
LAR-13463

Machinery

Rim-Supported Turbine Seal

An interstage seal would accommodate a large pressure drop across a vane stage.

Marshall Space Flight Center, Alabama

A proposed interstage seal for a turbine would be supported by the rim of the turbine disk. The seal concept was developed for such small rocket turbines as liquid-oxygen pumps. Usually, interstage seals in these turbines are positioned by snap lands and held in place by tie bolts. The new seal would reduce the number of parts and simplify the rotor configuration.

The seal concept would keep diaphragm-type areas small and thus ensure low axial loads on vanes, because the sealing surfaces are close to the innermost gas-flow path. It is thus well suited to turbines with high pressure drops across vane stages.

In the seal configuration shown in the figure, two blade stages would be supported by a single disk, which is broached over the entire width of the rim. Although a full ring seal is envisioned, segments could be used, as many as the number of blades if necessary.

This work was done by Kent O. Longenecker of United Technologies Corp. for **Marshall Space Flight Center**. *No further documentation is available.*

Inquiries concerning rights for the commercial use of this invention should be addressed to the Patent Counsel, Marshall Space Flight Center [see page 18]. Refer to MFS-28112.

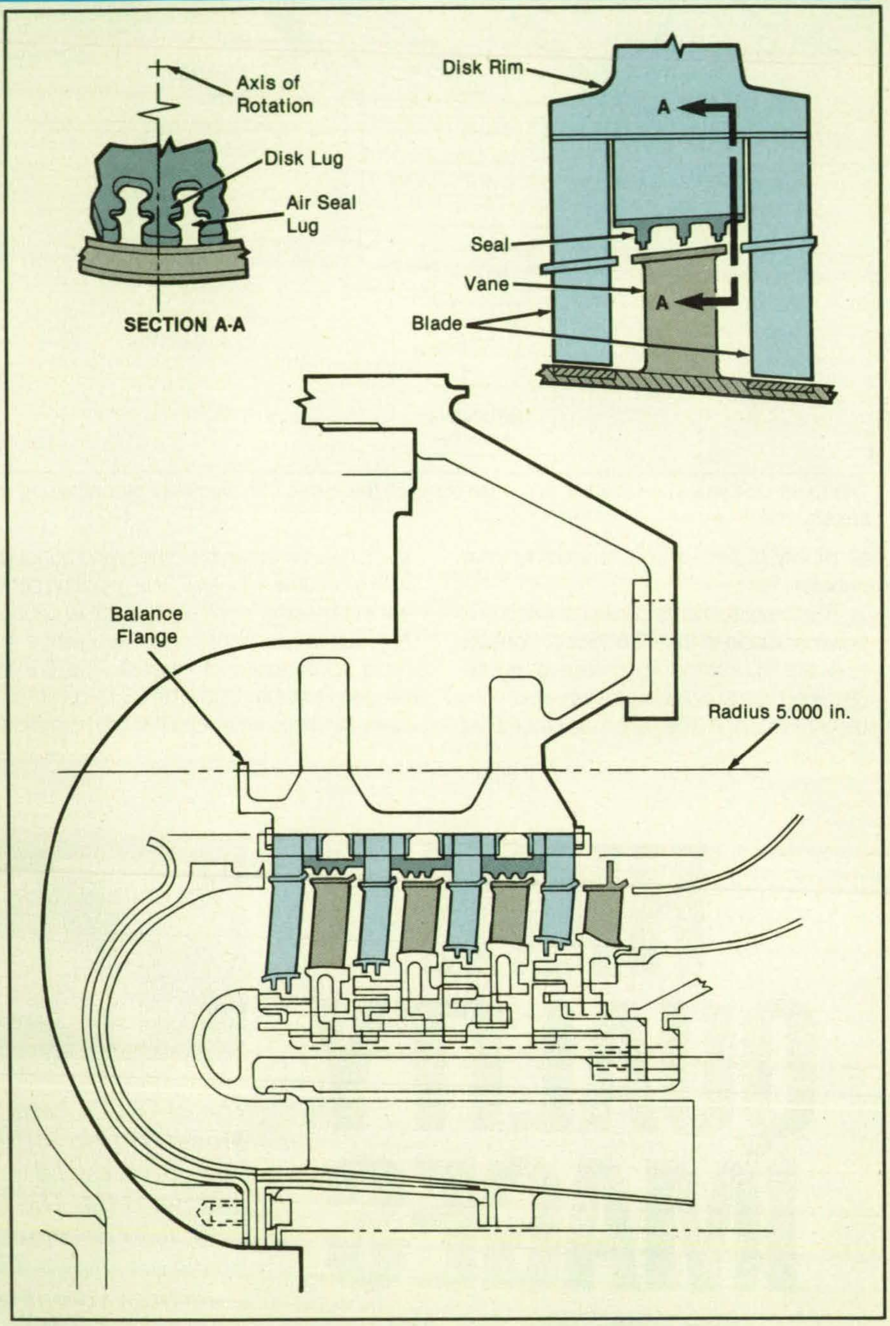

The **Sealing Surfaces Are Close** to the inner diameter of the gas-flow path.

Self-Centering Reciprocating-Permanent-Magnet Machine

The coil can be sized for the required efficiency and power.

Lewis Research Center, Cleveland, Ohio

A new design for a monocoil reciprocating-permanent-magnet electric machine provides a self-centering force. In previous machines of this type, the length of each repeatable section had to be equal to the length of a stroke. This limited the amount of copper that could be used for winding a coil. The only way to increase power at a given plunger diameter was to use multiple coils. Further, the arrangement of magnets on the plunger was such as to get the plunger locked at either extreme of its travel, because in these positions, the plunger magnets are directly under corresponding poles on the stator. Thus, in the absence of current in stator coils, there was a decentering force on the plunger, which gave rise to an undesirable negative-spring effect in the dynamics of the overall reciprocating system.

In the new design, the magnets are ar-

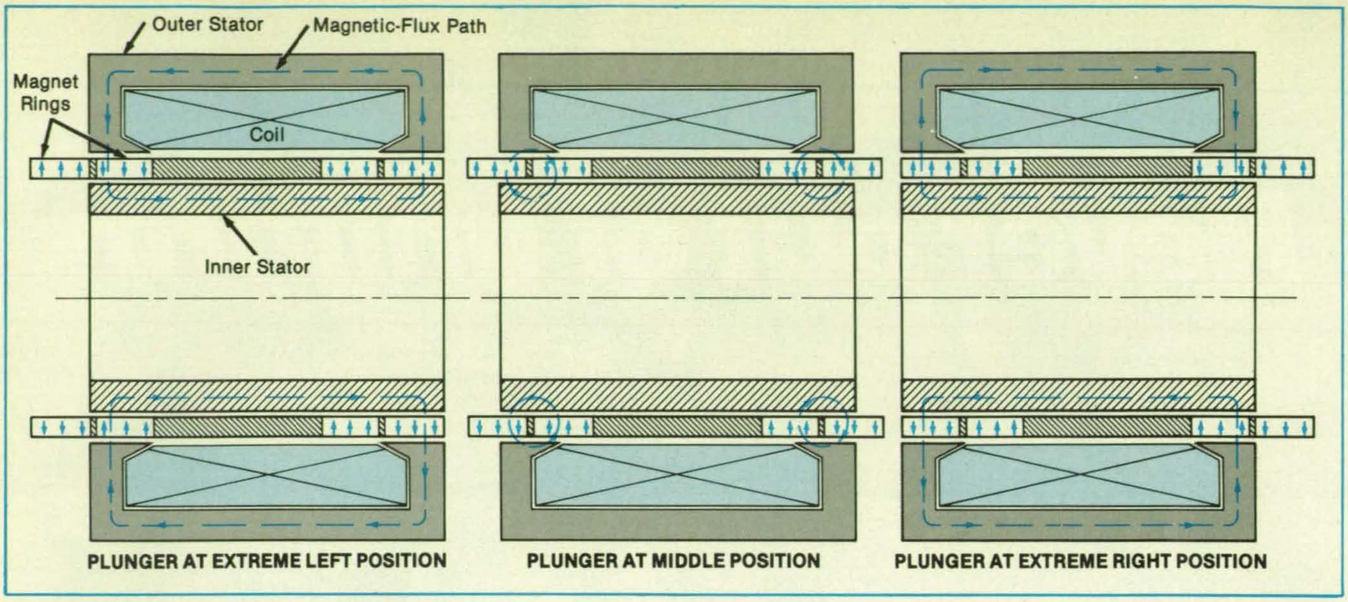

The **Linear Permanent-Magnet Electrical Motor** includes an outer stator, an inner stator, and a permanent-magnet plunger that oscillates axially between extreme left and right positions.

ranged to produce a centering force. The new design allows the use of only one coil of arbitrary axial length. Thus, the axial length of the coil can be chosen to provide the required efficiency and power output.

The figure shows the basic features of the machine. It has three separate parts: the outer stator, the movable plunger carrying radially magnetized magnets, and the inner stator. The inner stator has the shape of a cylindrical sleeve. The outer stator is shaped to receive a doughnut-shaped coil. Both stators are radially laminated to prevent the induction of circumferential electric currents. They are made of high-permeability, high-electrical-resistivity material like electrical steel.

The moving plunger includes four cylindrical rings of radially-polarized permanent magnets of samarium cobalt or other strongly magnetic material. Because the magnets are structurally very weak, they are held in the ring configuration by a lightweight, structurally-strong nonmagnetic material. All of these parts are concentric to each other: The moving plunger reciprocates in the annular space between the inner and outer stators.

The left side of the figure shows the plunger in the extreme left position and the corresponding magnetic-flux paths. When the plunger is moved to the extreme right, the flux paths are as shown at the right side of the figure. The middle of the figure shows the flux paths when the plunger is in the middle position. At this position, the net flux linking the coil is zero. When the plunger is reciprocated sinusoidally by the engine, the flux linking the coil varies sinusoidally, and a voltage is induced in the coil.

This work was done by Suresh Bhate and Nick Vitale of Mechanical Technology Inc. for **Lewis Research Center**. *No further documentation is available. LEW-14263*

Yaw Control at High Angles of Attack

Hinged, conformal forebody strakes provide control when rudders become ineffective.

Langley Research Center, Hampton, Virginia

In a conventional airplane, the rudder becomes ineffective when the craft is operating at a very high angle of attack because of massive flow separation on lifting surfaces. The use of articulated, conformal forebody strakes provides yaw control at such high angles of attack.

The device consists of a symmetric pair of longitudinally hinged strakes designed to fold completely into the forebody contour. The strakes can be rotated individually out into the external flow. The selective deployment of one of the strakes forces a stable, asymmetric vortex pattern on the forebody at high angles of attack, thereby generating a sideward force component. The sideward force, acting considerably forward of the craft center of gravity, produces a yawing moment. Reliance on forced asymmetry of forebody-vortex separation allows this yawing moment to continue unabated to high angles of attack, unaffected by flow separation on wings and aft surfaces.

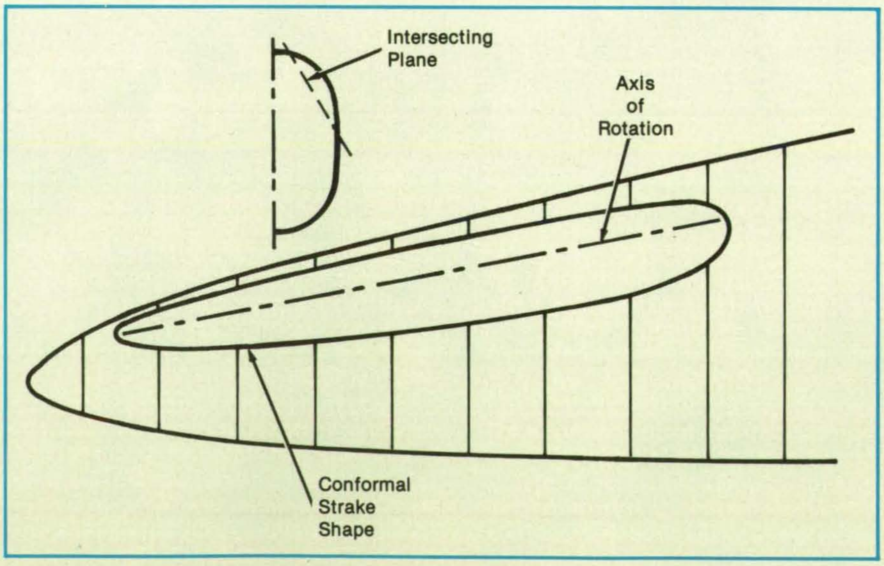

Figure 1. **Conformal Strake Shape** is generated by an oblique plane intersecting the forebody side.

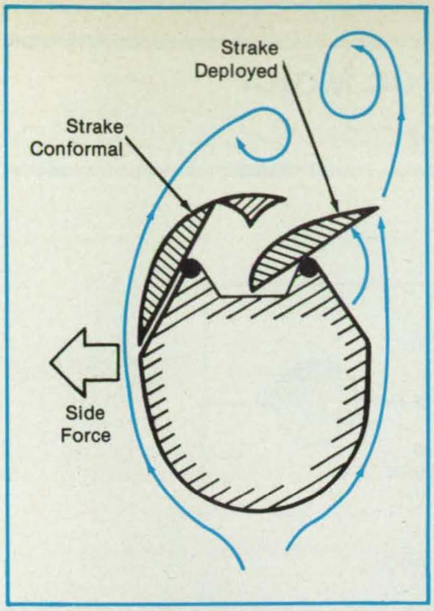

Figure 2. The **Asymmetric Flow** produced by a deployed strake generates a sideward force that causes the aircraft to yaw.

Figure 1 depicts a conformal strake generated by means of an oblique plane intersecting through the upper quarter to one side of the forebody plane of symmetry; a mirror image of the strake geometry is generated on the other side. The strakes are pivoted to rotate about a longitudinal axis contained in the respective intersection planes. Figure 2 shows a typical cross section of the forebody with one strake deployed. The consequent asymmetric separation of the crossflow at high angles of attack produces a skewed pressure distribution around the forebody circumference, which creates a net side force as indicated. Increasing the strake deflection causes progressive side force increments, thus providing a means of yawing moment modulation.

The principle is equally valid, as demonstrated in wind-tunnel tests, for forebodies of triangular and other noncircular cross sections. The forebody sideward force is maintained at angles of attack well above the typical limit of rudder effectiveness. Wind-tunnel tests have confirmed the effectiveness of this arrangement at angles of attack between 10° and 70°, and sideslip angles to 20°.

This work was done by Daniel G. Murri of **Langley Research Center** *and Dhanvada M. Rao of Vigyan Research Associates, Inc. No further documentation is available.*

In accordance with Public Law 96-517, the contractor has elected to retain title to this invention. Inquiries concerning rights for its commercial use should be addressed to

Dhanvada M. Rao
Vigyan Research Associates, Inc.
30 Research Drive
Hampton, VA 23666-1325

Refer to LAR-13472, volume and number of this NASA Tech Briefs *issue, and the page number.*

Gravity Compensation Technique Uses Small dc Motor

The motor is a lighter and more compact alternative to a counterbalance.

Ames Research Center, Moffett Field, California

A small dc servomotor powered by a simple constant-current source and with suitable gearing can be used to cancel the effect of gravity upon the load. The motor can be used in a variety of mechanical systems where a load is to be positioned or accelerated in the vertical plane.

Vertical positioning servosystems, robot arms, and drafting-table arms work better when the energy needed for a required movement is the same for both upward and downward motion. Generally, it is desirable that these systems or arms remain stationary when no motion is called for. Conventionally, these requirements are achieved by means of a counterbalance, some form of spring, or by offset-biasing a servoamplifier.

The dc motor offers the potential of lower weight and smaller size than a counterbalance, greater longevity than a constant-force spring, and servoamplifiers that are enabled to have symmetrical performance in both directions. Furthermore, the system is easily adjusted to accommodate changes in the weight of the load.

For example, in the lead-screw and ball-nut positioning system shown in Figure 1, the gravitational force acting on the load tends to cause the lead screw to rotate — the weight of the load applies torque to the lead screw. A supplementary dc motor is geared to the lead screw and powered so that a countertorque is applied. When this torque is set equal in magnitude but opposite in direction to that induced by the load, the effect of the load is cancelled. This holds true for both static and a wide range of dynamic conditions.

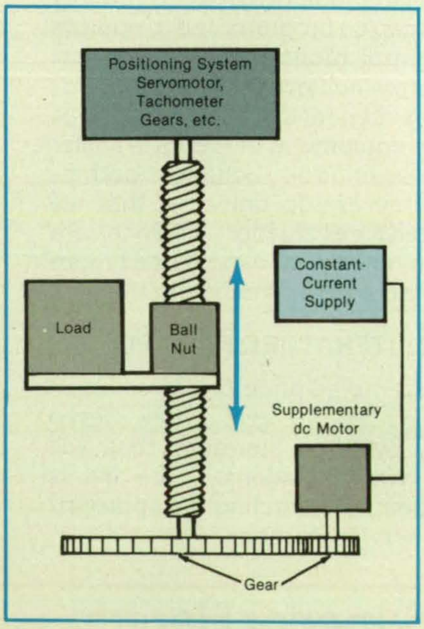

Figure 1. A **Lead-Screw Positioning System** has a load counterbalanced by a small supplementary motor powered by a constant-current source.

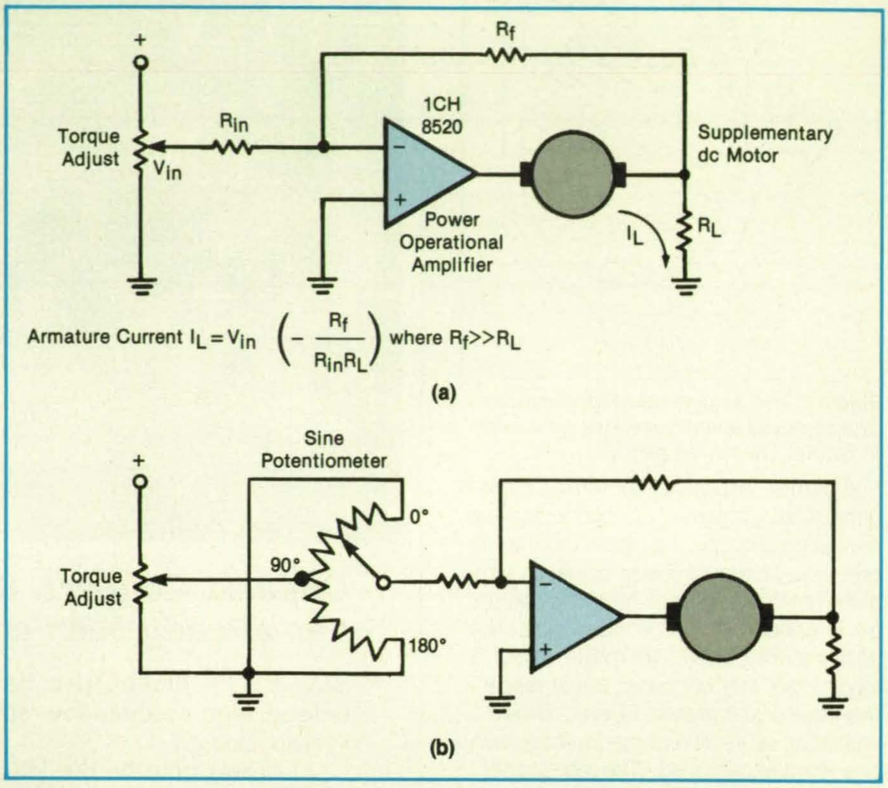

Figure 2. A **Supplementary dc Motor and a Method of Counterbalancing** are shown. Part (a) shows a 2-A constant-current power supply for a dc motor. A modification to this circuit (b) enables counterbalancing a vertically pivoting arm. The sine-potentiometer wiper is mechanically coupled to the arm and therefore positioned by it.

This occurs because dc servomotors in general are so designed that with a constant armature current they generate an almost constant torque over wide speeds and load range, and the power supply [see Figure 2(a)] for the supplementary dc servomotor is of the type that supplies a constant current. The output level of the supply is adjustable; therefore, adjusting this current sets the countertorque.

To enable the use of the smallest motor and most economical power supply, the gearing is chosen to give a large reduction ratio, but there are limitations. Assuming adequate torque is provided, the reduction-ratio limit is determined by the ability of the supplementary motor to accelerate itself and its gears at a high enough rate so that the positioning system motor has no tendency to drive the supplementary one.

In a lead-screw-positioning-system application, a 1 in.$^{-3}$ (16 cm^{-3}) sized motor, with a gear reduction of 5:1 and using the power supply shown, was employed to counterbalance different loads of up to approximately 8 lb (36 N).

This method of counterbalancing can also be applied to a vertically pivoting arm. The only changes required are the addition of a center-tapped "sine potentiometer" to the constant-current supply and mechanically coupling the potentiometer wiper to the arm [see Figure 2(b)].

With the arm horizontal, the supplementary motor torque is initially adjusted for counterbalance. Then, as the arm is driven by the positioning system, the small dc motor current varies as the sine of the arm angle, the current ranging from a maximum when the arm is horizontal to zero when vertical. For a situation in which the arm is required to rotate through 360°, a second potentiometer would be ganged to the first but staggered by 180°. An alternative to sine potentiometers could be a digital encoder, microprocessor, and D/A package. (It should be noted that counterbalancing ceases the moment that current to the supplementary motor is cut off.)

This work was done by Richard Hollow of **Ames Research Center**. *For further information, Circle 21 on the TSP Request Card.*

Inquiries concerning rights for the commercial use of this invention should be addressed to the Patent Counsel, Ames Research Center [see page 18]. Refer to ARC-11525.

Improved Robot-Joint Calculations

Modified Denavit-Hartenberg parameters are better for locating successive joint-axis systems.

Langley Research Center, Hampton, Virginia

The motion of a robot hand is the result of movements of joints in the robot arm. To transform commands from the operator to the robot hand into movements of joints and to pass information from sensors along the arm, the relative locations of successive joint-axis systems must be known. By far, the most popular way to describe the relative location and orientation of one joint-axis system with respect to another is to use the well-known Denavit-Hartenberg parameters.

However, a recent justifiable criticism is that one of these parameters approaches infinity when two successive joints have nearly-parallel rotational axes. Geometrically, this parameter removes the joint axis an excessive distance from the robot arm; computationally, this large parameter leads to an ill-conditioned transformation matrix.

A simple modification in the location of this axis system easily overcomes this disadvantage. This modification results from the insistence that a transverse vector between successive joint rotational axes be perpendicular to one of the rotational axes instead of to both axes. This simple modification leads to modified Denavit-Hartenberg parameters that favorably locate successive joint-axis systems.

In an example of a robot arm with elbow and shoulder joints (see figure), the regular and modified Denavit-Hartenberg parameters were extracted by an algebraic method with simulated measurements of three different locations of a point on the robot arm. For small misalignments of the elbow-and shoulder-joint rotational axes from a parallel condition, the regular Denavit-Hartenberg parameters locate the elbow-joint system far away from the robot arm; the modified parameters locate the axis system at the desired place on the robot arm. In addition, for a given accuracy of the measurements used in the parameter-extraction process, the extracted values for the Denavit-Hartenberg parameters yielded considerably larger errors than did the extracted values for the modified parameters. It is evident that the modified parameters provide a more natural location of successive joint-axis systems and would be useful in the industrial calibration of robot arms.

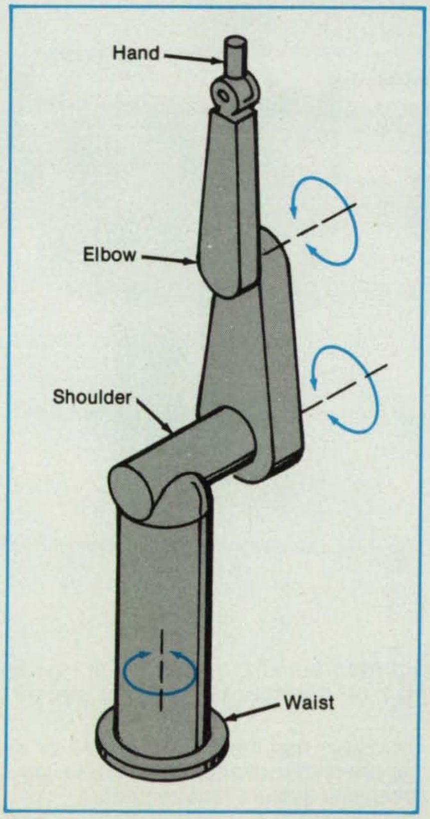

A Robot Arm With Elbow and Shoulder Joints was used as a mathematical model to test the modified Denavit-Hartenberg parameters.

This work was done by L. Keith Barker of **Langley Research Center.** *Further information may be found in NASA TP-2585 [N86-27953/NSP], "Modified Denavit-Hartenberg Parameters for Better Location of Joint Axis Systems in Robot Arms."*

Copies may be purchased [prepayment required] from the National Technical Information Service, Springfield, Virginia 22161, Telephone No. (703) 487-4650. Rush orders may be placed for an extra fee by calling (800) 336-4700. LAR-13682

Books and Reports

These reports, studies, handbooks are available from NASA as Technical Support Packages (TSP's) when a Request Card number is cited; otherwise they are available from the National Technical Information Service.

Predicting Life and Reliability of a Rotating Disk

The effects of design variables, temperature gradients, and speeds are examined.

A report presents a study of a generalized method for the prediction of the fatigue life and the reliability of a rotating disk. The method incorporates the computation of the life, at a given probability of survival, of elemental stressed volumes within the body of the disk.

The effects of speed and of such design variables as the diameter and thickness of the disk and the size, number, and location of boltholes on the life of the disk were determined. An investigation into the effect of a radial temperature gradient as well as the accompanying induced thermal stresses on the relative life of the disk was also performed. In addition, such characteristics of the material as the Weibull modulus and fatigue limit were incorporated into the method.

From the analysis, the concept of a dynamic-speed capacity, N_0, is introduced. This is defined as the speed that would produce a theoretical life of one million stress cycles at a 90-percent probability of survival. For any speed, N, the life, L, for a given disk at a 90-percent probability of survival is

$$L = \left(\frac{N_0}{N}\right)^{14.3} \times 10^6$$

This method would be useful in the analysis, design, and development of disks for aircraft-engine turbines and compressors and flywheels for industrial and automotive applications.

This work was done by Erwin V. Zaretsky of **Lewis Research Center** *and Todd E. Smith and Richard August of Sverdrup Technology, Inc. Further information may be found in NASA TM-88883 [N87-13755/NSP], "Effect of Design Variables, Temperature Gradients, and Speed of Life and Reliability of a Rotating Disk."*

Copies may be purchased [prepayment required] from the National Technical Information Service, Springfield, Virginia 22161, Telephone No. (703) 487-4650. Rush orders may be placed for an extra fee by calling (800) 336-4700.
LEW-14582

Cepstral Analysis Detects Ball-Cage Wear

Vibrational frequencies symptomatic of wear are found quickly.

A collection of letters and reports discusses an application of cepstral analysis to the diagnosis of wear in ball-bearing cages in rotating machinery. When the cepstral analysis is performed with the help of a suitable analog computer or digital computer and program, the ball-cage vibrations and changes in vibrations that are symptomatic of wear can be detected earlier in a test than they can be by more conventional methods based on strain-gauge measurements.

Although there are several alternative definitions of the cepstrum, it can be said in general that a cepstrum is a spectrum of a logarithmic power spectrum. Because of this, a peak in the cepstrum indicates periodicity in the spectrum; usually, this signifies a family of harmonics at equal frequency intervals.

Cepstral analysis is particularly useful in diagnoses of gearboxes and rolling-element bearings because the merging of data on vibrations at harmonically related frequencies into a single cepstral peak

makes it easier to assess qualitatively, at a glance, what changes are taking place at a multitude of significant points in the spectrum. The amplitude of a cepstral peak is a function of the individual harmonic amplitudes. Changes in the number and strengths of the harmonics, which usually indicate deterioration of the item under test, cause fluctuations in the amplitude of the cepstral peak. Thus, to detect wear during a test, it may be necessary to watch for changes in only one or a few cepstral peak(s), whereas it would be necessary to monitor many peaks in a spectrum.

For example, in the case of a turbopump ball-bearing cage that was the object of these studies, it was found that wear could be monitored by observing only the cepstral peak that corresponds to the fundamental frequency of the ball-cage vibrations: subsequent cepstra clearly showed the rise of the ball-cage frequencies and their modulation effects relative to the cepstral peak due to the rotation. This represents a great reduction in the analytical effort required by the previous spectral-analysis technique, which required the generation and examination of calibrated spectral isoplots throughout a test.

This work was done by Gary E. Weese and Michael G. Hine of Rockwell International Corp. for **Marshall Space Flight Center**. *To obtain a copy of the collection, "Ball-Cage Frequency Detection Using Cepstrum Analysis," Circle 130 on the TSP Request Card.*
MFS-29187

Solid Rocket With Integral Case

The propellant and case would be manufactured together.

A report describes a proposed solid-propellant rocket motor. The case of the motor would be integrated with the propellant and would itself burn and produce thrust as the propellant combustion proceeds outward. The proposed motor would increase the payload-weight capacity.

During manufacture, structural fibers would be embedded in a poured propellant matrix. When the matrix hardens, the fibers and matrix would form an integrated propellant and case. When the rocket motor is ignited, the stress created by the pressure of the burning core would be passed to and absorbed by the fibers. The propellant cylinder would be covered only by a thin shell, which would protect against fire and damage during handling.

The propellant would be formulated so that it produces a high pressure and thrust at lift-off. Later, as the burning region includes the integrated case, the formulation would burn more slowly, reducing internal pressure on the then-weaker wall. The rocket motor would thus be strong and stiff and would dampen vibration most effectively during lift-off and initial flight, when loads are highest.

On the Space Shuttle, the payload capacity of 32,000 lb (14,500 kg) would be increased by about 72 percent by use of the new solid rockets. To achieve this improvement, however, the weight of the integrated case would have to be no greater than that of the standard solid rocket motor with graphite/epoxy case. The total specific impulse will have to be as large as that of the standard case and propellant. In addition, the outer protective shell and any unburned integrated-case material would have to weigh no more than 20 percent of the standard case weight. The potential increase in payload would be even larger for launch vehicles that use only solid rocket motors, particularly multistage vehicles.

This work was done by Carleton J. Moore of **Marshall Space Flight Center**. *To obtain a copy of the report, "Integrated Case and Propellant Solid Rocket Motor," Circle 39 on the TSP Request Card.*

Inquiries concerning rights for the commercial use of this invention should be addressed to the Patent Counsel, Marshall Space Flight Center [see page 18]. Refer to MFS-28263.

Rotary Joint for the Space Station

Earthbound solar-power systems could also benefit from this development.

Solar-power-conversion units for the Space Station must be capable of tracking the Sun at an approximate orbital rate of 1 revolution per 94 minutes. The most critical mechanism aboard the station will be the rotary joint that performs this tracking function, because it must position the solar photovoltaic receiver and the solar dynamic collector to face the Sun within about 1° and 0.1°, respectively.

Due to the large inertias of these solar receivers and the lengths of the transfer booms, structural stiffness across the "alpha" joint must be maximized to reduce deflection and accelerations as well as to maximize the rate of response of the actuator. The joint must contain a rotary means to transfer electrical power and data signals across the rotary interface. Furthermore, the rotary drive mechanism must provide smooth motion, possess long life in a space environment, and have intrinsically fail-safe characteristics.

A study was conducted to determine the optimum mechanism for the rotary joint. The results of the study indicated that the best mechanism would be a continuously rotating joint based on the concept of a multiple, discrete bearing-supported joint driven by a self-loading, "pinch"-roller drive actuator.

This mechanism provides greater protection against catastrophic jamming, less sensitivity to adverse thermal gradients, greater accessibility to maintenance or replacement, and greater adaptability to very large truss members than do more-conventional continuous-support-bearing/gear joints. Furthermore, wear-life estimates show a continuous service life more than two orders of magnitude greater than that required for this application. This rotating-joint mechanism would be applicable not only to solar-power-conversion units but also to Earthbound solar-power farms and other related power-generation systems.

This work was done by Stuart H. Loewenthal and Fredrick T. Schuller of **Lewis Research Center**. *Further information may be found in NASA TM-88800 [N86-30206/NSP], "Feasibility Study of a Discrete Bearing/Roller Drive Rotary Joint for the Space Station."*

Copies may be purchased [prepayment required] from the National Technical Information Service, Springfield, Virginia 22161, Telephone No. (703) 487-4650. Rush orders may be placed for an extra fee by calling (800) 336-4700.
LEW-14542

Seals for Cryogenic Turbomachines

An analysis considers the effects of seals on stability.

A report presents a method of calculation of flows of cryogenic fluids through shaft seals. The calculations agree reasonably well with experimental data. Although the primary function of a seal is to control leakage, an important secondary purpose is to provide dynamic stability; a seal properly designed according to computational fluid dynamics and experience can enhance the stability of a turbomachine. The calculations take this secondary purpose into account.

The report discusses leakage rates and relations between pressure profiles and direct stiffnesses of three seal configurations. It relates the pressure profiles to postulated zones of secondary flow or separation.

The injection of fluid augments direct stiffness, the report notes. Flow choking can occur within a seal. In a stepped configuration, choking diverts the flow and causes a crossover of the pressure profiles in the upstream step and negative stiffness locally, but the flow separates within the step thereby increasing the overall direct stiffness. A similar effect occurs in a cylindrical seal. In a stepped labyrinth seal, carryover diminishes from the entrance and creates a crossover in the pressure profiles in each of the three steps. The local direct stiffness changes from positive to negative.

Pressure measurements taken at 0° and 180° along the axial length of a seal are not enough to define maximum-to-minimum pressure variations and zones of secondary flow. Instead, measurements must be augmented by three-dimensional computations and intuition.

The key to stability turns out to be the local average velocity in a seal. The local average velocity is strongly influenced by effects of the inlet and outlet and the injection of fluid. Thus, for accuracy, the local variations in the average dynamic coefficients must be integrated into the analysis.

This work was done by Robert C. Hendricks of **Lewis Research Center**, *L. T. Tam of CHAM, M. J. Braun of The University of Akron, and B. L. Vlcek of Rensselaer Polytechnic Institute. Further information may be found in NASA TM-88919 [N87-15442/NSP], "Evaluation of Seals for High-Performance Cryogenic Turbomachines."*

Copies may be purchased [prepayment required] from the National Technical Information Service, Springfield, Virginia 22161, Telephone No. (703) 487-4650. Rush orders may be placed for an extra fee by calling (800) 336-4700.
LEW-14556

Fabrication Technology

Erosion-Resistant Water-Blast Nozzle

A tapered design imparts long life and effectiveness.

Marshall Space Flight Center, Alabama

A new high-pressure water-jet nozzle for stripping coatings from structures lasts longer than traditional water-blast nozzles. The design of the nozzle reduces erosion of the orifice by the turbulent high-pressure water flowing through it.

The new nozzle has higher efficiency, as shown by the greater flow rate of 20 kpsi (138 MPa) water compared with that of a traditional nozzle of the same orifice size. In addition, the new nozzle strips away such coatings as paint, primer, and insulation more rapidly and more completely.

The improved performance and resistance to erosion were achieved by giving the interior nozzle surface a long, gradual convergence before the exit orifice and an abrupt divergence after the orifice (see figure) and by machining this surface to a smooth finish. Stainless-steel alloy 17-4 PH/900H (or equivalent) was selected as the nozzle material for its strength and hardness. The nozzle can be attached to the water source by a standard 3/4-in. (1.9-cm) connector.

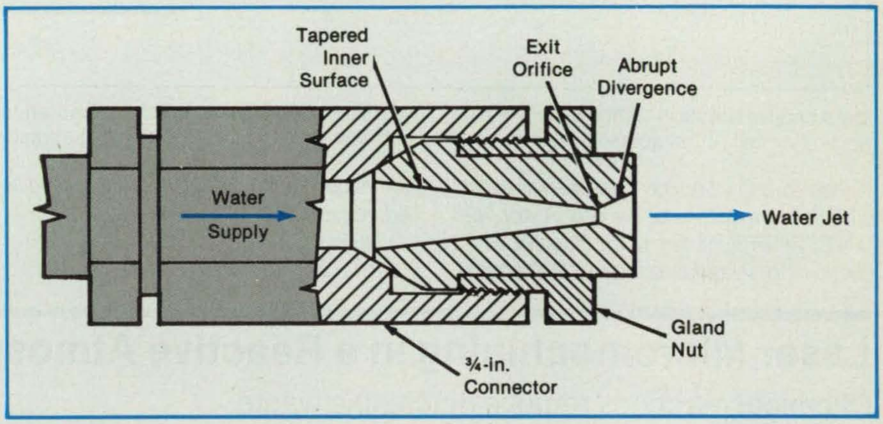

The **Taper in the Stripping Nozzle** reduces erosion. The nozzle mates with a standard connector.

The nozzle produces a jet with a long core. It can therefore be positioned farther from the work than traditional nozzles, so that the probability of a collision with the workpiece is reduced when the nozzle is used by a robot.

This work was done by Marion L. Roberts of **Marshall Space Flight Center** *and R. M. Rice and S. A. Cosby of USBI Booster Production Co. No further documentation is available.*

Title to this invention has been waived under the provisions of the NASA Act [42 U.S.C. 2457(f)], to the USBI Booster Production Co. Inquiries concerning licenses for its commercial development should be addressed to

USBI Booster Production Co.
P. O. Box 1900
Huntsville, AL 35907

Refer to MFS-28218, volume and number of this NASA Tech Briefs *issue, and the page number.*

Erosion-Resistant Water-and-Grit-Blasting Assembly

A unit releases a jet of abrasive-containing water.

Marshall Space Flight Center, Alabama

A nozzle assembly adds abrasive particles to a high-pressure water jet. The assembly includes the new tapered stripping nozzle described in "Erosion-Resistant Water-Blast Nozzle" (MFS-28218) in this issue of *NASA Tech Briefs*. The addition of abrasive particles to the jet from the tapered nozzle enhances the ability of the jet to remove coatings quickly and effectively. At the same time, the assembly shares the erosion resistance and longevity of the tapered nozzle.

The assembly includes an abrasive injector and an exit nozzle (see figure). The abrasive injector slips over the tapered stripping nozzle and screws into the standard 3/4-in. (1.9-cm) connector, replacing the gland nut that ordinarily retains the tapered nozzle. The connection uses no O-rings or backup rings. Commonly used as seals in conventional grit-blast nozzle assemblies, such rings tend to be extruded under high pressure and eventually fail.

The partial vacuum created in the abrasive-injector housing by the water flowing from the tapered nozzle draws the abrasive particles into the exit nozzle. Like the tapered nozzle, the exit nozzle is made of 17-4 PH/900H (UNS S17400) stainless-steel alloy and is gradually tapered and smoothly finished in its converging section to minimize erosion. It ends in a cylindrical exit orifice.

If desired, the nozzle assembly can be used for nonabrasive stripping by simply closing the abrasive-supply line. The long, straight jet created by the tapered stripping nozzle is retained, and it is not necessary to remove the abrasive injector from the tapered nozzle.

This work was done by Marion L. Roberts of **Marshall Space Flight Center** *and R. M. Rice and S. A. Cosby of USBI Booster Production Co. No further documentation is available.*

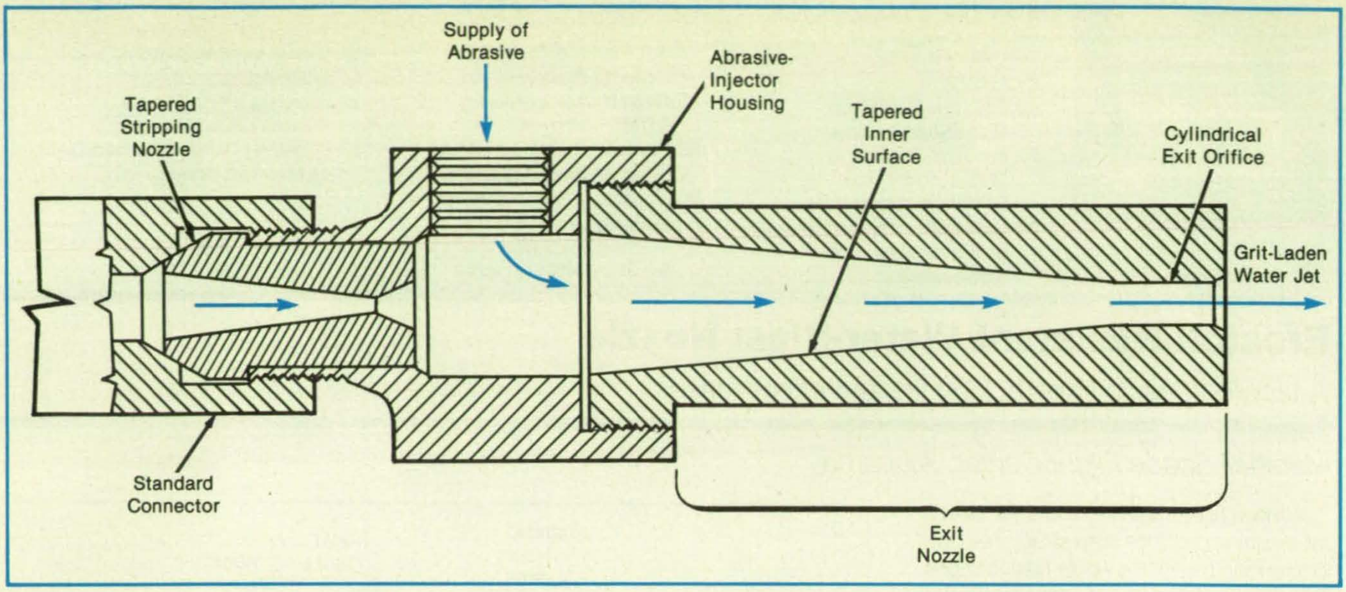

The **Abrasive Nozzle** is combined with a high-pressure tapered stripping nozzle and a standard connector. The partial vacuum in the relatively large chamber of the abrasive-injector housing entrains the grit particles from the abrasive supply.

Title to this invention has been waived under the provisions of the NASA Act [42 U.S.C. 2457(f)], to the USBI Booster Production Co. Inquiries concerning licenses for its commercial development should be addressed to

USBI Booster Production Co.
P. O. Box 1900
Huntsville, AL 35907

Refer to MFS-28219, volume and number of this NASA Tech Briefs *issue, and the page number.*

Laser Micromachining in a Reactive Atmosphere

Chemical reactions remove machining waste.

NASA's Jet Propulsion Laboratory, Pasadena, California

The drilling of deep holes in silicon by a laser beam is aided by conducting the operation in a reactive atmosphere. The atmosphere reacts with material ejected from the hole and converts the material to a gas that flows away from the work area. The hole is cleaner and more sharply defined, and debris do not spatter the surface of the work.

When holes are drilled in a silicon chip by a laser beam in air or in an inert atmosphere, solid debris collect around the holes. However, if the procedure is done in chlorine gas, the silicon vapor and droplets leaving the hole combine with the chlorine to form silicon tetrachloride gas.

In a demonstration, holes 0.030 and 0.003 in. (0.76 and 0.076 mm) in diameter were drilled in silicon wafers in various atmospheres. A portable manifold controlled the flow of air, oxygen, nitrogen, argon, or chlorine in a microscope-stage reaction chamber. A ruby-laser beam entered the chamber through a thin glass window.

The holes drilled in a chlorine atmosphere were more regular than those drilled in air, nitrogen, or argon and were completely free of debris (see figure). Drilling in oxygen converted the ejected silicon to fluffy white silica debris that interfered with visibility but probably did not damage the silica layer on the wafer surface.

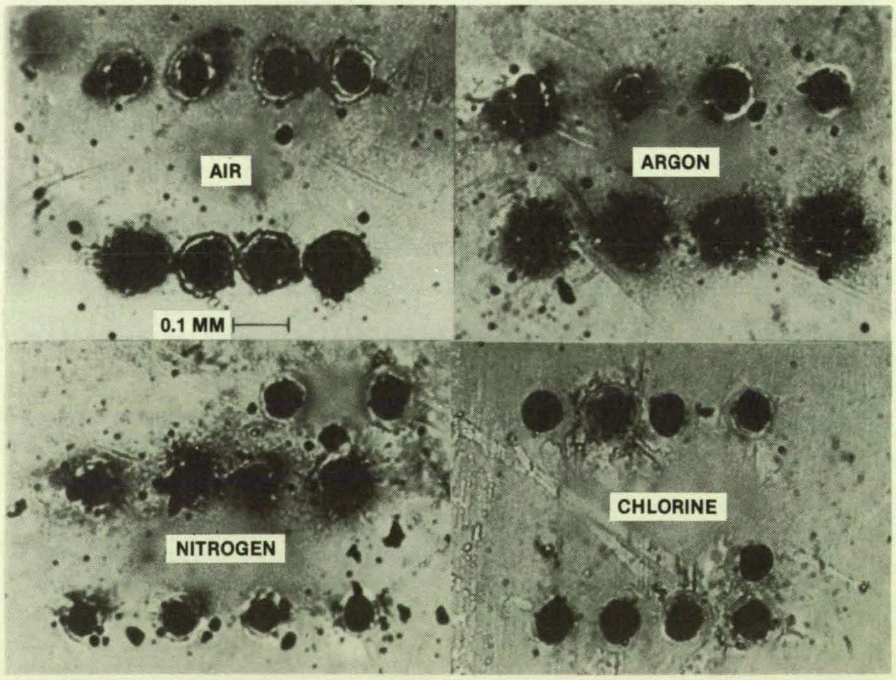

Spattered Silicon surrounds laser-drilled holes, except those made in a chlorine atmosphere. The reaction of silicon and chlorine not only eliminates debris but also makes the holes more nearly round.

This work was done by Paul J. Shlichta of Caltech for **NASA's Jet Propulsion Laboratory** *and George Zahaykevich of Advanced Laser Systems, Inc. For further information, Circle 76 on the TSP Request Card.*
NPO-16587

Arc Plasma Gun With Coaxial Powder Feed

Powder is injected directly through the cathode into the plasma jet.

Lewis Research Center, Cleveland, Ohio

A redesigned plasma gun provides improved metallic and ceramic coatings. In a present arc plasma gun, the particles to be sprayed are injected orthogonally to the plasma jets either outside the nozzles or internally through circularly distributed holes in the nozzles (see Figure 1). With this method of injection, only some of the particles penetrate to the central region of the jet, and a significant part of the injected particles becomes entrained in the external, relatively cooler region of the plasma jet. This causes the injected particles to acquire a spectrum of velocities and temperatures, and some of them are either partially melted or totally unmelted.

To provide a more-uniform temperature and velocity distribution of the particles in the improved plasma gun, the particles are injected directly through a coaxial bore in the cathode into the central region of the plasma jet (see Figure 2). In this manner, the particles are introduced into the hotter and faster region of the plasma jet.

In addition, the coaxial injection increases the time of residence of the particles in the plasma jet and eliminates the cooling effect of the feeder gas on the plasma. In this case, the feeder gas becomes a part of the arc gas. Another feature of the new design is the cooling of the cathode by the feeder gas. To optimize the performance of the plasma gun for various powder and arc gases, the position of the cathode can be adjusted.

This work was done by Isidor Zaplatynsky of **Lewis Research Center**. *No further documentation is available.*

Inquiries concerning rights for the commercial use of this invention should be addressed to the Patent Counsel, Lewis Research Center [see page 18]. Refer to LEW-14539.

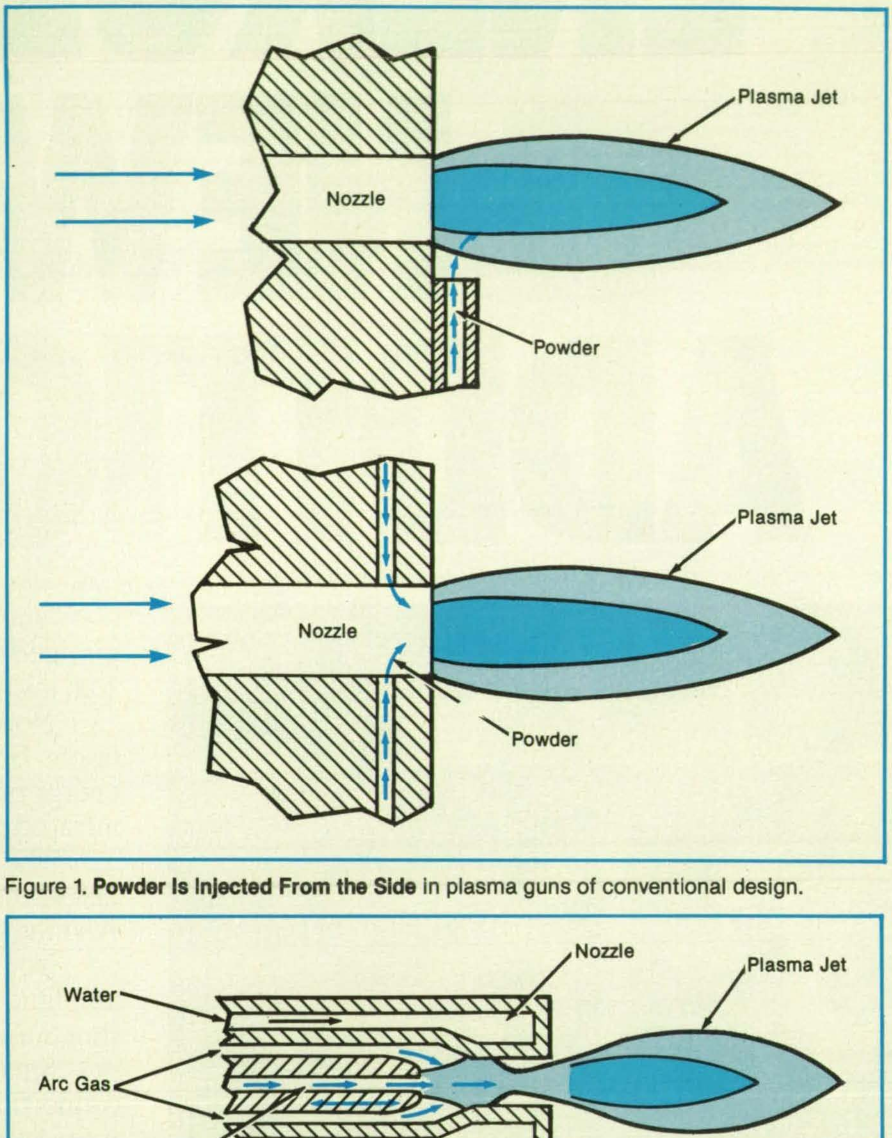

Figure 1. **Powder Is Injected From the Side** in plasma guns of conventional design.

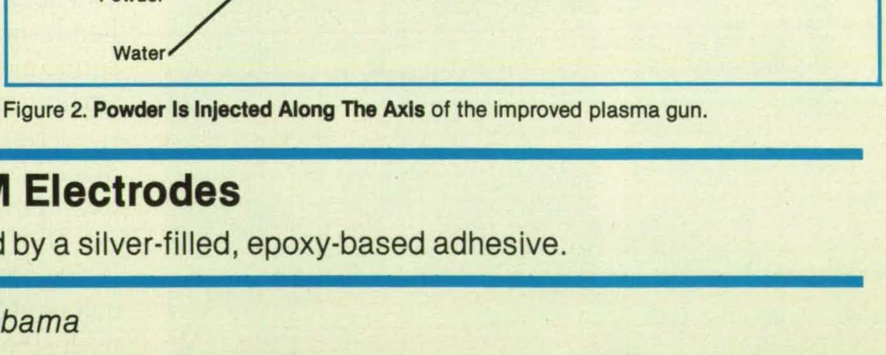

Figure 2. **Powder Is Injected Along The Axis** of the improved plasma gun.

Repair of Graphite EDM Electrodes

These electrodes can be repaired by a silver-filled, epoxy-based adhesive.

Marshall Space Flight Center, Alabama

The cost of electrical-discharge machining (EDM) can be reduced by use of an electrically conductive adhesive to repair worn or damaged sections of the graphite electrodes. Previously, damaged electrodes had to be replaced, because they were made without extra stock for remachining.

To provide extra material for remachining, pieces of graphite can be bonded to a damaged electrode with Eccobond (or equivalent) silver-filled, epoxy-based adhesive. Because this adhesive is electrically conductive, the electrical conductivity of the electrode is not impaired. Once repaired, the electrode is machined to the designed configuration and returned to service.

This work was done by Glenn Burow of Rockwell International Corp. for **Marshall Space Flight Center**. *For further information, Circle 51 on the TSP Request Card. MFS-29138*

Forming n/p Junctions With an Excimer Laser

Compact equipment yields high-quality solar cells.

NASA's Jet Propulsion Laboratory, Pasadena, California

Heating with the concentrated ultraviolet energy of an excimer laser has proved successful in driving liquid dopants into silicon to form shallow n/p junctions for solar cells. The laser equipment is more compact than the furnaces conventionally used to form junctions by diffusion of vapors. The laser equipment can fit on a tabletop.

In preparation for tests of the laser manufacturing technique, liquid dopants were applied to silicon wafers. The wafers were then heated at 200 to 400 °C for 10 to 15 minutes to drive off solvents; the dopants formed hard, glasslike layers. The wafers were then exposed to the excimer laser. Finally, they were metalized.

The excimer laser is a table model that can be pulsed at rates up to 100 Hz. It produces 20 mJ of energy per pulse at a wavelength of 193 or 308 nm (the higher wavelength was used in the tests).

Mirrors directed the light from the laser to the wafer (see figure). Lenses focused the beam from its original cross-sectional area of 1 cm^2 to 0.01 cm^2 at the wafer. The wafer was held in place by a vacuum chuck on a two-stage motorized *x-y* translation stage. A computer synchronized the motion of the stage with the firing of the laser pulses so that the laser completely scanned the wafer.

The wafers were p-type Czochralski-grown silicon with a <100> crystal orientation, coated on one side with phosphorus-doped liquid to form an n-type layer upon diffusion into the silicon. The wafers were 4 cm^2 in area; the energy density of the laser beam, 1.2 J/cm^2; the duration of the laser pulses, 25 ns; and the beam path overlapped by 50 percent on each pass.

Under these conditions, the system produced solar cells that had an average efficiency of 9.1 percent without an antireflective coating. This is equivalent to over 13 percent efficiency with an antireflective coating — comparable to that of the best cells made by conventional gaseous diffusion.

The process is also suitable for silicon made by the dendritic-web-growth process. Efficiencies range up to 13 percent with <111> p-type material, 10 cm^2 in area.

This work was done by Paul Alexander, Jr., of Caltech, Robert B. Campbell of Westinghouse Electric Corp., David C. Wong and William L. Bottenberg of Arco Solar, and Stanley Byron of Spectra-Physics, Inc., for **NASA's Jet Propulsion Laboratory**. *For further information, Circle 19 on the TSP Request Card.*

This invention is owned by NASA, and a patent application has been filed. Inquiries concerning nonexclusive or exclusive license for its commercial development should be addressed to the Patent Counsel, NASA Resident Office-JPL [see page 18]. Refer to NPO-16994.

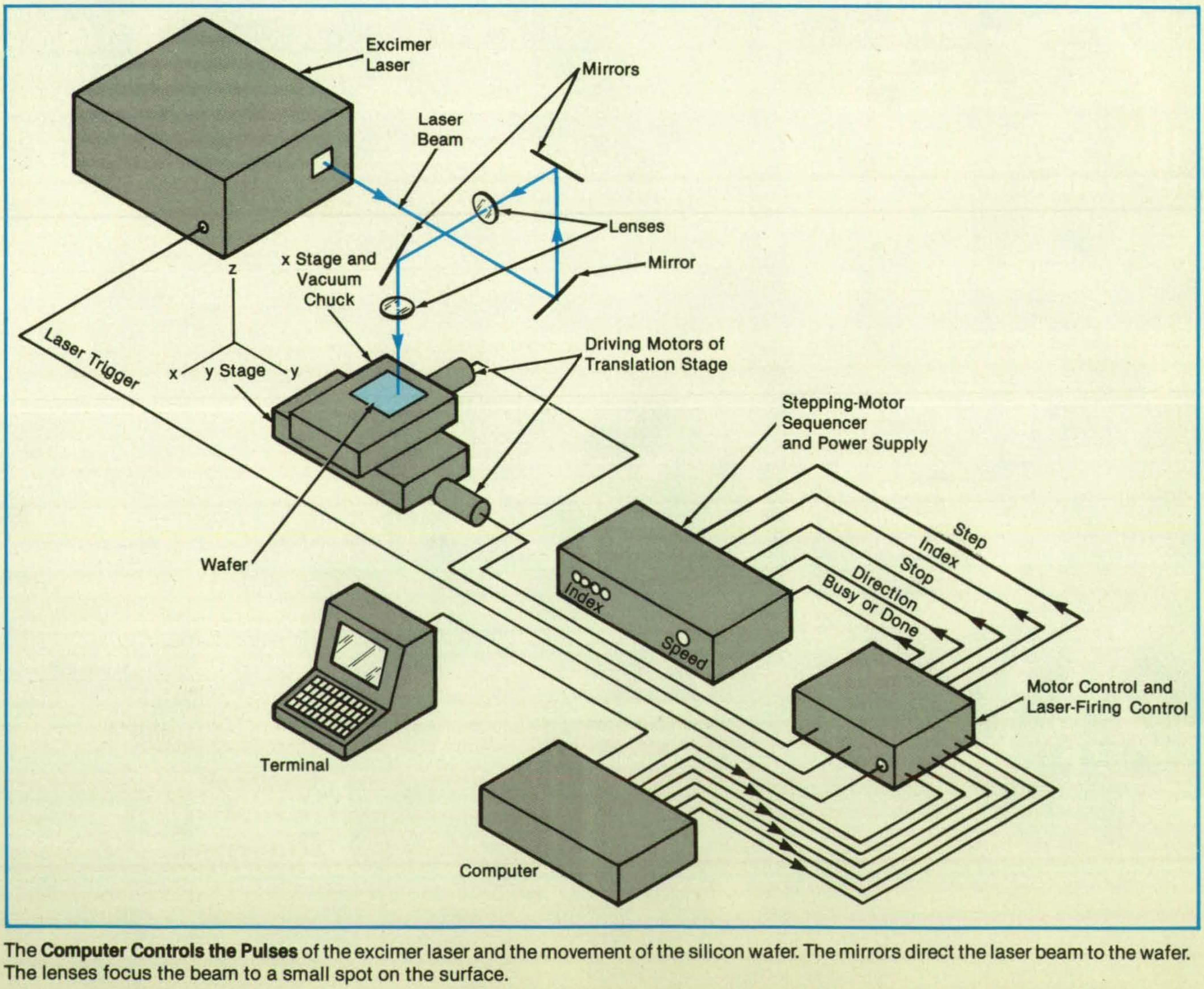

The **Computer Controls the Pulses** of the excimer laser and the movement of the silicon wafer. The mirrors direct the laser beam to the wafer. The lenses focus the beam to a small spot on the surface.

Shaping Plastic Covers Quickly and Cheaply

A cover of complicated shape can be made in only half an hour.

Marshall Space Flight Center, Alabama

A fixture enables the thermal forming of custom-contoured plastic covers in only half an hour. Previously, two workers needed 12 hours to form such a cover by hand. The fixture is inexpensive and compact.

The fixture (see figure) includes an aluminum baseplate and an aluminum forming plate with an opening cut out to match the cover outline. The pair of plates is mounted on a set of four rods, one rod at each corner of the plates. A spring on each rod pushes the forming plate toward the baseplate.

A wood mandrel is built to match the internal dimensions of the cover. The mandrel is secured to the baseplate and a sheet of plastic is placed on the top of it. The forming plate is placed on the plastic sheet, which may be of a material like acrylonitrile/butadiene/styrene (ABS). The forming plate is spring-loaded against the baseplate.

The fixture and its contents are heated in an oven to soften the plastic, allowing it to deform to the contour of the mandrel. Once the plastic sheet meets and seals against the baseplate due to spring pressure, a vacuum is applied from below to finish the forming operation by forcing the plastic tightly against the mandrel.

Because the mandrel tends to deform in the heat of the oven, it is not used repeatedly. Instead, a new mandrel is made by pouring plaster into the first plastic part made on the wooden mandrel.

This work was done by I. Gurman and D. Muckey of Rockwell International Corp. for **Marshall Space Flight Center**. *No further documentation is available.*
MFS-29188

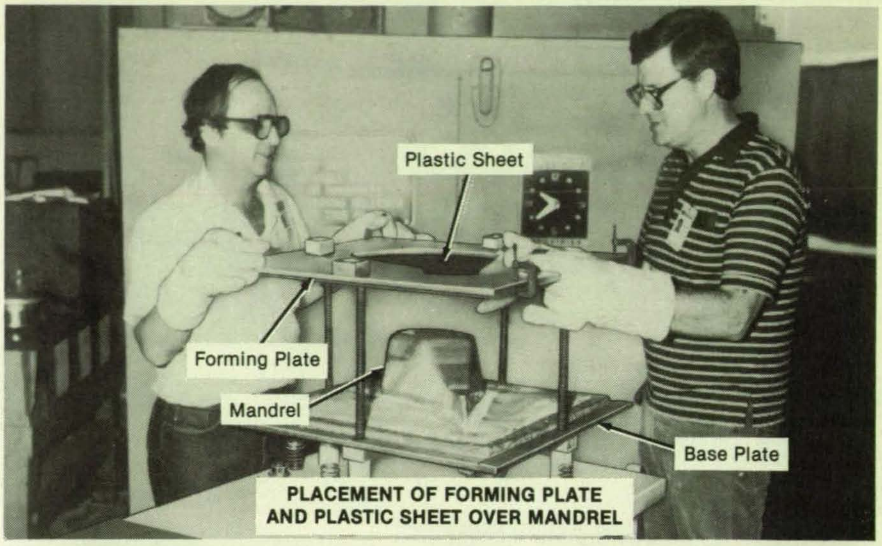

PLACEMENT OF FORMING PLATE AND PLASTIC SHEET OVER MANDREL

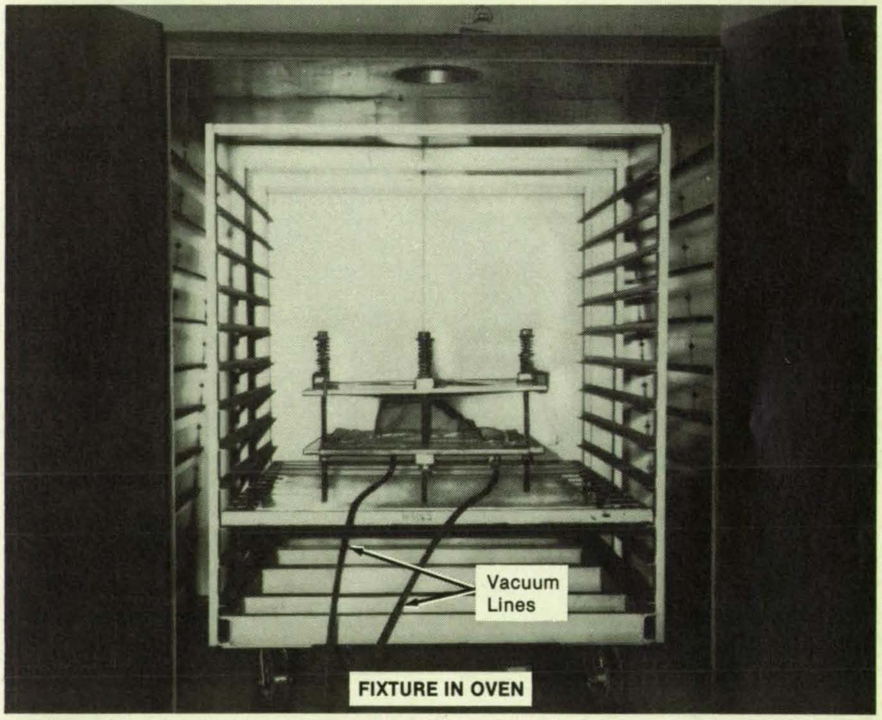

FIXTURE IN OVEN

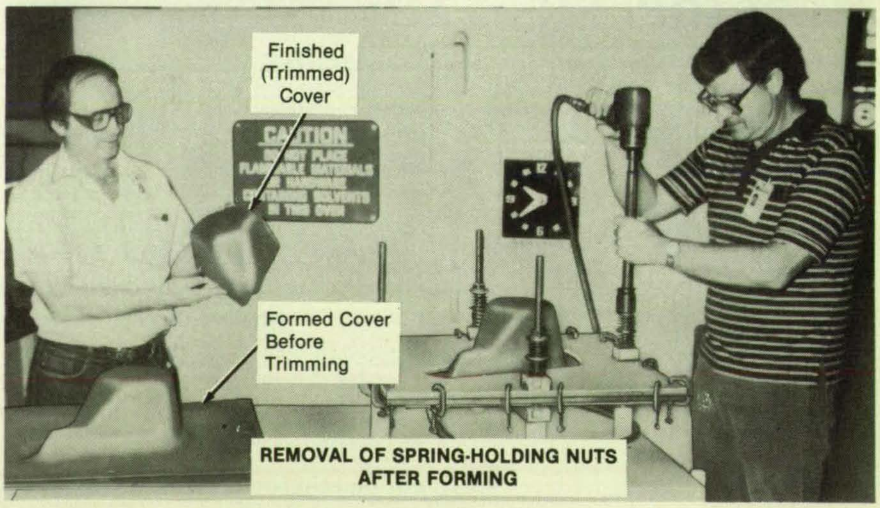

REMOVAL OF SPRING-HOLDING NUTS AFTER FORMING

In the **Assembled Cover-Forming Fixture**, the spring-loaded forming plate presses the plastic sheet toward the baseplate. Finished covers are stacked at the left side of the table.

Making EDM Electrodes by Stereolithography

Electrodes with complicated shapes are made quickly from computer models.

Marshall Space Flight Center, Alabama

Stereolithography can be used to make models and molds of electrodes for electrical-discharge machining (EDM). By use of stereolithography, an engineer can quickly turn the design of an object into a plastic model, bypassing the machining and other intermediate fabrication steps that normally consume much time (see figure). The technique has been proposed for use in making turbopump impellers for the Space Shuttle main engine and can be used to make EDM electrodes for the manufacture of other objects that have complicated shapes.

Stereolithography is a computer-aided manufacturing technique that is practiced in conjunction with computer-aided design and engineering. The three-dimensional computer model of the surface of the object to be made is converted to vector data, which are passed to the data processor of the stereolithography system. This processor uses the data to control an ultraviolet laser, a galvanometer mirror that scans the laser beam in the *x* and *y* (horizontal) directions, and a vertical translation stage in a vat of monomer of a photopolymer below the laser.

The laser beam is focused to a spot in the liquid, causing the monomer to polymerize at that point. The laser beam is scanned across each *x-y* plane; then the vertical translation stage is moved slightly, and the laser beam is scanned across the next *x-y* plane. The process continues, gradually building up the model in layers of accreting polymer. Once the model is thus completely grown, it is hardened in a bath of ultraviolet light.

A negative or positive plastic model could be made by this process. A negative model could be used as mold to make positive models, epoxy abrasive dies, or electroformed copper EDM electrodes. It could also be coated with an abrasive and used as an abrasive die to make graphite electrodes. A positive model could be used as a template for tracing by a pantograph or as an injection mold to make EDM electrodes.

This work was done by Philip A. Barlas of Rockwell International Corp. for **Marshall Space Flight Center**. *No further documentation is available.*
MFS-29480

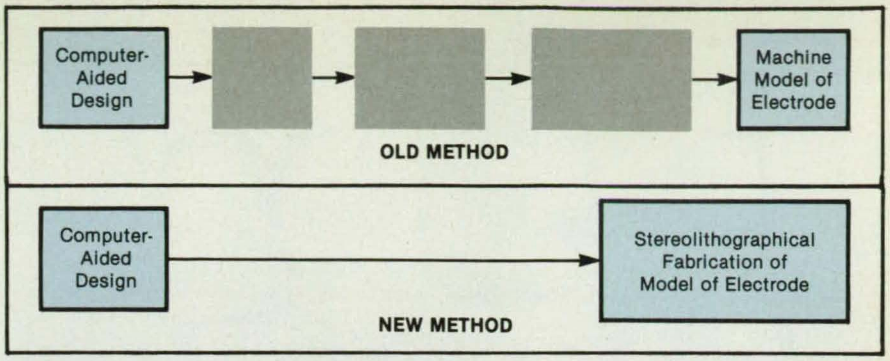

Stereolithography Eliminates Intermediate Steps in the fabrication of a plastic model of an object to be used in making an EDM electrode to manufacture the object or a mold for the object.

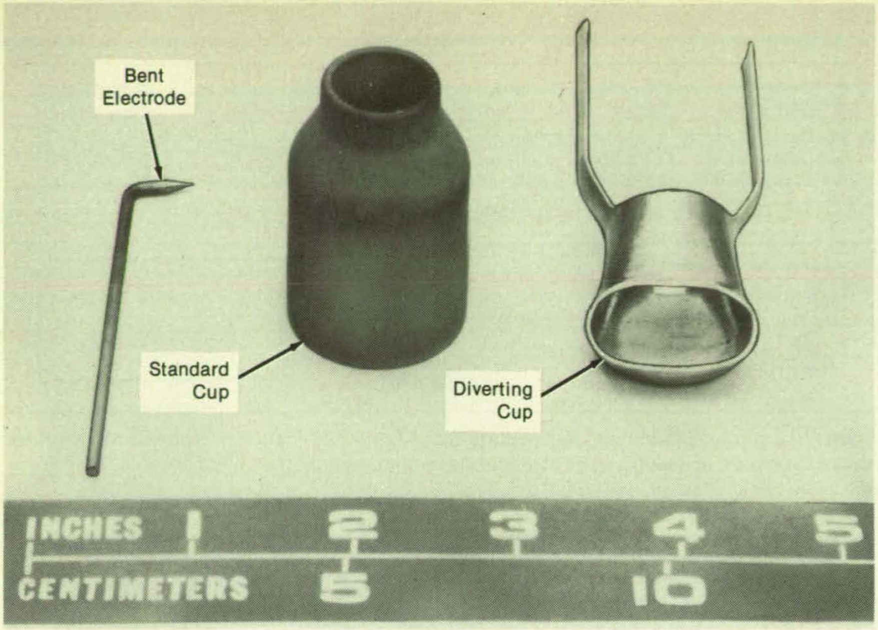

PARTS SHOWN SEPARATELY

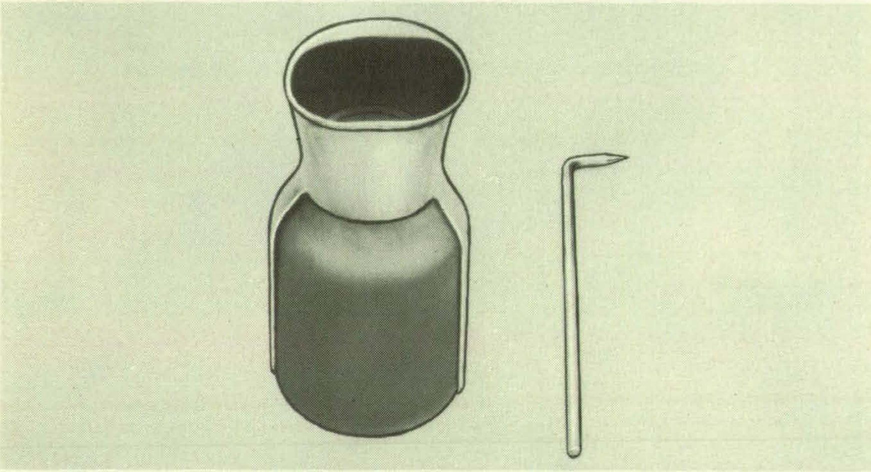

DIVERTING CUP INSTALLED ON STANDARD CUP

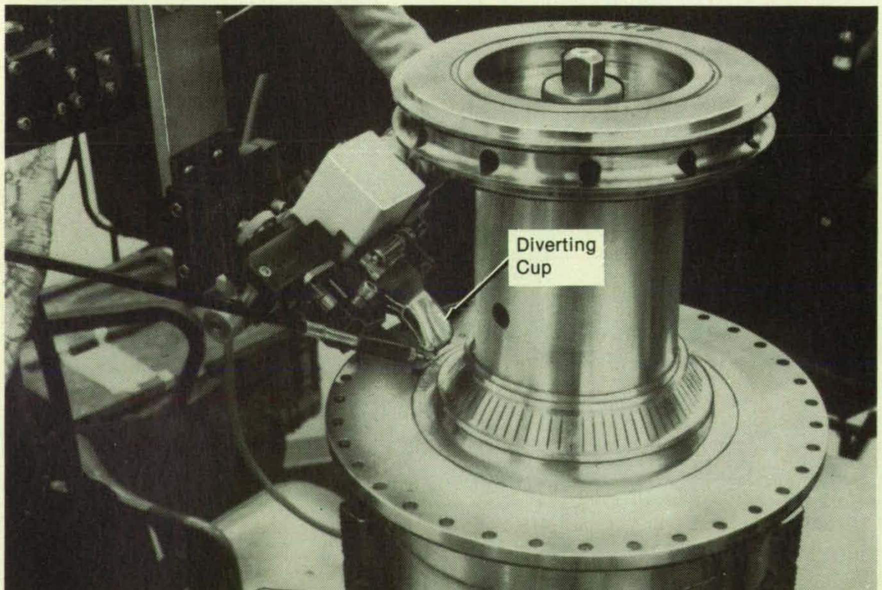

DIVERTING CUP IN USE ON WELDING TORCH

The **Stainless-Steel Diverting Cup** shown at the right in the top photograph slips over the standard torch cup as shown in the middle photograph, and the bent electrode is inserted in the torch. The assembly can reach weld joints that are inaccessible to a straight welding torch, as shown in the bottom photograph.

Gas-Diverting Cup for Welding at an Angle

An attachment makes automatic arc welders more versatile.

Marshall Space Flight Center, Alabama

A simple add-on cup for a gas/tungsten arc-welding torch makes it possible to weld in previously inaccessible places. The cup, made of stainless steel, is slipped over a welding torch equipped with a standard No. 10 cup. The add-on cup changes the angle of the gas flow, diverting it 60° away from its usual direction. The tungsten electrode is also bent 60° a short distance from its tip (see figure).

With the add-on cup and the bent electrode, an automatic welding machine can reach joints between protrusions that would interfere with the movement of a straight electrode and gas stream.

This work was done by G. E. Dyer of Rockwell International Corp. for **Marshall Space Flight Center**. *No further documentation is available.*
MFS-29206

Starting VPPA Welds Without Pilot Holes

Welding current is turned on gradually.

Marshall Space Flight Center, Alabama

Variable-polarity plasma-arc (VPPA) "keyhole" welds can be initiated without pilot holes or starting tabs, by use of a simple gradual-turn-on technique. Although pilot holes have typically yielded 80-percent repeatability, tests in the laboratory and in production show that the gradual-turn-on technique is 100 percent reliable.

In VPPA keyhole welding, the welding parameters (standoff distance, voltages or currents, speed of the torch along the weld, and times at the two polarities) are set at values that cause the weld to penetrate the workpiece and the molten metal to flow around the opening in a pattern reminiscent of a keyhole. The conventional method for starting such a weld was to drill a pilot hole to serve as the initial keyhole, carefully align the welding torch over the pilot hole, adjust the standoff distance, and

then turn on the torch at full power. The success of this method depended on the operator's ability to perform this alignment and adjustment precisely.

The new starting technique does not depend on precise manual alignment. The welding torch is positioned with no more than the usual care. As the torch begins to move along the weld, the welding current is gradually increased toward the full operating level, causing the depth of the weld to increase gradually until the keyhole is formed (see figure). The standoff is controlled by the automatic-voltage-control portion of the welding equipment. At the end of a circumferential weld, the torch can continue a short distance past the starting point to overlap and thereby complete the weld in the starting transition region.

This work was done by W. F. McGee of Martin Marietta Corp. for **Marshall Space Flight Center**. *No further documentation is available.*

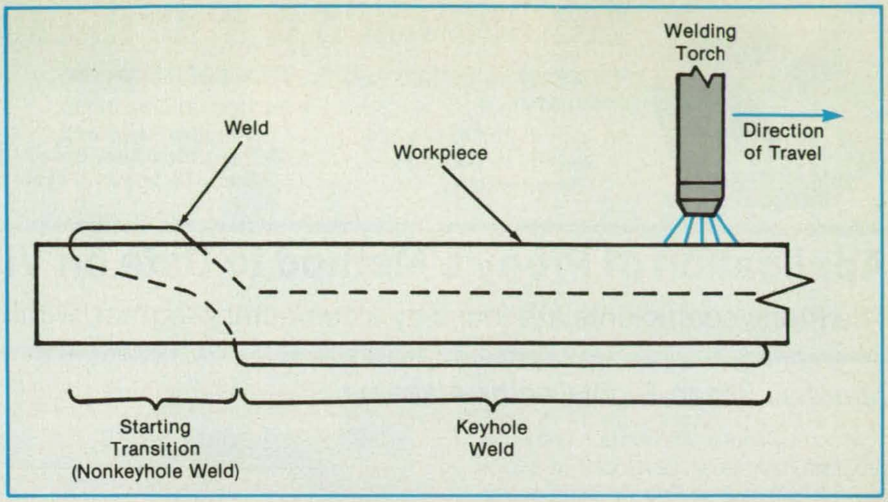

The **Welding Current Is Increased Gradually** over a short distance until the full operating current is reached, and welding proceeds in the "keyhole" mode.

Inquiries concerning rights for the commercial use of this invention should be addressed to the Patent Counsel, Marshall Space Flight Center [see page 18]. Refer to MFS-28268.

Mapping Redistribution of Metal in Welds

Displacements are detected with radioactive tracers.

Marshall Space Flight Center, Alabama

A radioactive-tracer technique can be applied to map the redistribution of metal caused by a welding process. This technique can be used to verify the predictions of computer codes for the dynamics of fluids in weld pools. These codes are important because they contribute to understanding of the dynamics and thereby may help to provide better welds that have lower residual stresses. Before the advent of the new technique, there was no way to verify the predictions of the codes after the completion of welds.

Before welding, the surfaces of the parts to be welded are irradiated by particle-beam generators to make them slightly radioactive to a specified depth in the range of 0.001 to 0.100 in. (0.025 to 2.5 mm). The total radioactivity can be less than 10 μCi — less than the level that requires licensing.

During welding, the radioactive material from the surface layer is churned with the other molten material. Eventually, the radioactive and nonradioactive components solidify in new positions. The new distribution of radioactivity can be imaged by gamma-ray detectors or photographic film. For finer three-dimensional detail, the weld region can be sliced into thin layers prior to imaging.

This work was done by Sarkis Barkhoudarian of Rockwell International Corp. for **Marshall Space Flight Center**. *No further documentation is available.*
MFS-29487

Mathematics & Information Sciences

Application of Prony's Method to Data on Viscoelasticity

The Prony coefficients are found by a computer program, without trial and error.

Marshall Space Flight Center, Alabama

A computational method and computer program have been developed to exploit the full potential of Prony's interpolation method in the analysis of experimental data on the relaxation modulus of a viscoelastic material. Because the relaxation modulus has a component that decays with time, it is well approximated by the first few terms in the Prony series

$$\bar{f}(t) = A + \sum_{i=1}^{m} B_i C^{\gamma_i t}$$

where $\bar{f}(t)$ denotes the approximation to the true value $f(t)$ of the relaxation modulus (or other quantity) that varies with time, A and the B_i and γ_i are the Prony coefficients that are sought, and t = time.

Typically, experimental values of $f(t)$ are available for discrete times t_k at unequal intervals. Heretofore, there have usually been too many unknowns for the number of data points and equations, making it necessary to solve for A and the B_i by trial and error, using assumed values of the γ_i. Moreover, it has not been possible to exploit the full capabilities of Prony's method because the method, in its traditional form, cannot give the best-fit curve through a set of data unless the data are at equal intervals of time.

In the new method, the first step is to fit the experimental data with a curve composed of a succession of third-degree curves. This is done with the help of the "B-spline interpolation" feature that is incorporated into the Intergraph Interactive Graphics Design System computer program. This interpolation is then used to manufacture data at the equal intervals required to obtain the Prony coefficients.

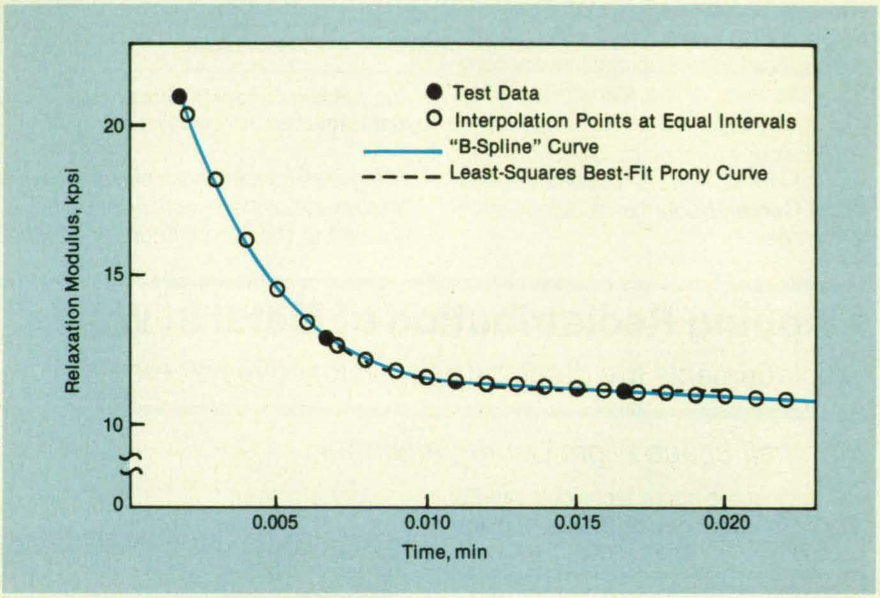

The **Prony Interpolation Curve** is chosen to give a least-squares best fit to a "B-spline" interpolation of experimental data.

The FORTRAN computer program PRONY calculates the γ_i from the roots of an mth-order equation, the coefficients of which are obtained through a matrix equation in products of differences between equal-interval-interpolated values. Using the calculated values of γ_i, the coefficients A and B_i are then chosen to make the least-squares best fit of the Prony curve to the B-spline curve (see figure).

This work was done by Pedro I. Rodriguez of **Marshall Space Flight Center**. *Further information may be found in NASA TM-86579 [N87-17455/NSP], "On the Analytical Determination of Relaxation Modulus of Viscoelastic Materials by Prony's Interpolation Method."*

Copies may be purchased [prepayment required] from the National Technical Information Service, Springfield, Virginia 22161, Telephone No. (703) 487-4650. Rush orders may be placed for an extra fee by calling (800) 336-4700. MFS-27179

Books and Reports

These reports, studies, handbooks are available from NASA as Technical Support Packages (TSP's) when a Request Card number is cited; otherwise they are available from the National Technical Information Service.

Three-Dimensional Complex Variables

Recent theoretical advances are reported.

A report presents some results of a new theory of analytic functions of three-dimensional complex variables. Mathematicians have long been frustrated in the search for a three-dimensional system of complex variables that would correspond closely to the well-known two-dimensional complex-number system. While the new three-dimensional system is subject to more limitations and is more difficult to use than is the two-dimensional system, it may nevertheless be useful in the analysis of three-dimensional fluid flows, electrostatic potentials, and other phenomena involving harmonic functions.

The author defines a three-dimensional complex number $Z = x + \delta y + \varepsilon z$, where x, y, and z are customary two-dimensional complex numbers and 1, δ, and ε are the basis vectors of the three-dimensional space, with 1 being the identity element of the algebra. The rules of multiplication are defined by

$$\delta^2 = -\tfrac{1}{2}(1 + i\varepsilon),$$
$$\varepsilon^2 = -\tfrac{1}{2}(1 - i\varepsilon),$$
$$\delta\varepsilon = \varepsilon\delta = -\tfrac{1}{2}(i\delta)$$

where $i^2 = -1$. An important property of

MACSYMA DOES THE JOBS EVEN FORTRAN DOESN'T WANT.

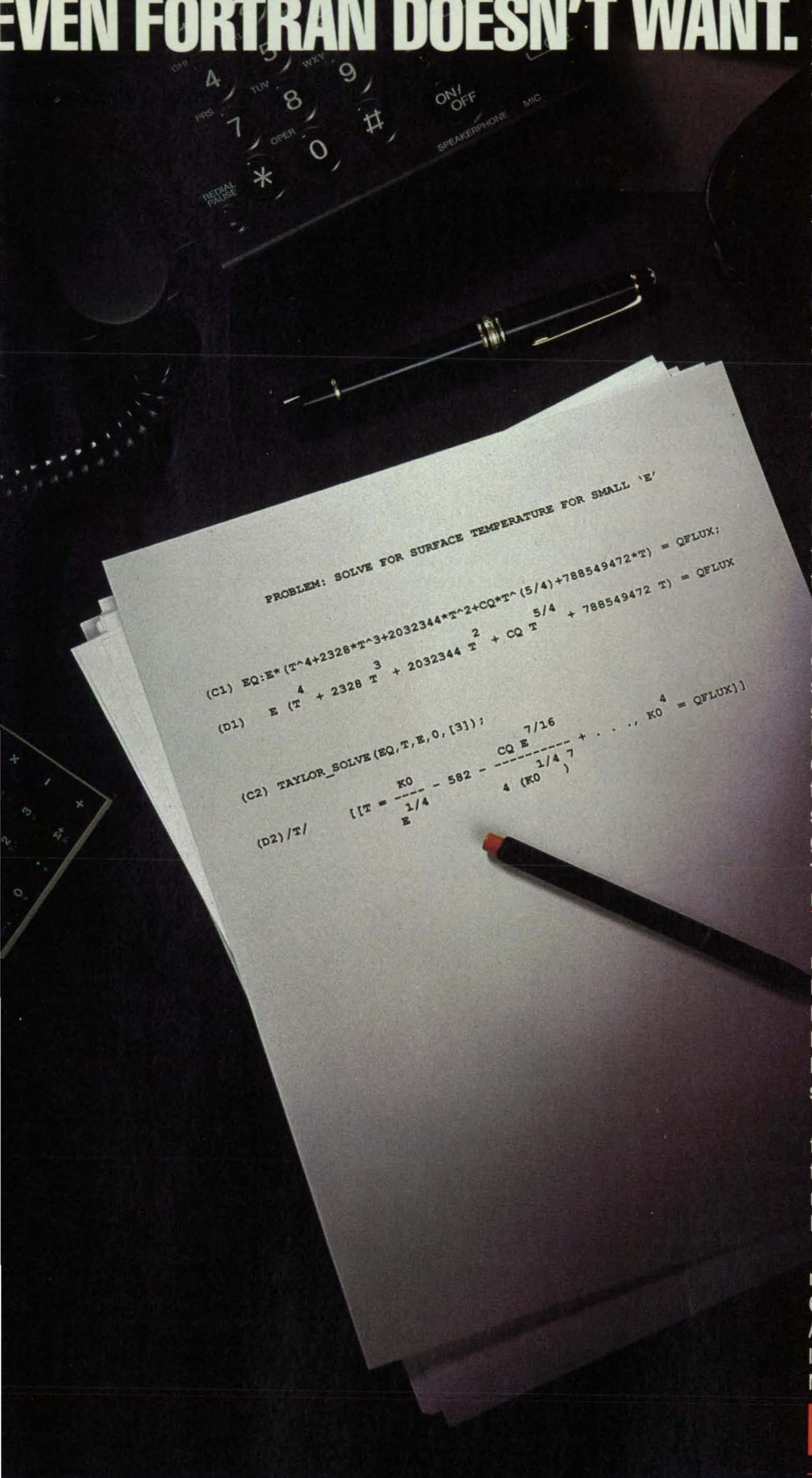

Your time is a terrible thing to waste.

Cumbersome mathematical models ar mind-numbing computations are all part your job. But the fact is, your **real** job is to solve problems on a much larger scale, a the pencil pushing is really slowing you down. Even the mainframe can't help, because Fortran just isn't up to the job.

Enter Macsyma, the symbolic mathem ics software package that lets you tackle y worst grunt work, in either batch or intera tive mode.

Give Macsyma the problems that would keep you busy for days or weeks, and you have your answer in minutes or hours. So you can solve your bigger problems faster Without wasting a lot of your valuable tim

Dare to tackle problems you could never consider before.

Most of today's complex math modeling is performed using numerical analysis tec niques and Fortran. Not necessarily becau numerical techniques are appropriate for the job, but because they're appropriate for Fortran.

With Macsyma, though, you can use th best techniques for the task. Macsyma wil give you closed-form symbolic solutions, symbolic approximations, and arithmetic solutions as well as numerical solutions. Plots and graphs, too. Without the tedium and errors associated with manual compu tations. Macsyma will even convert your solutions into Fortran code that can be int grated right into your existing programs.

Try Macsyma for 30 days and discover how much time it can save you every month.

Most professionals never realize how much time they can save until they try Macsyma. So we've made it easy for you. For a nominal installation fee, you can ha Macsyma up and running on your VAX, MicroVAX, Sun, APOLLO, or Symbolics system for a 30 day trial.

Put it through the paces. Throw your toughest problems at Macsyma. And when the 30 days are over, you will realize how much more productive you can be with Macsyma handling the math.

For a 30-day trial, or for more information, call 1-800-MACSYMA (in MA, 617-621-7770.) Or write the Computer Aided Mathematics Group, Symbolics, Inc., Eleven Cambridge Center, Cambridge MA, 02142.

Macsyma®

Productivity Tools for Mathematical Computing

symbolics

the algebra, therefore, is that all elements commute in multiplication.

The general set of three-dimensional complex numbers is denoted as C_3. It is also useful to define the more restricted set, C_3', for which x, y, and z are real numbers. The author presents several theorems and derivations relating to numbers and functions in C_3 and C_3'.

An important item concerns the multiplicative inverse, Z^{-1}: one of the peculiarities of this three-dimensional system is that Z^{-1} is undefined for some nonzero values of Z. In C_3', it is defined everywhere except along six rays (two of which form the y axis) spaced at equal angles in the plane $x = 0$.

The author defines $\bar{Z}$, the "bijugate" of Z in C_3, by the equation

$$\bar{Z} = \tfrac{1}{2}x - \delta y - \varepsilon z$$

The bijugate is somewhat analogous to the two-dimensional complex conjugate. In a theorem that states the necessary conditions for the three-dimensional analyticity of a function $\bar{G} = F(Z)$, the bijugate plays a role analogous to that of the two-dimensional complex conjugate in the Cauchy-Riemann analyticity conditions for two dimensions. Furthermore, as it would be in two dimensions, G is an irrotational and solenoidal vector in three dimensions.

A corollary of the analyticity theorem states that if $\bar{W} = dF/dZ$, then W is also an irrotational and solenoidal vector. Under suitable conditions, the harmonic real or imaginary parts (in the customary two-dimensional-complex sense) of the components of G can be related to a three-dimensional velocity potential and to general three-dimensional stream functions.

This work was done by E. Dale Martin of **Ames Research Center**. *To obtain a copy of the report, "A System of Three-Dimensional Complex Variables," Circle 137 on the TSP Request Card.*
ARC-11756

Integrated Analysis of Static Distributed Systems

An integrated approach encompasses modeling, identification of parameters, estimation of states, and control.

A report discusses aspects of an integrated methodology for the mathematical modeling, identification of parameters, and estimation of the states of a structure or other distributed system, for the purpose of controlling the system. The approach is appropriate for systems in which time-dependent effects are negligible and where control forces can be applied without exciting significant dynamic behavior.

The approach applies to models specified in part by possibly interconnected elliptic partial differential equations for deflections of structures under static loads. The authors cite the example of a wrap-rib antenna equipped with deflection sensors and with actuators that alter its reflecting surface. In this case, the mathematical model also provides for the analysis of measurements of the electromagnetic far field, which is affected by the deflections and can therefore be used to infer the deflections.

Errors in the mathematical model and in the measurements are treated as white noise; this leads to a second-order analysis of the related statistical errors. The identification (that is, the parameter-estimation) techniques are based on the method of maximum likelihood, in which the values of parameters in the mathematical model are obtained by maximizing an appropriately-defined likelihood functional that corresponds to the model equations and that incorporates the measurements. The maximization procedure is based on a Newton iteration of the functional, involving simultaneous approximations in the state and parameter spaces.

The state is estimated by use of a derived conditional mean of the state, given the measurements and parameter values. The resulting estimate is represented as a least-squares superposition of shape functions derived from the model of the structure. Batch processing of different kinds of measurements (e.g., deflections measured at a limited number of points on the antenna or far-field data taken at a finite number of points) yields recursive formulations for the state estimate similar to Kalman gains.

Computer simulations have demonstrated the validity of the general approach. A simplified model of the wrap-rib antenna with 6 actuators and 6, 9, or 12 deflection sensors yielded fairly accurate estimates of the rib-stiffness parameters, with little improvement as the number of sensors was increased. With a simplified planar antenna model, the approach yielded a small spurious deflection in a state-estimation test that used simulated far-field measurements along a ring and simulated electro-optical deflection measurements along a ring and at the center of the antenna surface.

This work was done by Guillermo Rodriguez and Robert E. Scheid, Jr., of Caltech for **NASA's Jet Propulsion Laboratory**. *To obtain a copy of the report, "Integrated Approach to Modeling, Control, Estimation and Identification for Static Distributed Systems," Circle 5 on the TSP Request Card.*
NPO-17010

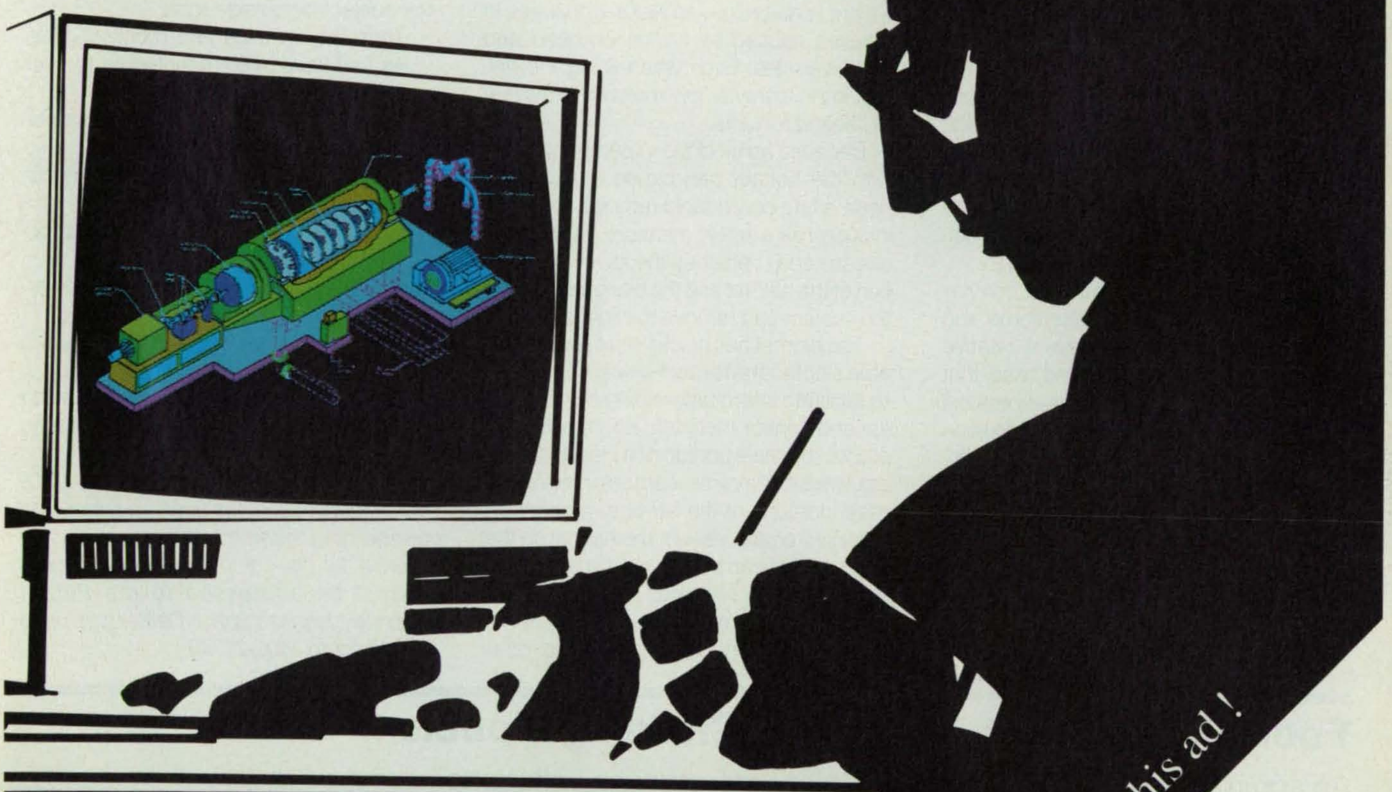

Life Sciences

Hardware Techniques, and Processes

Lightweight Helmet for Eye/Balance Studies

A bite board, sized liners, and inflatable bladders fix the helmet to the head.

Lyndon B. Johnson Space Center, Houston, Texas

A comfortable lightweight helmet serves as a mounting platform for stimulus and sensor modules used in experiments on the role of the vestibulo-ocular reflex in motion sickness and space-adaptation syndrome. These experiments require prevention of relative motion between the subject's head and the helmet-mounted modules. To achieve this without discomfort to the subject, the helmet has a fitted liner and five inflatable air bladders that stabilize the helmet with respect to the subject's head. A personal bite board attached to a chin-bar assembly makes the hard palate in the subject's mouth serve as a final position reference for the helmet.

The new helmet replaces a heavier metal helmet that was cumbersome and very uncomfortable. To prevent relative movement between helmet and head, that helmet used padded screws that pressed against the subject's head — a fixation technique that adversely affected both data collection and the subject's mental attitude.

The new helmet is easy to put on and take off. Its relatively low cost and simple manufacturing process make it attractive for a variety of neurosensory investigations. It is easily adapted to different wearers and experiments.

The new helmet is made of a lightweight polyethylene material (Spectra 900 or equivalent), fiberglass, and layers of graphite fibers. Without modules or accelerometers, it weighs less than 4 lb (1.8 kg). Low weight is necessary to reduce changes in reflexes caused by forces on head and neck muscles. Even when using the helmet in zero gravity, low mass is necessary to minimize inertia.

Because some of the experiments done with the helmet can cause motion sickness, a bite-board rapid-removal system is included as a safety measure. Pulling on a release cord detaches the lower front portion of the helmet and the bite board so that the subject can remove the helmet rapidly.

The helmet has quickly- and easily-operable electrical and mechanical connectors to facilitate interchangeability of the stimulus and sensor modules. Each module includes the male portion of a Hasselblad (or equivalent) bayonet camera mount. Female portions of the bayonet mounts are mounted on the visor of the helmet so that the modules can be mounted in front of the subject's eyes. Flattened areas on the top, back, and sides of the helmet allow for the mounting of accelerometers and other mechanical connections for sensing the position and acceleration of the head. Instructions can be communicated to the subject via headphones mounted in the helmet lining. A foam pad at the nose and cheeks prevents unwanted stimulation of the subject by outside light.

Thus far, stimulus and monitoring devices that have been mounted on the helmet include the following:

- Accelerometers to measure the acceleration of the head;
- Video cameras to record eye movements;
- An optokinetic stimulus module;
- Various light filters, including complete occlusion; and
- Calibration modules for electro-oculargrams.

This work was done by M. Catherine McStravick, David R. Proctor, and Scott J. Wood of Technology Inc. for **Johnson Space Center**. *No further documentation is available.*

This invention is owned by NASA, and a patent application has been filed. Inquiries concerning nonexclusive or exclusive license for its commercial development should be addressed to the Patent Counsel, Johnson Space Center [see page 18]. Refer to MSC-21249.

Food-Growing, Air- and Water-Cleaning Module

An apparatus produces fresh vegetables and removes pollutants from the air.

Lyndon B. Johnson Space Center, Houston, Texas

A hydroponic apparatus performs the dual function of growing fresh vegetables and purifying air and water. The system was developed for the production of salad vegetables in microgravity during long Space Shuttle missions and for experimentation with the recycling of air and water. The concept may be adaptable to the production of food and the cleaning of air and water in such closed environments as those in underwater research stations and submarines.

The apparatus is housed in a shell designed to fit in a locker (see figure). Fluorescent lamp tubes provide light. Fans circulate air from the cabin through the shell; besides providing one of the ingredients for photosynthesis, the flowing air cools the lamps. The vegetable leaves remove carbon dioxide from the air as they photosynthesize carbohydrates.

The walls of the shell hold a soillike growth medium, a granular calcined clay with particles ranging in size from 1 to 2 mm. The medium supports the plant roots; holds water, nutrients, and useful microbes; and allows the exchange of ions.

An aeration subsystem draws air through the growth medium and roots. It serves to remove excess water in the capillaries of the medium, bring fresh oxygen into the root zone, and bring organic pollutants into contact with micro-organisms that feed on them.

An "on-demand" watering subsystem supplies water and nutrients in quantities just sufficient for the needs of the roots. It fills the small capillaries adjacent to the roots but leaves the large capillaries clear for the movement of air. The subsystem may be active, employing moisture sensors, feedback circuits, and pumps; or it

may be passive, depending entirely on the capillary properties of the growth medium. A control module contains electronic circuitry that regulates the lighting cycle, the aeration of roots, and the supplies of water and nutrients.

Many variations of the system are possible. For example, it can be modified to accommodate such tall plants as dwarf tomato or bell pepper instead of such short ones as lettuce. In this case, the growth medium would occupy only one wall of the shell instead of two walls. The lamp tubes would be placed on the opposite wall instead of in the center. In another variation, the growth medium would be plastic foam incorporating ion-exchange resin beads as the supply of nutrients.

This work was done by R. L. Sauer of **Johnson Space Center** *and H. W. Scheld and J. W. Magnuson of PhytoResource Research, Inc. For further information, Circle 122 on the TSP Request Card.*

Inquiries concerning rights for the commercial use of this invention should be addressed to the Patent Counsel, Johnson Space Center [see page 18]. Refer to MSC-21301.

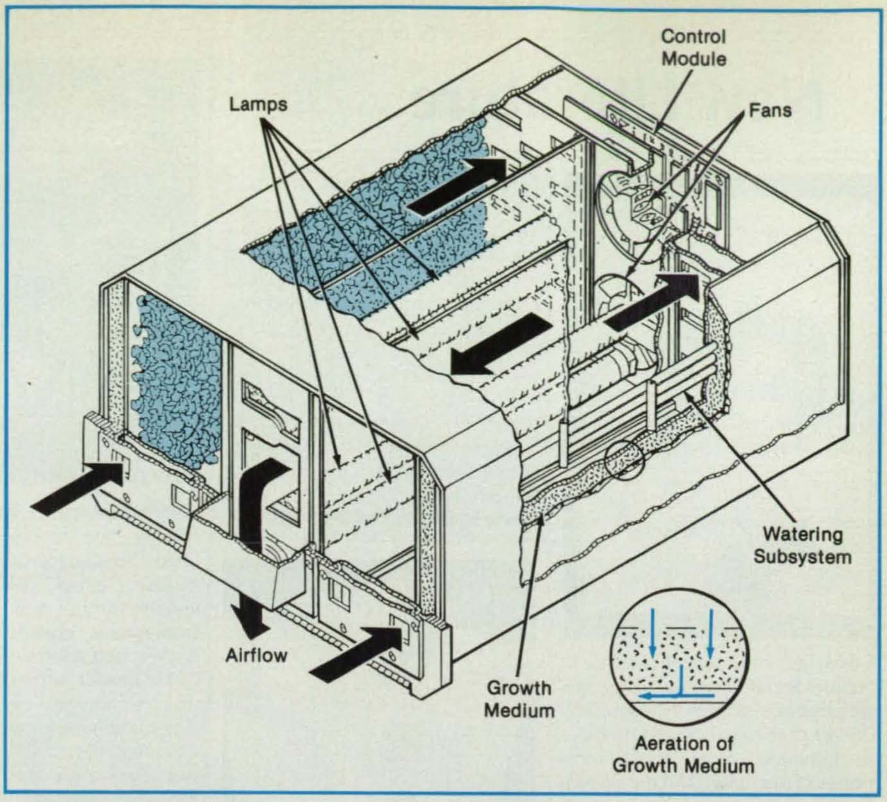

Leafy Vegetables rooted in a granular growth medium grow in the light of fluorescent lamps. Air flowing over the leaves supplies them with carbon dioxide and receives fresh oxygen from them.

Three-Dimensional Ultrasonic Imaging of the Cornea

A proposed technique would generate pictures of curved surfaces.

NASA's Jet Propulsion Laboratory, Pasadena, California

A concept for creating three-dimensional ultrasonic images would give images of such small curved objects as the cornea for medical diagnoses. The concept is adaptable to other types of reflection measurement systems as well — sonar and radar, for example.

The usual ultrasonic scanning along perpendicular x and y axes can be supplemented by gating the receiver to obtain information about small variations in depth (see figure); i.e., the receiver is held on for a brief "window" period for each reflected sound pulse. The window extends from slightly before to slightly after the expected time of return of a transmitted sound pulse. Variations in the elapsed time between transmission and reception correspond to variations in range of the target surface. These variations can be converted by time-delay spectrometry to depth variations over the cornea.

The depth variations can be displayed in any of several ways:

- As shades of gray on a video screen;
- As changing colors on a color screen; or
- As a stereoscopic image. For this presentation, two ultrasonic transmitter/receivers would be positioned to represent the left and right eyes. Their separate displays could be viewed through polarizers simultaneously so that the observer would experience visual sensations of depth variation.

This work was done by Richard C. Heyser and James A. Rooney of Caltech for **NASA's Jet Propulsion Laboratory.** *For further information, Circle 41 on the TSP Request Card.*

In accordance with Public Law 96-517, the contractor has elected to retain title to this invention. Inquiries concerning rights for its commercial use should be addressed to

Edward Ansell
Director of Patents and Licensing
Mail Stop 301-6
1207 East California Boulevard
Pasadena, CA 91125

Refer to NPO-16570, volume and number of this NASA Tech Briefs *issue, and the page number.*

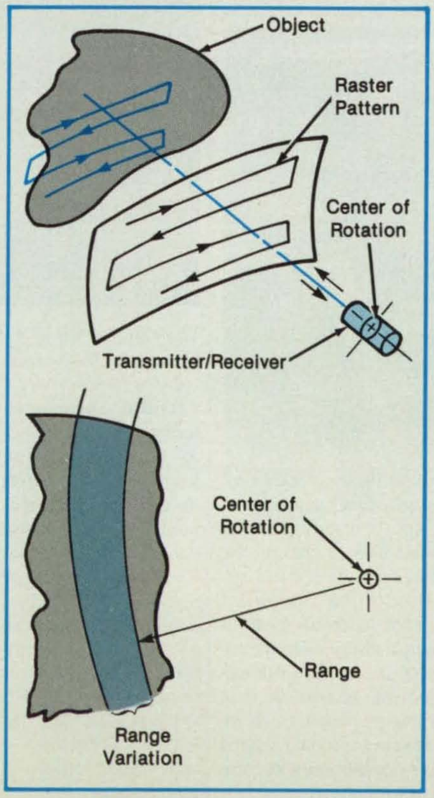

An **Object Is Ultrasonically Scanned** in a raster pattern generated by a scanning transmitter/receiver. Meanwhile, the receiver is turned on at frequent intervals to measure depth variations of the scanned object.

New Literature

A new four-color reference guide to **vacuum technology** is available free of charge from Balzers, Hudson, NH. The 40 page handbook emphasizes the principles, types, applications, modes of operation, and design fundamentals of turbomolecular pumps. A "design fundamentals" section includes formulas for calculating resistance and conductance, effective volume flow rate for geometrical configurations, and pump-down times.
Circle Reader Action Number 724.

A new brochure from CIDTEC Inc., Liverpool, NY, includes complete product specifications for CIDTEC's CID2710 **video camera**. The four-page brochure describes the camera's antiblooming and command stop motion capabilities, and discusses potential applications, including industrial inspection and testing, military guidance and tracking, and medical imaging.
Circle Reader Action Number 730.

"CADAM Step By Step," a self-training book for **learning CADAM software**, is available from CAD/CAM Consulting, Chicago, IL. The book contains 12 lessons featuring more than 300 illustrations. No previous computer knowledge is required.
Circle Reader Action Number 728.

Future Technologies Inc., Madison, GA, has published a **Survey on High-Temperature Superconductor Applications** that provides a timetable for superconductor product development, based on the combined forecasts of leading U.S. superconductivity experts. The commercialization and economic impact of high-temperature superconductors are projected for 28 classes of electronic, magnetic, communications, transportation, industrial, and power generation products.
Circle Reader Action Number 714.

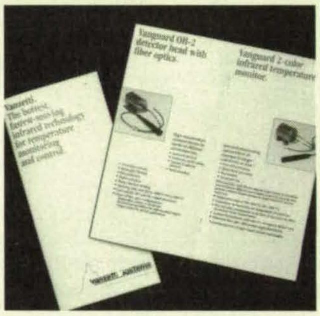

A new brochure from Vanzetti Systems, Stoughton, MA, highlights 11 non-contact **infrared temperature sensing and control products**. The brochure describes Vanzetti's infrared temperature transmitters, detector heads, infrared temperature monitors, signal processors, and linearized head assemblies.
Circle Reader Action Number 722.

Omega Engineering Inc., Stamford, CT, has released a new Data Acquisition and Computer Interface Handbook. Available free of charge, the handbook features over 350 full color pages describing hundreds of products from **software to complete data acquisition systems**. Included are sections on communication-based acquisition systems, data acquisition software, plug-in cards, industrial process controls, data logging systems, signal conditioners, recorders, printers, and plotters.
Circle Reader Action Number 718.

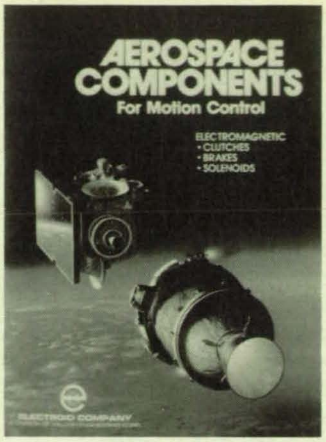

Electroid Company, Springfield, NJ, is offering a free four-color brochure entitled "Aerospace Components for Motion Control" which illustrates various torques and sizes of **electromagnetic clutches, couplings, brakes, and solenoids.**
Circle Reader Action Number 726.

A free brochure offered by Integrated Computer Systems, Culver City, CA, describes nine **technical short courses** for managers in technical environments. The courses cover topics in management skills, finance, managing projects, managing people in technical environments, and business skills.
Circle Reader Action Number 716.

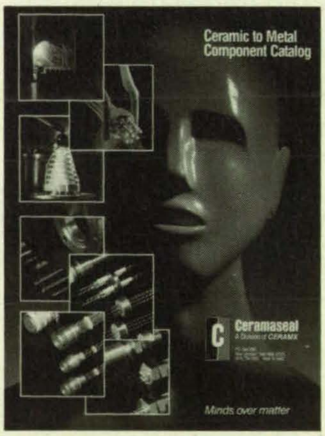

The Ceramic to Metal Component Catalog published by Ceramaseal, New Lebanon, NY, illustrates new **vacuum products** for high-temperature, high-vacuum, cryogenic, and superconducting environments. The four-color catalog describes Ceramaseal's full line of feed-thrus, connectors, thermocouples, and view-ports.
Circle Reader Action Number 706.

Over 3,000 **linear, rotational, and elevational motion devices and systems** are illustrated in a new catalog from the Klinger Scientific Corp., Garden City, NY. The catalog also features a technical explanation of micropositioning theory and technologies.
Circle Reader Action Number 704.

Hewlett-Packard's newly revised **Fiber Optics Handbook** highlights the latest technical developments in the photonics industry. The 250 page handbook is organized alphabetically and features many cross-references.
Circle Reader Action Number 702.

A free catalog from Grayhill Inc., La Grange, IL, illustrates the company's full line of **switches, keyboards, relays, and I/O modules**. Military qualification and UL and CSA recognition are listed for applicable DIP, rotary, and pushbutton switches, as well as solid state relays and I/O modules. **Circle Reader Action Number 712.**

A free brochure from the Soltec Corp., San Fernando, CA, spotlights Soltec's new DS-8000 **Digital Servo Recorder**. Unlike most strip chart recorders, the DS-8000 contains a microprocessor that converts all analog signals to a high-resolution, digital format.
Circle Reader Action Number 708.

New on the Market

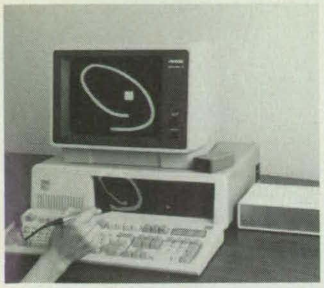

ISCAN Inc., Cambridge, MA, has introduced the OPTIMOUSE™, a **remote control cursor system** designed for rapid computer data entry. The OPTIMOUSE consists of a miniature real-time digital image processor that automatically tracks the position of a handheld pointer. The pointer can interface with any computer to control cursor position on the computer's video terminal. Unlike conventional mouse, trackball, or tablet data entry devices, the OPTIMOUSE has no desktop footprint and requires no physical contact with the computer system.
Circle Reader Action Number 800.

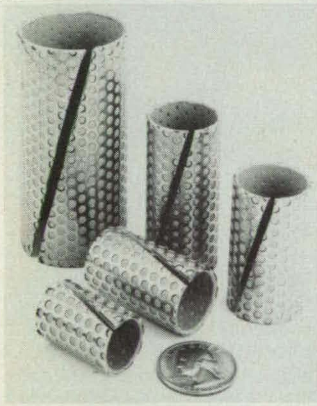

A line of stainless steel backed Teflon® **bearings** capable of withstanding loads up to 15,000 psi is now available from Engineering Plastics Inc., Westboro, MA. Designed for medium to low speed applications in corrosive environments, Engineering Plastics' HY-LOAD bearings operate over a -240° to 450°F range. No lubrication is required.
Circle Reader Action Number 790.

A new MicroVAX and VAXstation 3XXX-compatible **memory series** consisting of 8, 16, and 32 metabyte boards has been introduced by Clearpoint Research Corp., Hopkinton, MA. Using a custom gate array design, Clearpoint's MV3000 delivers 32 or 16 megabytes of memory using one megabit DRAMs. The MV3000/8MB uses 256 Kbit ZIP DRAMs. The MV3000 can also be used by MicroVAX II customers who upgrade their CPU boards to the MicroVAX 3000.
Circle Reader Action Number 780.

TCI Software Research Inc., Las Cruces, NM, has developed the T^3 **Scientific Word Processing System**, a technical document preparation program for IBM PCs and compatibles. Using a menu-driven interface and graphics screen display, T^3 offers a simple way to produce documents containing complex expressions. Mathematics, chemical structures, foreign languages, and other special characters are entered directly with T^3; no command language or markup code is required. Features include a built-in spelling checker, proportional and fixed character spacing, user-defined line and page formatting, and a macro capability.
Circle Reader Action Number 776.

The SPEECH THING™ from Covox Inc., Eugene, OR, is an eight bit digital-to-analog **sound converter** that attaches in-line with the parallel printer port of an IBM PC/XT/AT or compatible, allowing the computer to reproduce high-fidelity speech and music. Software includes a talking calculator, a graphics-based sound editor, a music sampler keyboard, and a special effects control panel. The complete hardware/software speech system costs $69.95.
Circle Reader Action Number 762.

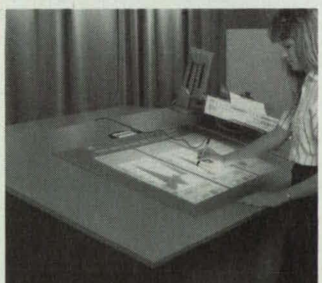

Showcase Systems Inc., Belmont, CA, has unveiled the Showcase Display Processing Workstation, a large screen (24″x36″) **digitizing drawing table** that combines a stylus or cursor with a high-resolution computer-generated color image. The image appears directly on the surface of the drafting table, thereby eliminating the "hand-to-eye" problem of using a cursor/mouse and monitor. Applications include design, control, and simulation.
Circle Reader Action Number 794.

CHR Industries Inc., New Haven, CT, is offering for evaluation a free sample of the company's new low-density **silicone foam**. The COHRlastic® foam material provides broad chemical and environmental resistance, low-compression set, and densities as low as 11 pounds/cu. ft. Applications include thermal barriers, noise and vibration dampeners, insulation, gaskets, and seals.
Circle Reader Action Number 784.

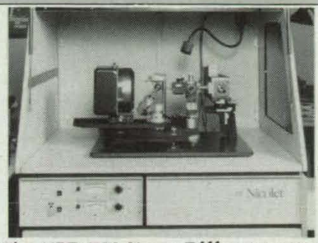

The XPD-700 **X-ray Diffractometer** from Siemens Analytical X-ray Instruments Inc., Madison, WI, offers enhanced beam brilliance, sample orientation, and x-ray detectability over previous micro-diffraction methods. The system couples dual nickel-coated x-ray mirrors for beam focusing and monochromatization. Sample orientation is achieved via a three-axis camera.
Circle Reader Action Number 786.

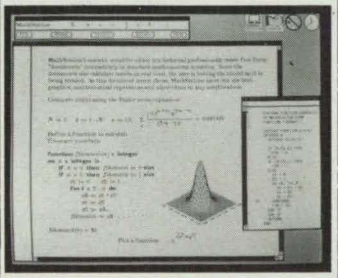

MathSoft Inc., Cambridge, MA, has introduced MathStation™, an interactive **software tool** used to design and build mathematical models and to perform numerical analysis. MathStation allows users to work directly with mathematics and spend less time programming. The workstation software integrates mathematics, text, and graphics with a WYSIWYG display, generates FORTRAN automatically from mathematical models, and integrates with existing FORTRAN code and libraries.
Circle Reader Action Number 770.

Tribo/Comp™ TFD, a new self-lubricating **composite material** produced by the Tiodize Company, Huntington Beach, CA, offers a strength-to-weight ratio which is one-fifth the weight of steel and one-half the weight of aluminum. The three-dimensional graphite fiber composite exhibits a .04 friction coefficient with no creep when exposed to 30,000 PSI compressive loads at 600°F continuously. Tribo/Comp TDF can be processed into a variety of shapes, including aircraft fasteners, bearings, gears, and fittings.
Circle Reader Action Number 772.

Dianachart Inc., Rockaway, NJ, has introduced an **XT Turbo Computer** for harsh industrial environments. The 19 inch rack-mounted computer is enclosed in a sealed metal case that maintains positive pressure against dirt and dust. Air is drawn into the case through a replaceable filter. 640K memory, parallel and serial ports, and a 5-¼ inch floppy disk are standard.
Circle Reader Action Number 760.

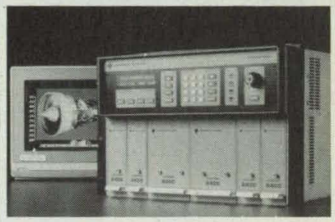

The new 8400 **Digital Pressure Measurement System** from Pressure Systems, Hampton, VA, allows users to digitally program calibration pressures in real time for on-line calibration of PSI's electronic pressure scanners. In addition to pressure scanning, the 8400 can measure extraneous parameters such as temperature and flow. The unit's parallel processing design permits acquisition rates up to 400,000 measurements per second.
Circle Reader Action Number 777.

The QL3600 **Laser/Microcomputer Pyrometer** from Quantum Logic Corp., Hackensack, NJ, automatically measures total radiance and reflectivity or true temperatures of diffuse surfaces in research and industrial control applications. Absolute accuracies of + 5°F are attainable, with various ranges available to cover 840-5430°F. An on-board digital link transfers either emissivity-corrected temperatures or target radiance and in-situ reflectivity data to an external computer for data acquisition, analysis, and presentation. Analog output options are available.
Circle Reader Action Number 758.

(Continued on the next page)

New on the Market *(continued from previous page)*

A **free demonstration disk** of MINI-GAM II, a menu-driven software package for gamma spectroscopy with high-purity germanium detectors, is now available from EG&G Ortec, Oak Ridge, TN. The sample is offered on either 3½ inch or 5¼ inch, double-sided, double-density diskettes, and is accompanied by a text of walkthrough instructions.
Circle Reader Action Number 782.

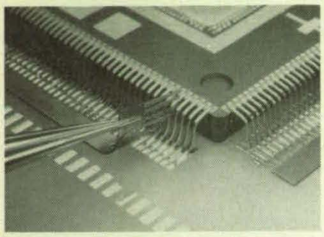

Six new **SolderQuik® tapes** from the Raychem Corp., Menlo Park, CA, align and precisely deliver solder to a variety of surface-mount components. The tapes are suited for soldering of leaded chip carriers and edge connectors to printed wiring boards, as well as soldering of flat packs, jumpers, and flexible circuits. With the proper reflow equipment, the tapes can virtually eliminate bridging.
Circle Reader Action Number 774.

The new Antares™ Q-switched, modelocked **Nd:YAG laser** from Coherent Inc., Palo Alto, CA, provides the highest pulse energy and repetition frequency of any commercially available laser system. The Antares Model 7800 delivers 4 mj Q-switched at 1064 nm; 3 mj Q-switched and modelocked at 1064 nm; and 1 mj at 532 nm. In Q-switched CW operation, the Model 7800 offers selectable pulse repetition rates from 10 Hz to 20 KHz, using a built-in digital display.
Circle Reader Action Number 798.

A new millimeter-wave **power meter** from the Dorado Company, Seattle, WA, can measure power from 26.5 to 170 GHz with a single sensor. The Dorado Model PS-28-6 can take up to 1.5 watts CW without burnout and measure pulse signals up to 100 watts peak.
Circle Reader Action Number 778.

The new **CIR-KIT®** from Pace Inc., Laurel, MD, offers a low-cost way to quickly repair and/or replace damaged or missing lands, conductors, and edge connectors on printed circuit boards. Each kit contains over 30 sizes of eyelets, tracks of various widths, an abrasive stick, a setting tool, and instructions.
Circle Reader Action Number 752.

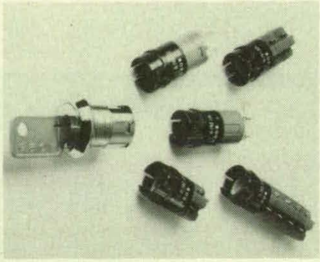

The new Series 15, ¾" round **keylock concept** created by EAO Switch Corp., Milford, CT, offers the design engineer a low-cost, five tumbler lock mechanism with a choice of contact materials and standard EAO switch elements. The Series 15 gives the engineer the flexibility to design-in an assembled, two-position keylock with the exact power requirements for the application.
Circle Reader Action Number 764.

The Monarch **Color Graphics Converter** (CGC) from Folsom Research Inc., Folsom, CA, converts high-resolution black and white or color computer graphics to NTSC or PAL format in real-time, for use with video recorders, projectors, and video disks. The Monarch CGC accepts either interlaced or non-interlaced graphics output video at a horizontal scan frequency of up to 72 KHz and a maximum of 1024 active lines. Applications include CAD/CAM/CAE, animation, and marketing and commercial television presentations.
Circle Reader Action Number 796.

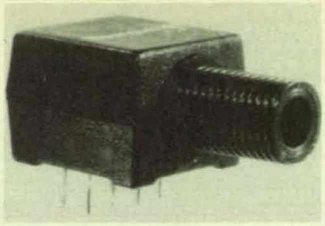

Two new series of **fiber optic transmitters and receivers** in a fiber-DIP plastic package have been developed by the Optoelectronics operation of Micro Switch, a Honeywell division. The Honeywell HFE4400 series offers a wide range of minimum output power for standard 850 nm LEDs, while the Honeywell HFD3400 series are fiber optic receivers ranging from 5 Mbit direct-coupled integrated receivers to 35 MHz analog integrated receivers. Both series come with an optical connector that accepts standard 905- or 906-type SMA fiber optic connectors.
Circle Reader Action Number 768.

Scanivalve Corp., San Diego, CA, has introduced the Hyscan™ 2000 **Pressure Measurement System**, a PC/AT-based data acquisition system that scans and stores pressure and analog input signals at 100,000 channels per second. Engineering unit converted data can be downloaded to a host computer at throughput rates up to 50,000 measurements per second. Unlike other pressure data systems available today, the Hyscan 2000 is both a high-speed computer and a pressure measurement system. The DAQ provides processing power with either the 80286 or 80386 CPU.
Circle Reader Action Number 792.

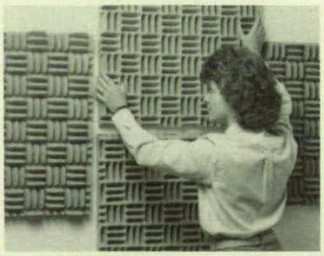

New SONEX Juniors from Illbruck, Minneapolis, MN, are designed to **control noise problems** in the office, plant, warehouse, or home. The sculptured panels, each 24" square and 2" thick, feature a porous acoustic construction that helps alleviate such common sound problems as standing waves, slap echo, and peak resonances. SONEX Juniors can be arranged in a uniform pattern or at various angles for design versatility.
Circle Reader Action Number 766.

A new **thermoplastic powder prepreg process** that can combine virtually any polymer with any reinforcement has been developed by Thermoplastic Composites, an operating unit of BASF Structural Materials Inc., Charlotte, NC. The solvent-free process eliminates the need for lengthy mold cycle times, concerns over void formation, and the problems associated with solvent removal. The powder preform is presently available as unidirectional tape. Products under development include single-end towpregs, unidirectional broad goods, and woven fabric.
Circle Reader Action Number 788.

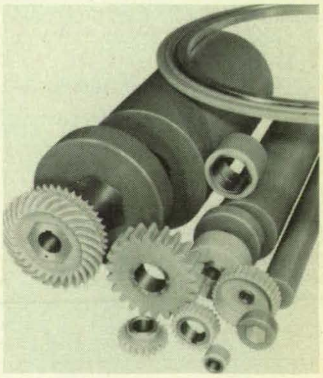

Intech, Fort Lee, NJ, is offering samples of its new Power Core™ **composite material**, designed to solve noise, vibration, corrosion, and alignment problems in gear applications. Power Core machinable blanks are cast of Lauramid® -nylon 12 around a hexagonal metal core to assure high torque delivery at elevated temperatures.
Circle Reader Action Number 748.

The new HC-4000 **Holographic System** from Newport Corp., Fountain Valley, CA, provides real-time holographic data for non-destructive testing and evaluation. Using a compact on-board laser diode source and a CCD camera, the HC-4000 records holograms every 1/30 of a second and produces deformation measurements accurate to half the wavelength of light.
Circle Reader Action Number 750.

Subject Index

A

B

C

D

(Continued on page 110)

Advertiser's Index

***RAC** stands for **Reader Action Card.** For further information on these advertisers, please circle the RAC number on the Reader Action Card elsewhere in this issue. This index has been compiled as a service to our readers and advertisers. Every precaution is taken to ensure its accuracy, but the publisher assumes no liability for errors or omissions.

Subject Index

(Continued from page 108)

NASA Tech Briefs, ISSN 0145-319X, USPS 750-070, copyright © 1988 in U.S., is published monthly except July/August and November/December (10x per year) by Associated Business Publications Co., Ltd. 41 E. 42nd St., New York, NY 10017-5391. The copyrighted information does not include the individual Tech Briefs which are supplied by NASA. Editorial, sales, production and circulation offices at 41 E. 42nd Street, New York, NY 10017-5391. Subscriptions for non-qualified subscribers in the U.S., Panama Canal Zone, and Puerto Rico, $75.00 for 1 year; $125.00 for 2 years; $200 for 3 years. Single copies $15.00. Remit by check, draft, postal or express orders. Other remittances at sender's risk. Address all communications for subscriptions or circulation to NASA Tech Briefs, 41 E. 42nd Street, New York, NY 10017-5391. Second-class postage paid at New York, NY and additional mailing offices. **POSTMASTER: please send address changes to NASA Tech Briefs, 41 E. 42nd Street, Suite 921, New York, NY 10017-5391.**

HEADGEAR THAT HOLDS EVERYTHING NEEDED TO TACKLE AIRCRAFT MAINTENANCE PROBLEMS.

Searching through the millions of instructions needed to maintain the many systems on today's advanced aircraft is no easy task. But McDonnell Douglas logistics specialists have found a way to store massive amounts of data on computers linked to a miniature TV mounted on a technician's helmet. Detailed instructions needed to get the job done are instantly available as text, graphics or video at the touch of a button, leaving hands free to carry out the work. Engineers at McDonnell Douglas are giving America its money's worth with new data displays —not only for maintenance, but for spacecraft and aircraft mission management— that save time and improve performance.

For more information, write: Data, McDonnell Douglas, Box 14526, St. Louis, MO 63178.

MCDONNELL DOUGLAS

TRAINING   INFORMATION SYSTEMS   HELICOPTERS   SPACECRAFT & MISSILES   FINANCING   MILITARY & COMMERCIAL AIRCRAFT

Circle Reader Action No. 501